

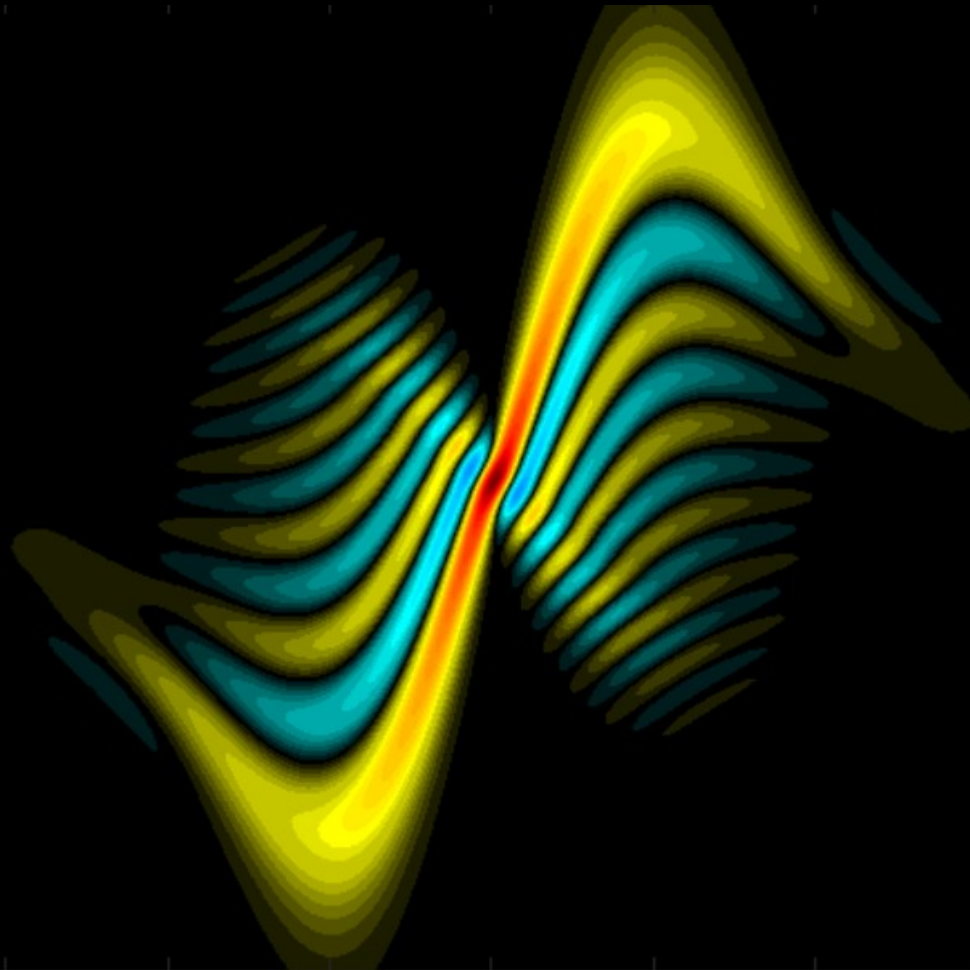
How to deal with femtosecond pulses

Baptiste Fabre, CELIA, Université de Bordeaux – CEA – CNRS

Yann Mairesse, CELIA, Université de Bordeaux – CEA – CNRS

Sébastien Weber, CEMES Toulouse, CNRS

I – Manipulation



Introduction: time-frequency travel

Keeping ultrashort pulses ultrashort

Self-phase modulation – the enemy within

Mirror mirror

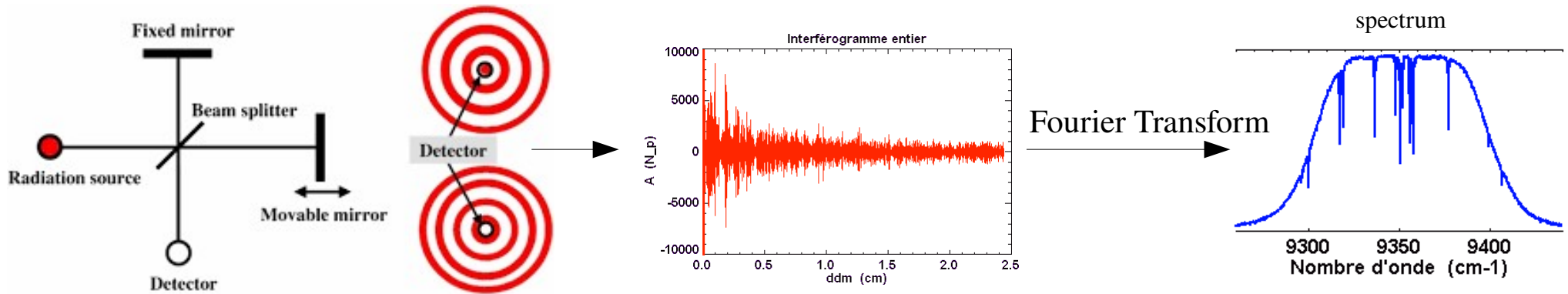
Producing circularly polarized pulses – a perfect circle

Focus

Time and spectrum

The spectral width of a light source defines its **coherence time** $\tau_c = 1/\Delta\nu$
(coherence = ability to produce interferences)

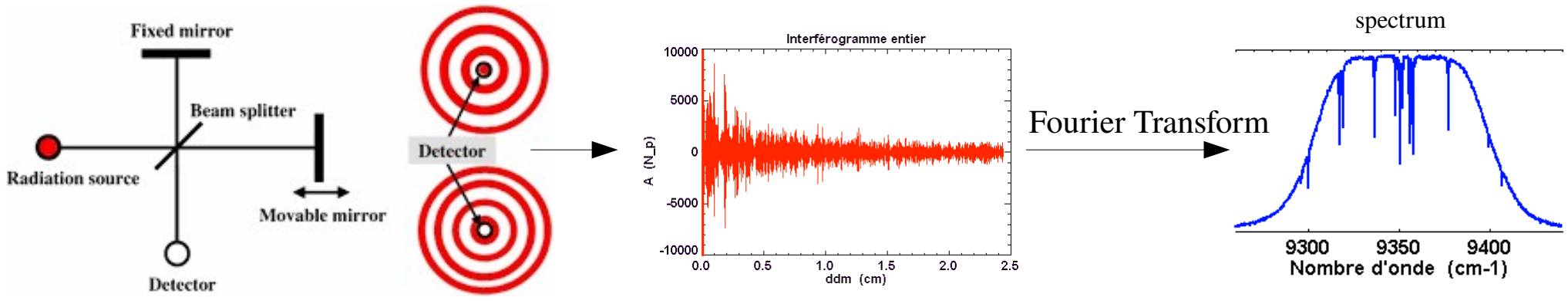
Measurement: linear (field) autocorrelation = Fourier transform spectroscopy



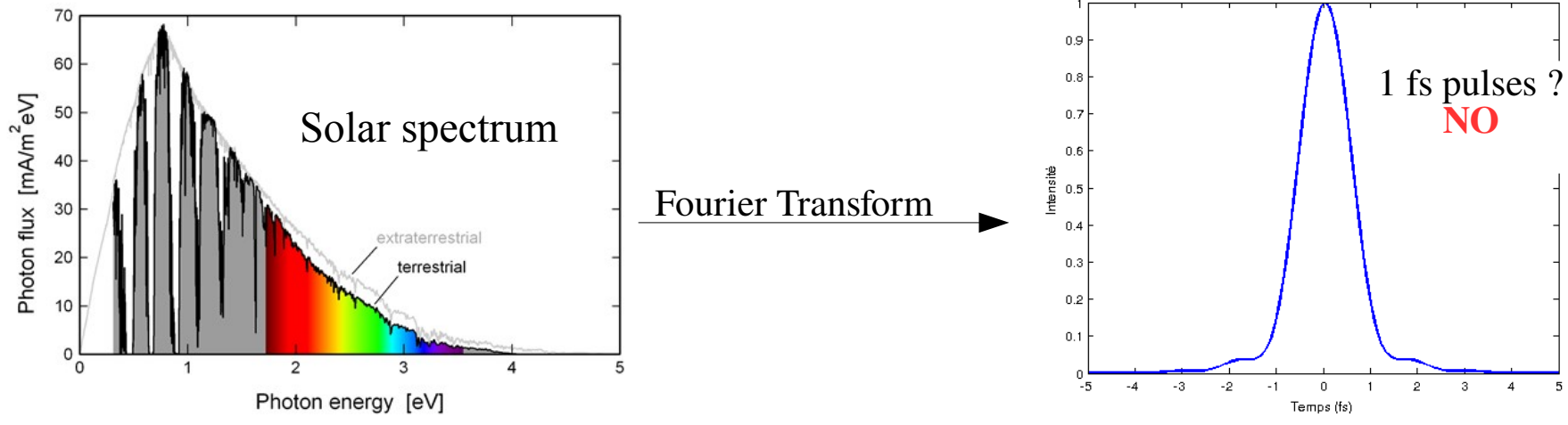
Time and spectrum

The spectral width of a light source defines its **coherence time** $\tau_c = 1/\Delta\nu$
(coherence = ability to produce interferences)

Measurement: linear (field) autocorrelation = Fourier transform spectroscopy



An ultrashort light pulse necessarily has an ultrashort coherence time, and thus a **broad spectrum**
This is a necessary, but not sufficient, condition



The temporal profile is obtained by FT the complex spectrum

Definitions :

$$E(t) = |E(t)| e^{i\varphi(t)}$$

$$\mathcal{F} [E(\omega)] = \int E(\omega) e^{-i\omega t} d\omega = E(t)$$

$$E(\omega) = |E(\omega)| e^{i\varphi(\omega)}$$

Real Gaussian function $I(t) = I_0 \exp\left(-\frac{4 \ln(2) t^2}{\Delta t^2}\right)$

Δt Full Width at Half Maximum

$$I(\omega) = |\mathcal{F} [E(t)]|^2 \propto I_0 \exp\left(-\frac{4 \ln(2) \omega^2}{\Delta \omega^2}\right) \quad \Delta \omega \quad \text{FWHM}$$

$$\Delta \omega \Delta t = 4 \ln(2) \approx 2.77$$

Fourier transform

Definitions :

$$E(t) = |E(t)| e^{i\varphi(t)}$$

$$\mathcal{F} [E(\omega)] = \int E(\omega) e^{-i\omega t} d\omega = E(t)$$

$$E(\omega) = |E(\omega)| e^{i\varphi(\omega)}$$

Real Gaussian function

$$I(t) = I_0 \exp\left(-\frac{4 \ln(2) t^2}{\Delta t^2}\right)$$

Δt Full Width at Half Maximum

$$I(\omega) = |\mathcal{F} [E(t)]|^2 \propto I_0 \exp\left(-\frac{4 \ln(2) \omega^2}{\Delta \omega^2}\right)$$

$\Delta \omega$ FWHM

$$\Delta \omega \Delta t = 4 \ln(2) \approx 2.77$$

Effect of a linear phase

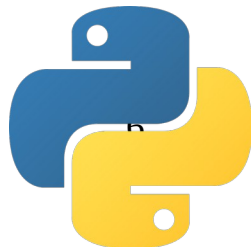
$$\mathcal{F} [E(\omega) e^{i\omega t_0}] = \mathcal{F} [E(\omega)] * \mathcal{F} [e^{i\omega t_0}] = E(t) \delta_{t_0} = E(t - t_0)$$

→ temporal shift

Group delay

$$\tau_g(\omega) = \partial \varphi(\omega) / \partial \omega$$

Linear spectral phase $\omega \tau_0 \rightarrow$ group delay $\tau_g = \tau_0$



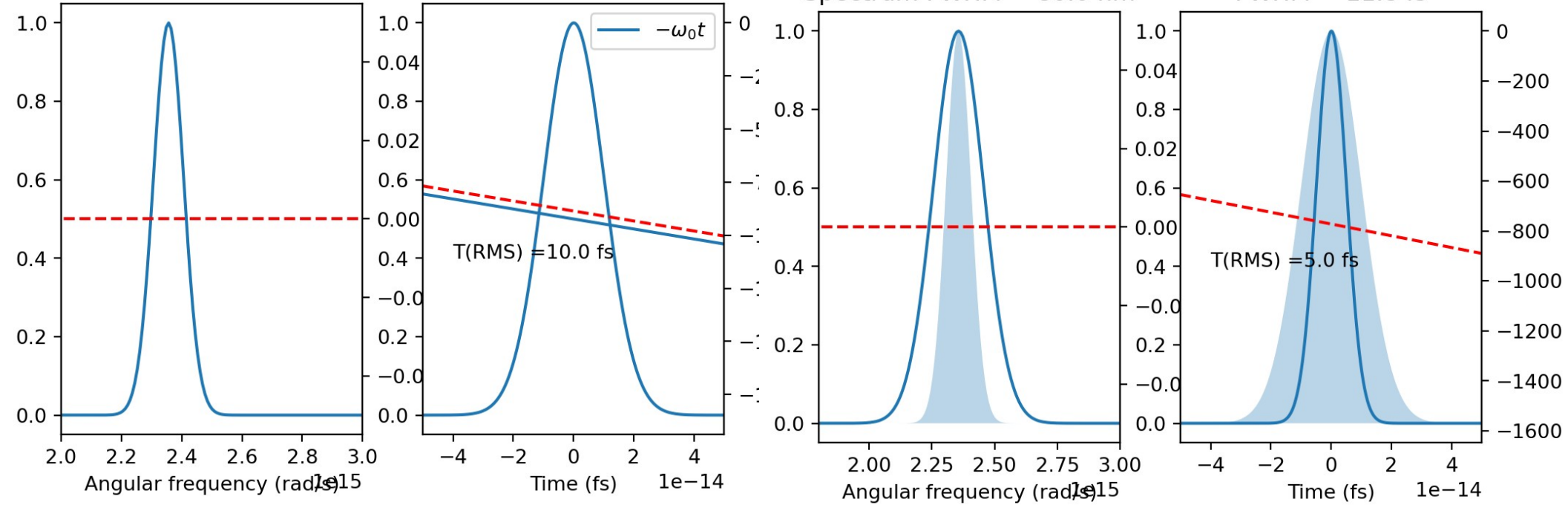
Fourier transform

Spectrum FWHM = 40.0 nm

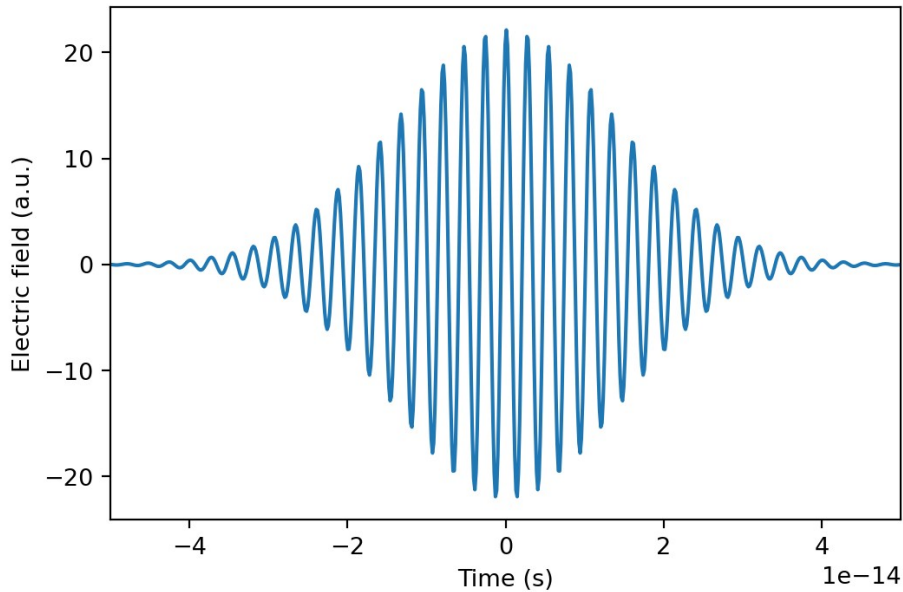
FWHM = 23.4 fs

Spectrum FWHM = 80.0 nm

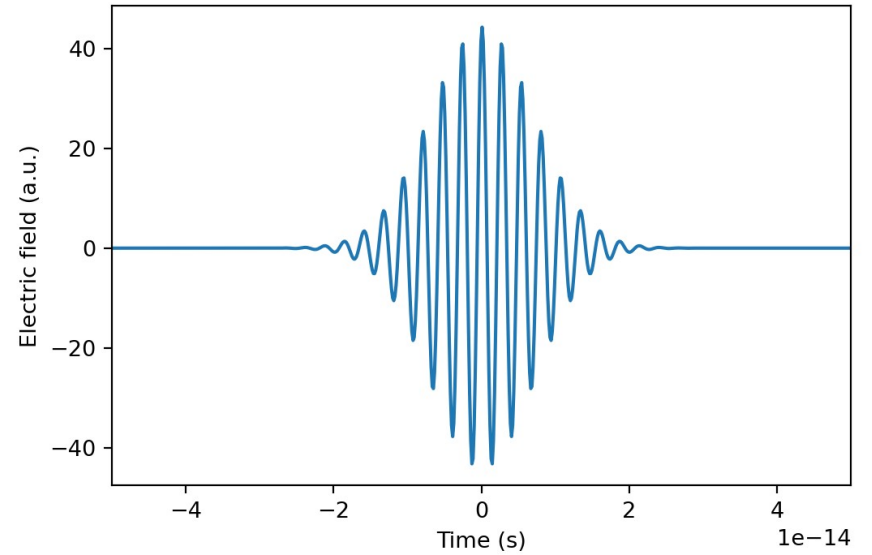
FWHM = 11.8 fs



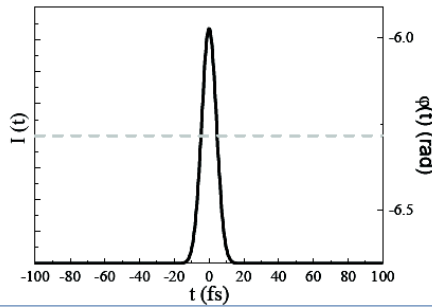
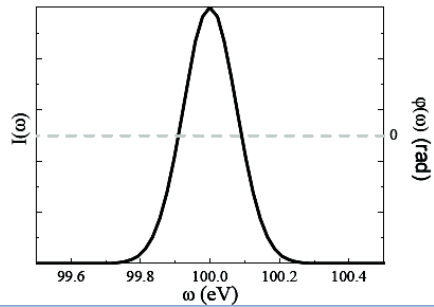
Electric field



Electric field

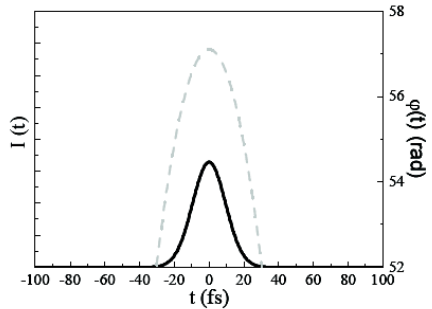
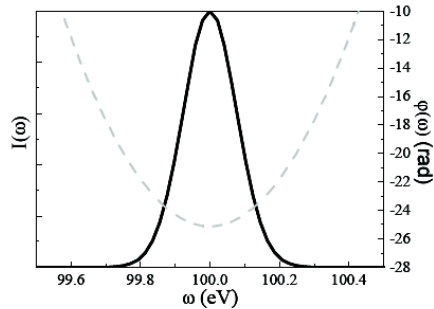


Fourier transform of a Gaussian



Constant spectral phase
Shortest pulse
= **Fourier Limit**

$$\Delta\omega\Delta t = 4 \ln(2) \approx 2.77$$

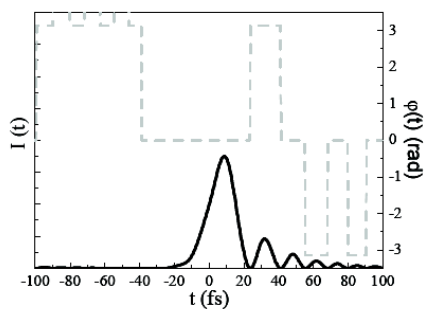
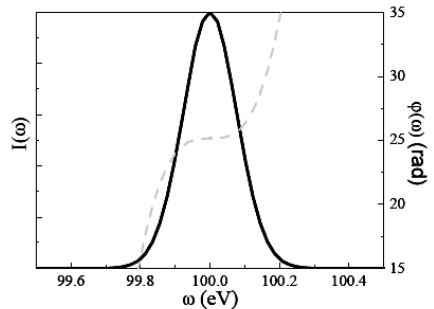


Quadratic spectral phase :

Gaussian pulse, but stretched
The group delay varies linearly with frequency

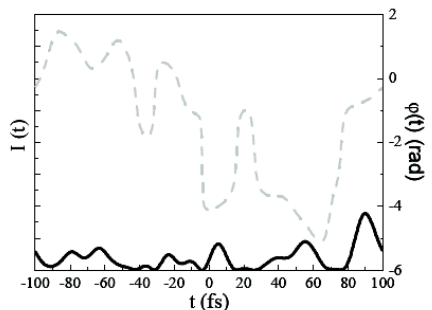
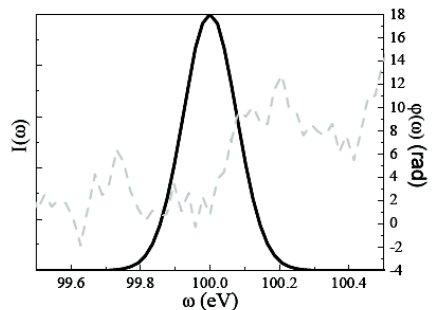
$$\tau_g(\omega) = \partial\varphi(\omega)/\partial\omega$$

(and the instantaneous frequency varies linearly in time)
→ **linear chirp**



Cubic spectral phase :

Non gaussian pulse, asymmetric, with pre or post pulses
(temporal interference of the red and blue wings of the spectrum)



Random spectral phase :

No ultrashort pulse

Time-frequency representations

A Fourier-limited Gaussian narrowband pulse and a chirped broadband Gaussian pulse can have the same intensity profile.

The temporal/spectral phase may not be the most intuitive representation

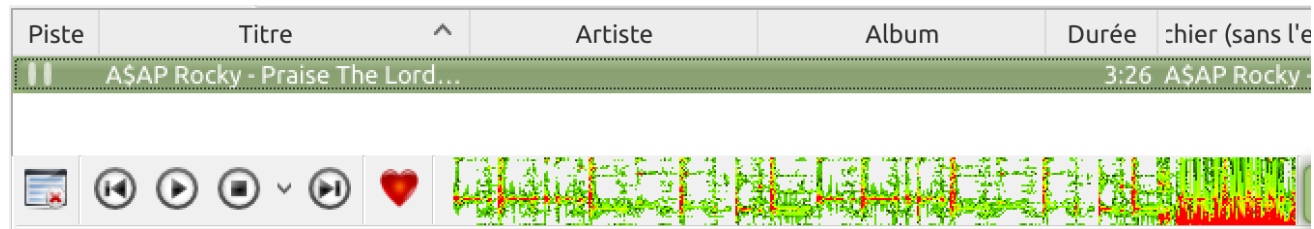
→ Time frequency distributions: spectrogram

Goal: resolve temporally the evolution of the spectrum of a signal

→ Principle of the music score

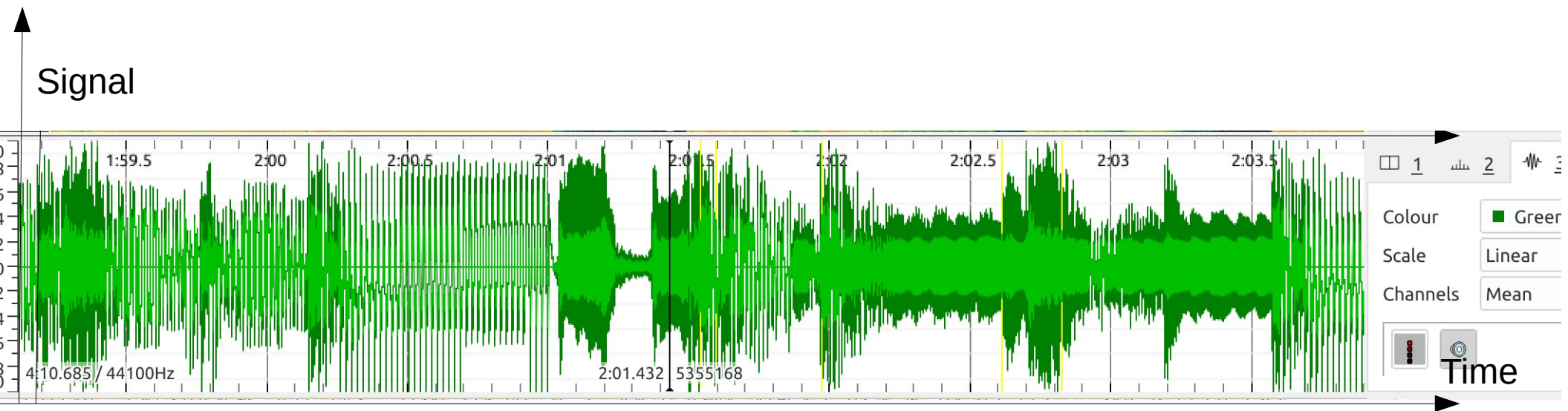


Time-frequency representations are common in acoustics



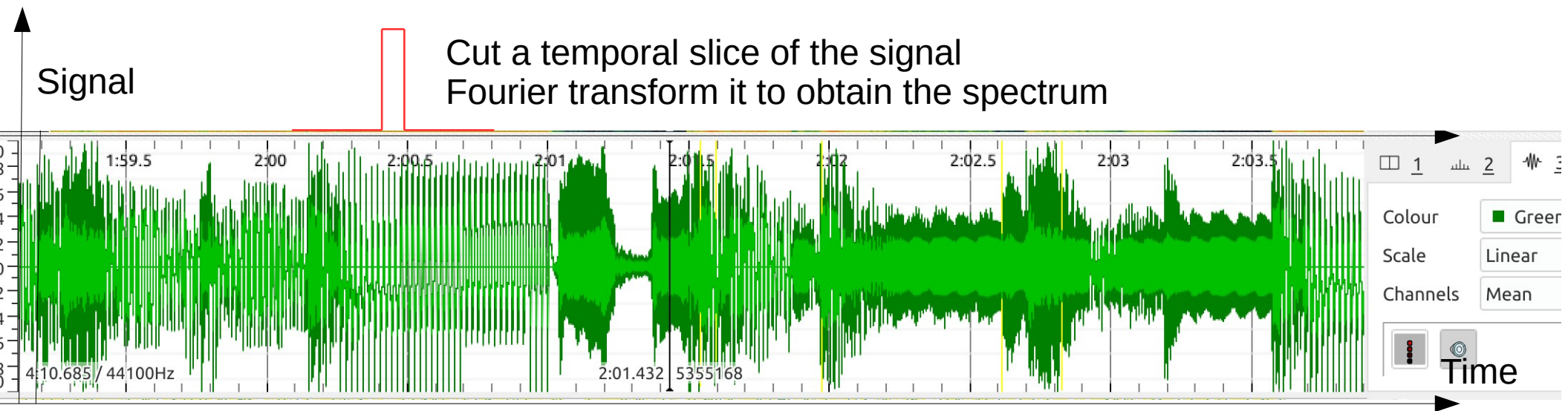
Time-frequency representations

A sonogram using Sonic Visualiser
Track: Ultra Heat Treated, by Slugabed



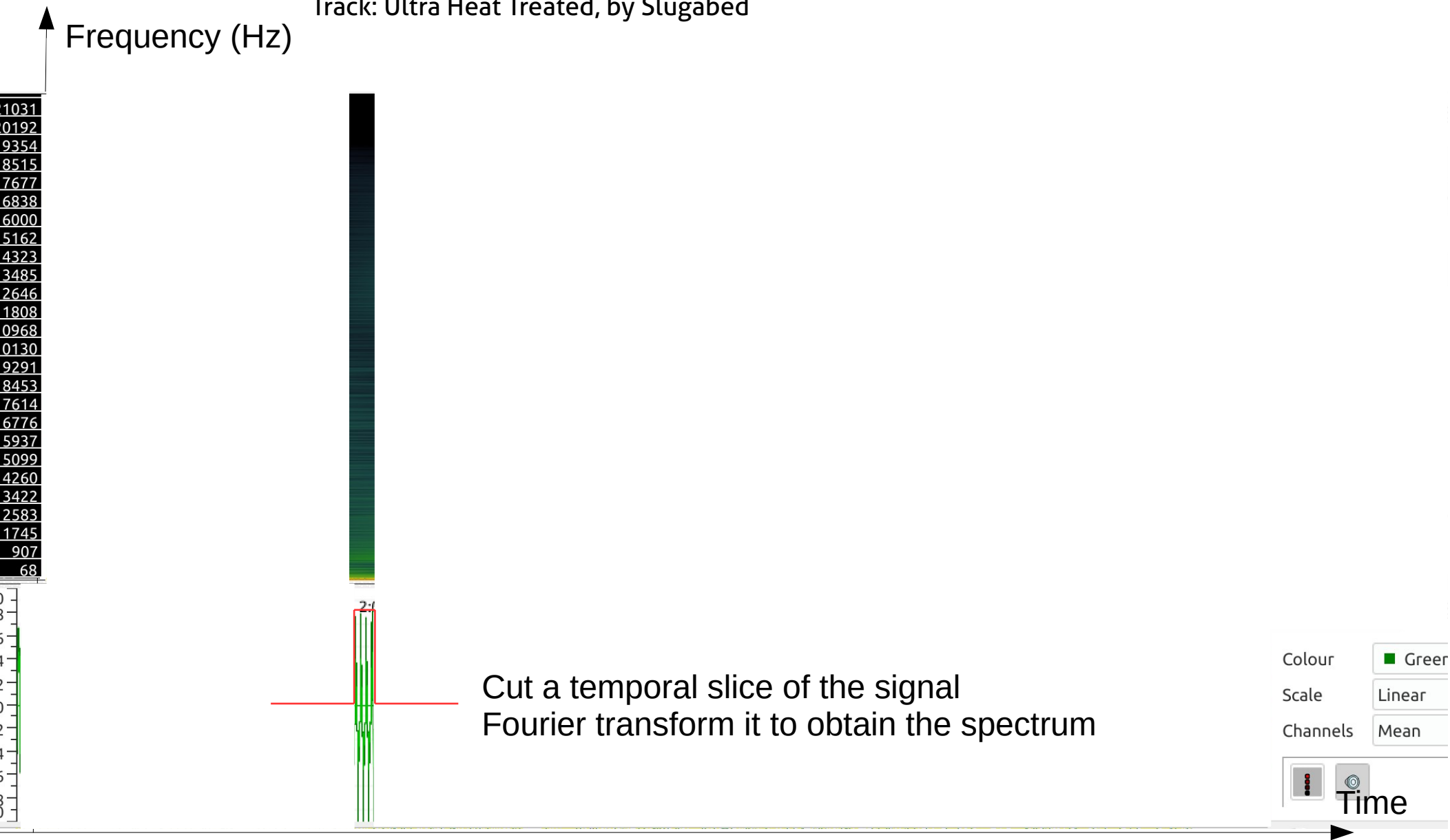
Time-frequency representations

A sonogram using Sonic Visualiser
Track: Ultra Heat Treated, by Slugabed



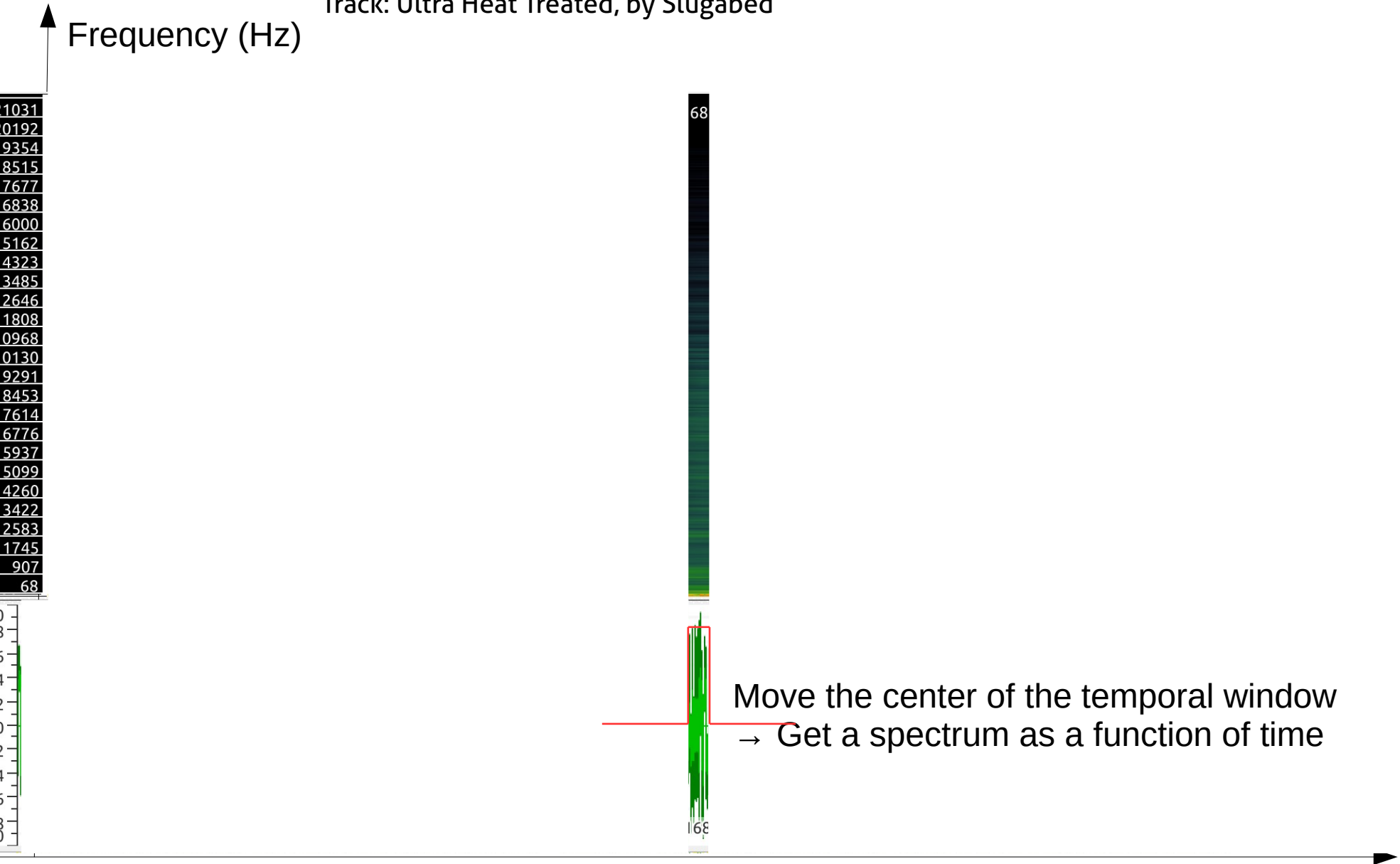
Time-frequency representations

A sonogram using Sonic Visualiser
Track: Ultra Heat Treated, by Slugabed



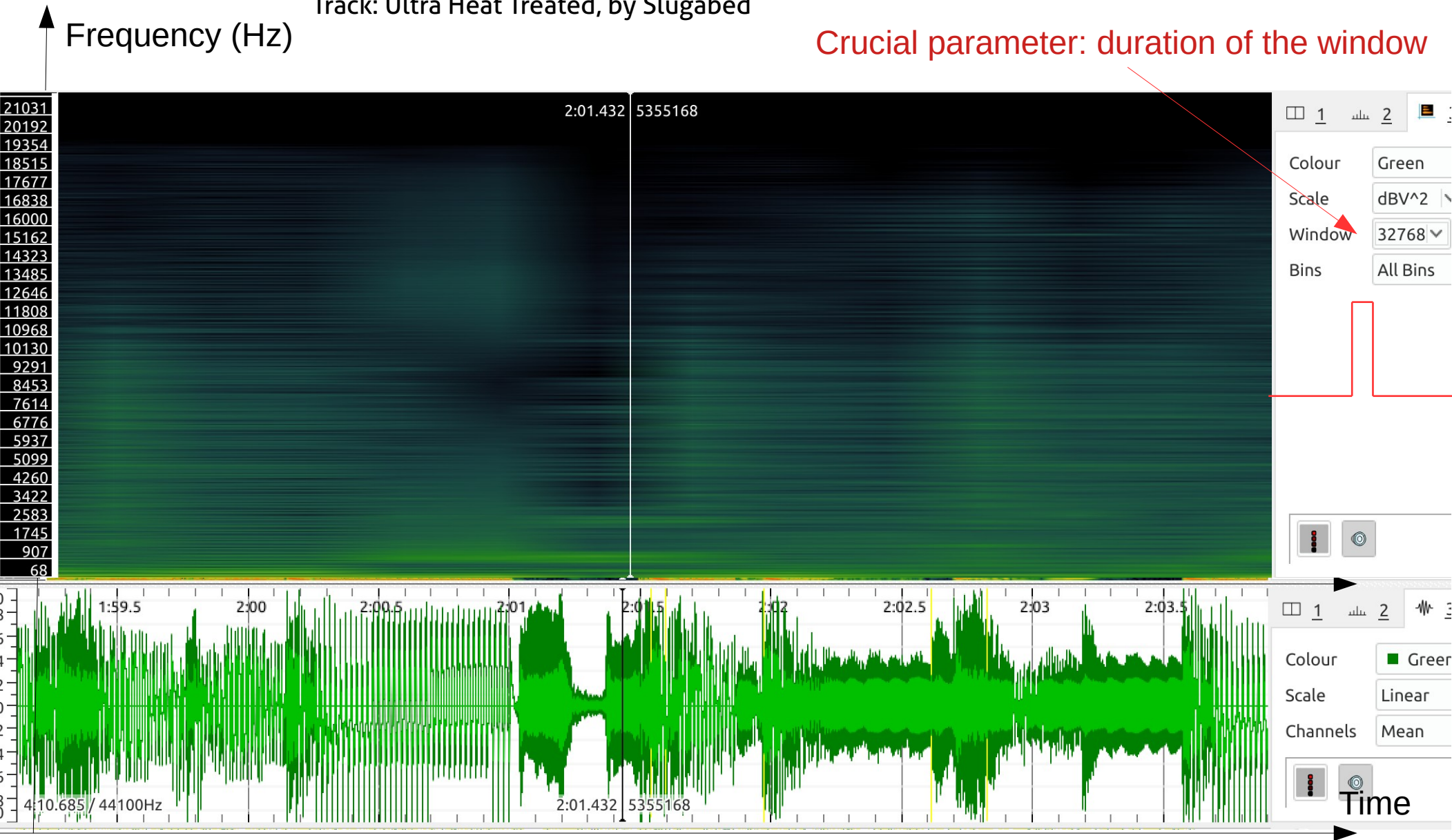
Time-frequency representations

A sonogram using Sonic Visualiser
Track: Ultra Heat Treated, by Slugabed



Time-frequency representations

A sonogram using Sonic Visualiser
Track: Ultra Heat Treated, by Slugabed



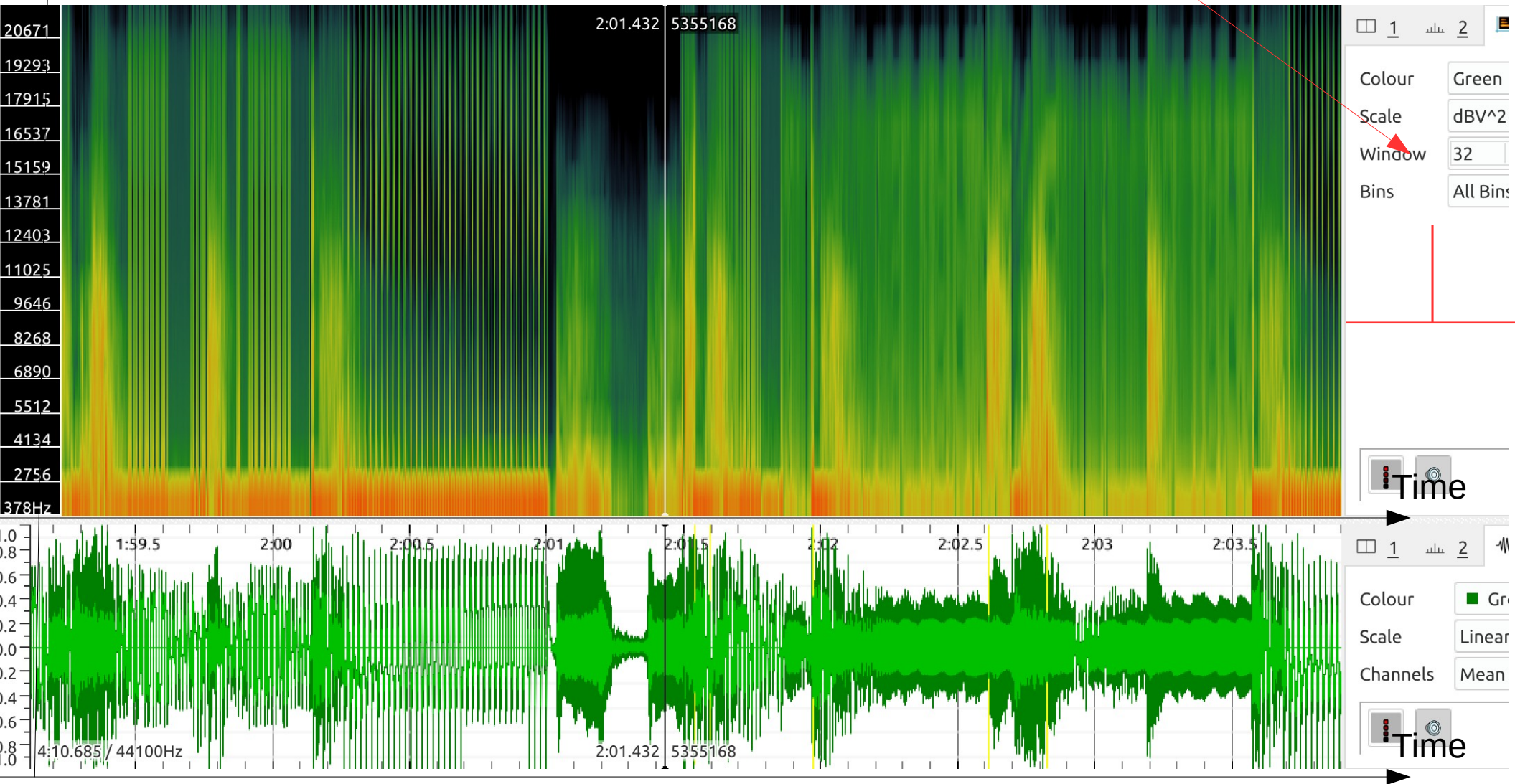
Long temporal window → Good spectral resolution but bad temporal resolution

Time-frequency representations

A sonogram using Sonic Visualiser
Track: Ultra Heat Treated, by Slugabed

↑
Frequency (Hz)

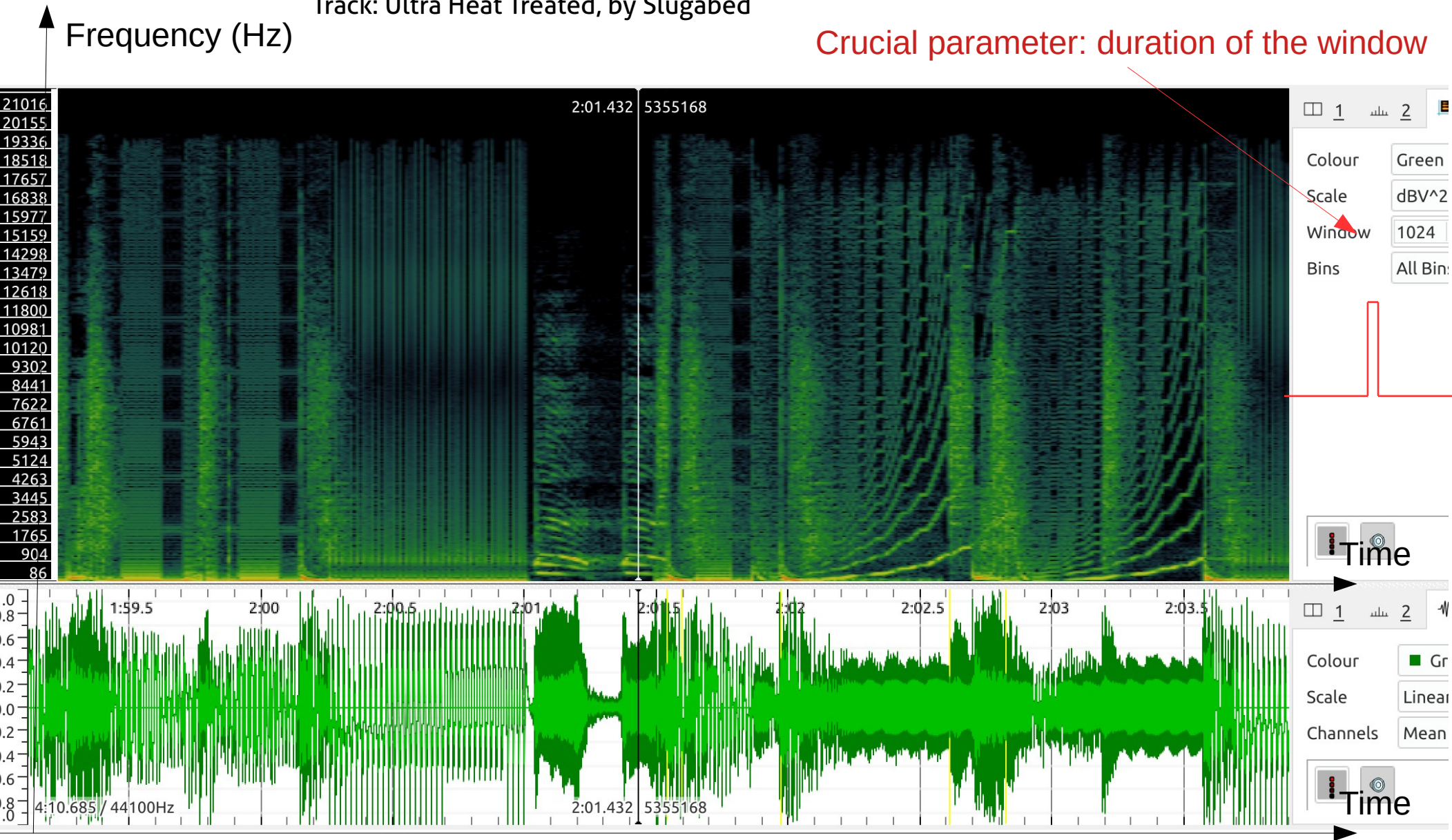
Crucial parameter: duration of the window



Long temporal window → Good spectral resolution but bad temporal resolution
Short temporal window → Good temporal resolution but bad spectral resolution

Time-frequency representations

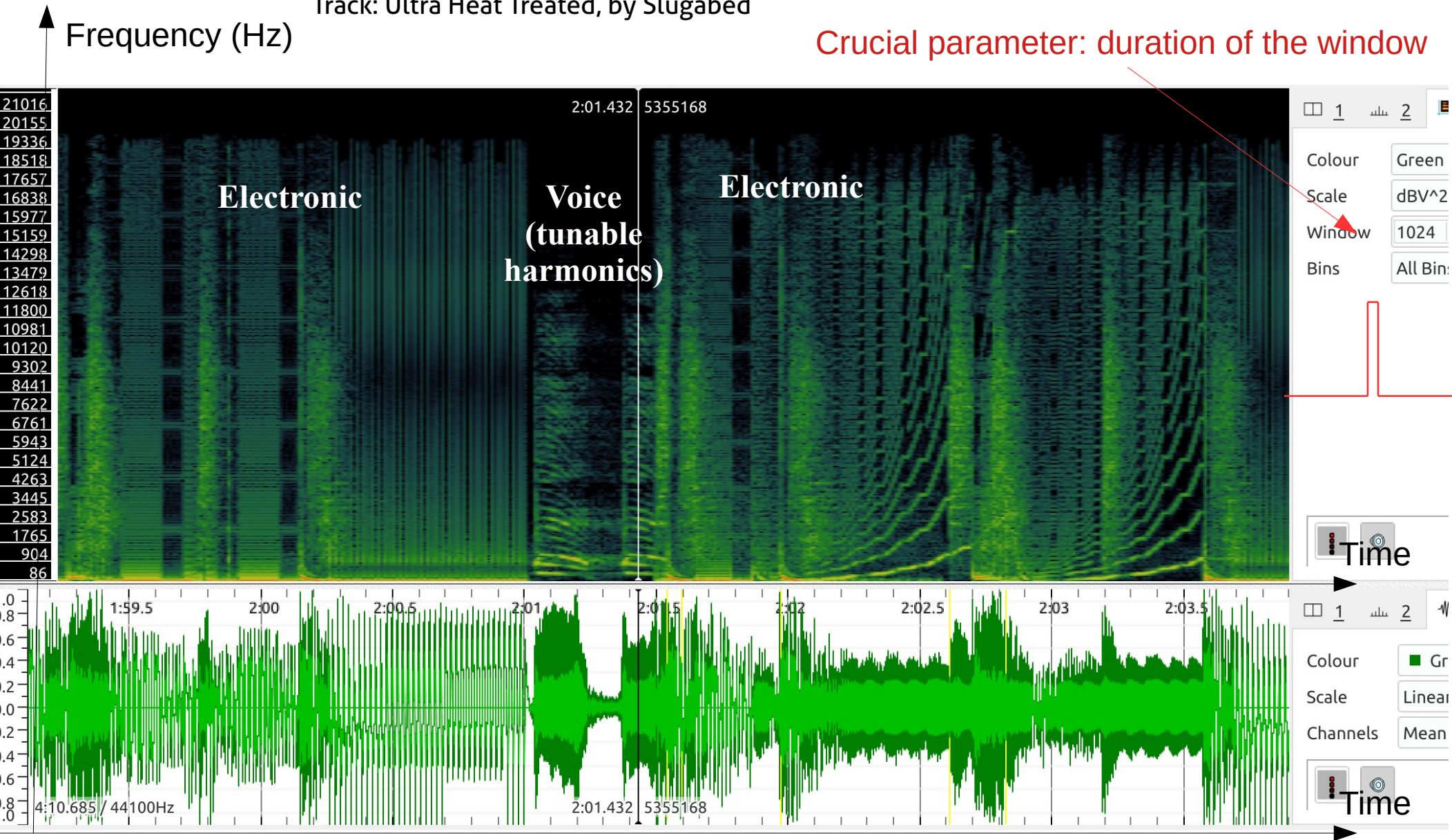
A sonogram using Sonic Visualiser
Track: Ultra Heat Treated, by Slugabed



Long temporal window → Good spectral resolution but bad temporal resolution
Short temporal window → Good temporal resolution but bad spectral resolution
Optimal window → Reveals the temporal evolution of the spectrum

Time-frequency representations

A sonogram using Sonic Visualiser
Track: Ultra Heat Treated, by Slugabed



Long temporal window → Good spectral resolution but bad temporal resolution
Short temporal window → Good temporal resolution but bad spectral resolution
Optimal window → Reveals the temporal evolution of the spectrum

Time-frequency representations of femtosecond pulses

Gabor Analysis: building a spectrogram

$$S(\omega, \tau) = \left| \int E(t)G(t - \tau)e^{i\omega t} dt \right|^2$$

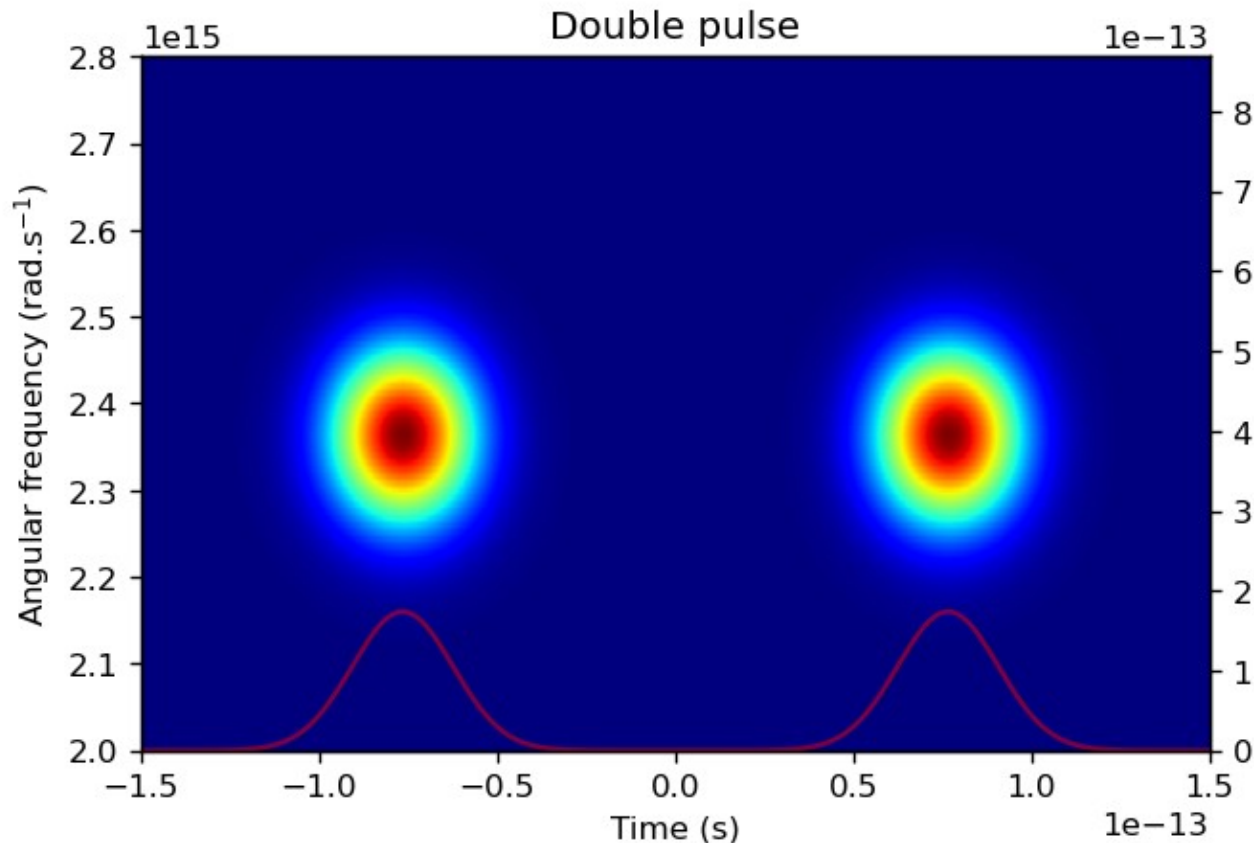
```
def gabor(t,E_t,zp,alpha):  
    def gaussian(t,alpha):  
        return 1./2*sqrt(pi*alpha)*exp(-t**2/(alpha)**2)  
    S=zeros((len(t),zp),dtype=complex)  
    for i,tau in enumerate(t):  
        S[i,:]=ifftshift(ifft(E_t*gaussian(t-tau,alpha),zp))  
    return transpose(E_w)
```

Define Gaussian gate function G

Calculate the spectrum of the gated signal

Slide the gate

Example: Spectrogram of two delayed Fourier Limited pulses



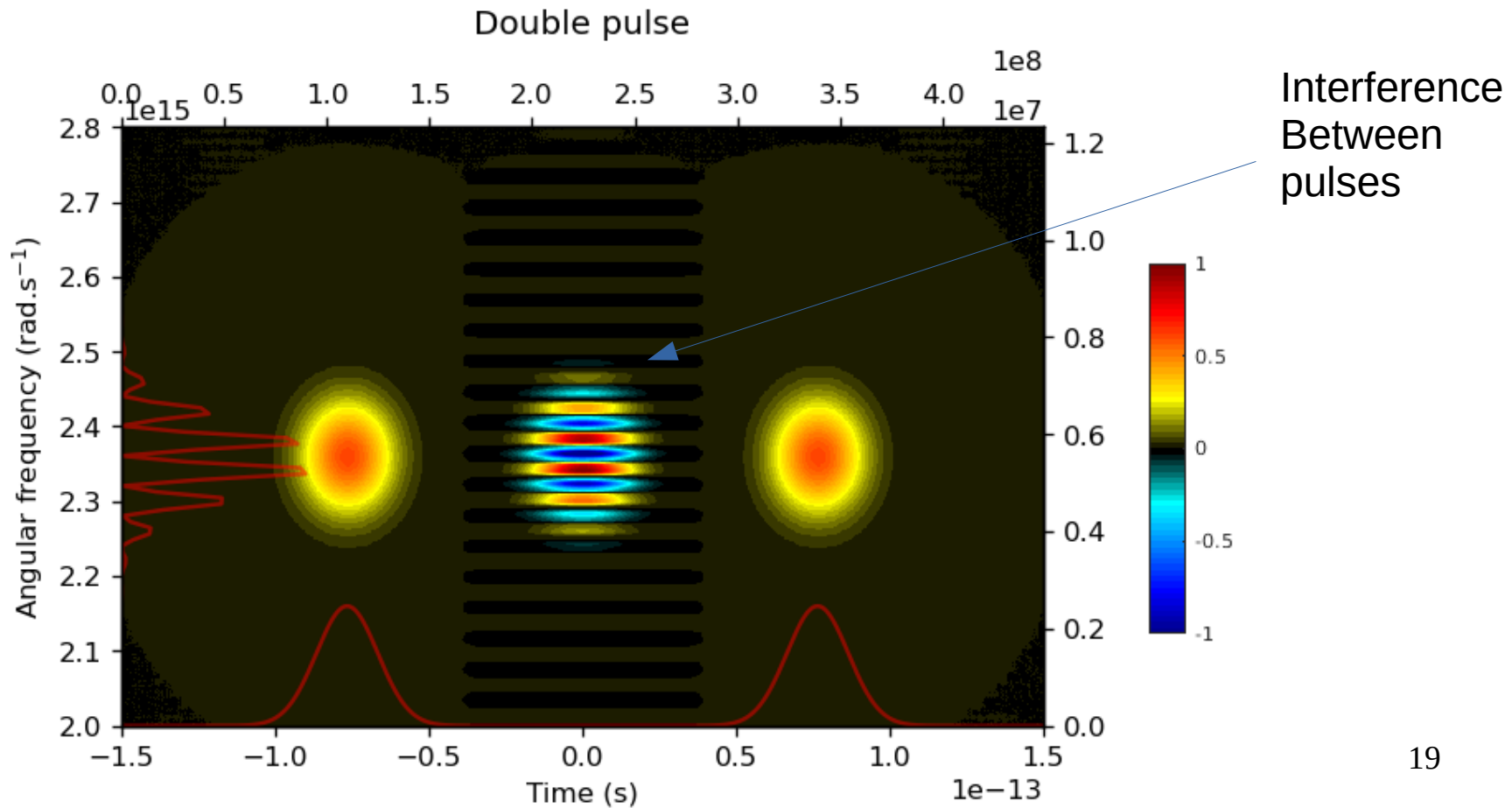
Time-frequency representations of femtosecond pulses

Wigner distribution

$$W(\omega, \tau) = \int E(t + \tau/2)E^*(t - \tau/2)e^{i\omega t} dt$$

Marginals: $I(t) = \int W(\omega, \tau) d\omega$

$$I(\omega) = \int W(\omega, \tau) d\tau$$





Time-frequency representations of femtosecond pulses

IOP PUBLISHING

JOURNAL OF PHYSICS B: ATOMIC, MOLECULAR AND OPTICAL PHYSICS

J. Phys. B: At. Mol. Opt. Phys. 43 (2010) 103001 (34pp)

doi:10.1088/0953-4075/43/10/103001

PhD TUTORIAL

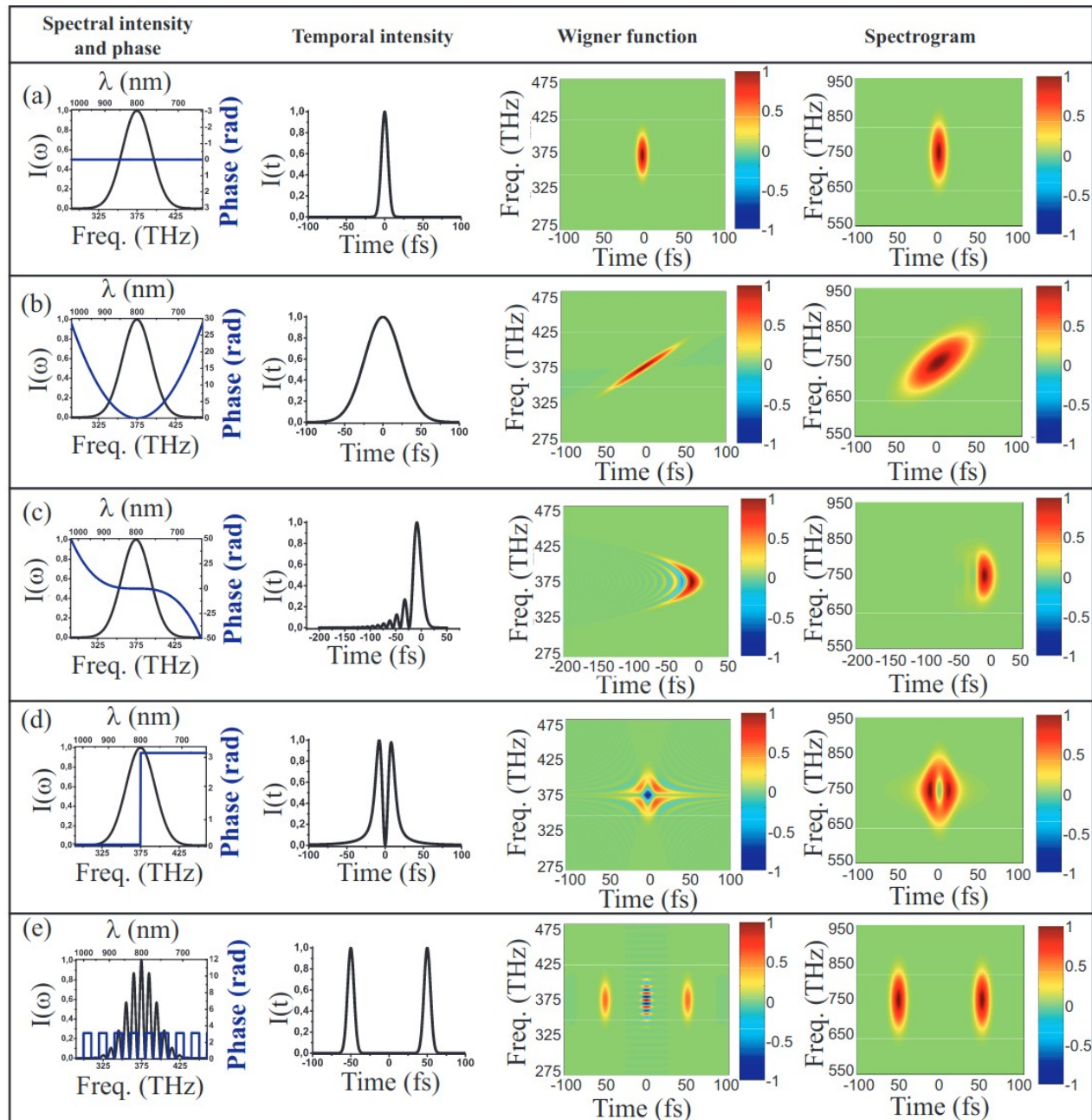
A newcomer's guide to ultrashort pulse shaping and characterization

Antoine Monmayrant^{1,2}, Sébastien Weber³ and Béatrice Chatel³

¹ CNRS-LAAS, 7 avenue du colonel Roche, F-31077 Toulouse, France

² Université de Toulouse, UPS, INSA, INP, ISAE : LAAS, F-31077 Toulouse, France

³ CNRS-Université de Toulouse; UPS, Laboratoire Collisions, Agrégats Réactivité, IRSAMC, F-31062 Toulouse, France.



Introduction: time-frequency travel

Keeping ultrashort pulses ultrashort

Self-phase modulation – the enemy within

Mirror mirror

Producing circularly polarized pulses – a perfect circle

Focus

A typical femtosecond experimental setup

Aurore: A platform for ultrafast sciences

Cite as: Rev. Sci. Instrum. 91, 105104 (2020); <https://doi.org/10.1063/5.0012485>
Submitted: 01 May 2020 . Accepted: 16 September 2020 . Published Online: 06 October 2020

N. Fedorov, S. Beaulieu, A. Belsky, V. Blanchet, R. Bouillaud, M. De Anda Villa, A. Filippov, C. Fourment, J. Gaudin, R. E. Grisenti, E. Lamour, A. Lévy, S. Macé, Y. Mairesse, P. Martin, P. Martinez, P. Noé, I. Papagiannouli, M. Patanen, S. Petit, D. Vernhet, K. Veyrinas, and D. Descamps

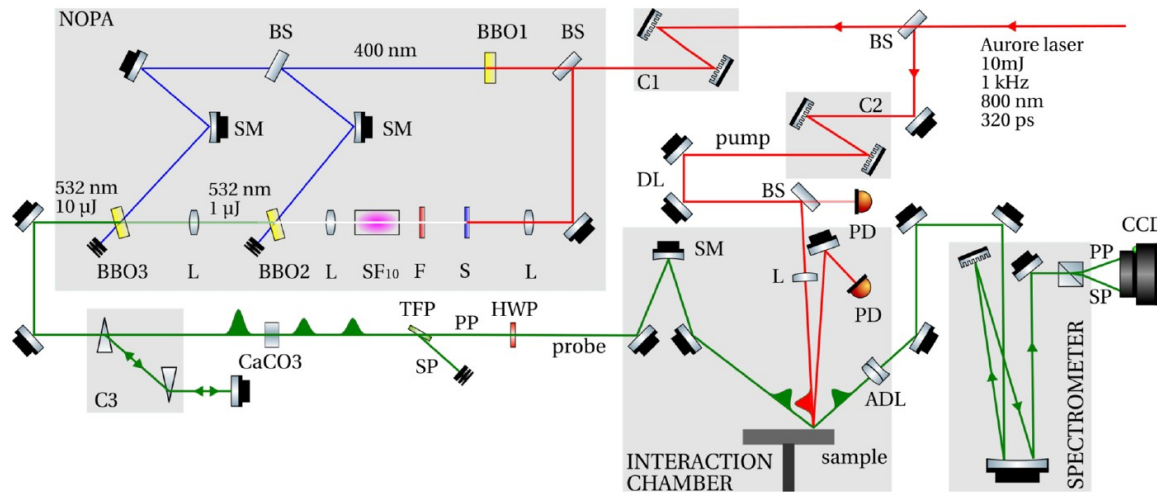


FIG. 9. FDI setup including the NOPA (BS: beam splitter, BBO: beta-barium borate crystal, S: sapphire plate, F: 800 nm notch-filter, SM: spherical mirror, L: lens, SF₁₀: heavy-flint glass, CaCO₃: calcite crystal, TFP: thin film polarizer, PP: P polarized beam, SP: S polarized beam, C1, C2: double pass grating compressor, C3: prism compressor, PD: photodiode, ADL: achromatic doublet lens, DL: delay line, and HWP: zero order half-wave plate).

Propagation in various media (air, glass...)

Reflections on mirrors

Polarization manipulation

Focusing by lenses, mirrors

Entrance windows to vacuum chambers

→ All of this can bring trouble, in particular stretch your pulses

This is an issue if:

- you need time resolution
- you need high intensity to drive extreme processes
- you need high intensity for multiphoton microscopy
- you simply want ultrashort pulses to remain ultrashort because it's so satisfying (and you paid for that).

Dispersion

RefractiveIndex.INFO
Refractive index database

about

ENHANCED BY Google

Shelf

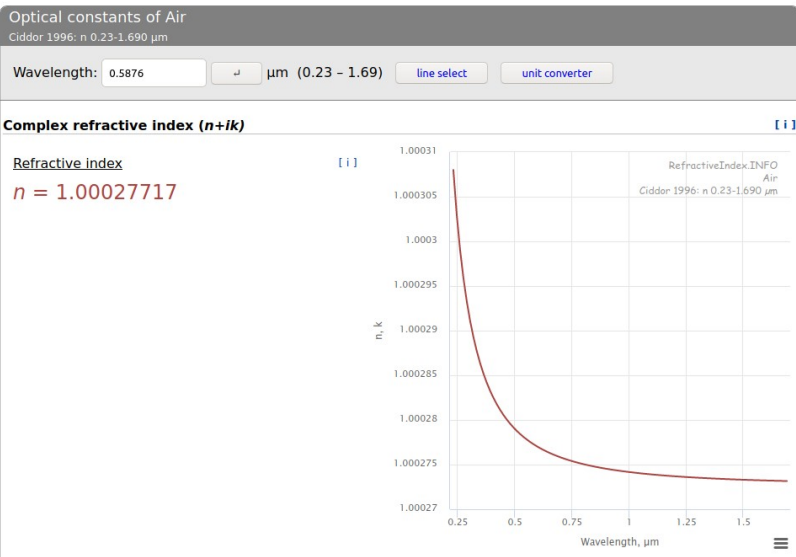
- MAIN - simple inorganic materials
- ORGANIC - organic materials
- GLASS - glasses
- OTHER - miscellaneous materials
- 3D - selected data for 3D artists

Book

Air

Page

Ciddor 1996: n 0.23-1.690 μm



Dispersion \rightarrow group velocity dispersion
The different frequency components travel at different speeds
Effect on fs pulse?

\rightarrow Get the dispersion formula $n(\omega)$
and calculate the accumulated spectral phase :

$$\varphi(\omega) = n(\omega)l\omega/c$$

over propagation distance l

Derivative of the spectral phase = group delay

Linear spectral phase: constant group delay

Quadratic spectral phase: group delay dispersion (GDD, fs^2)

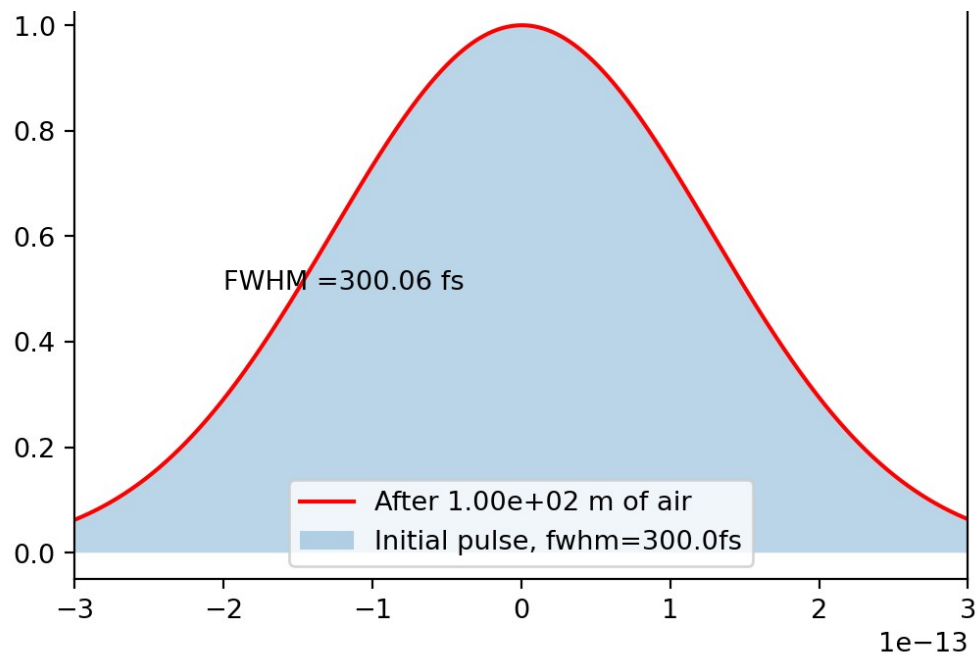
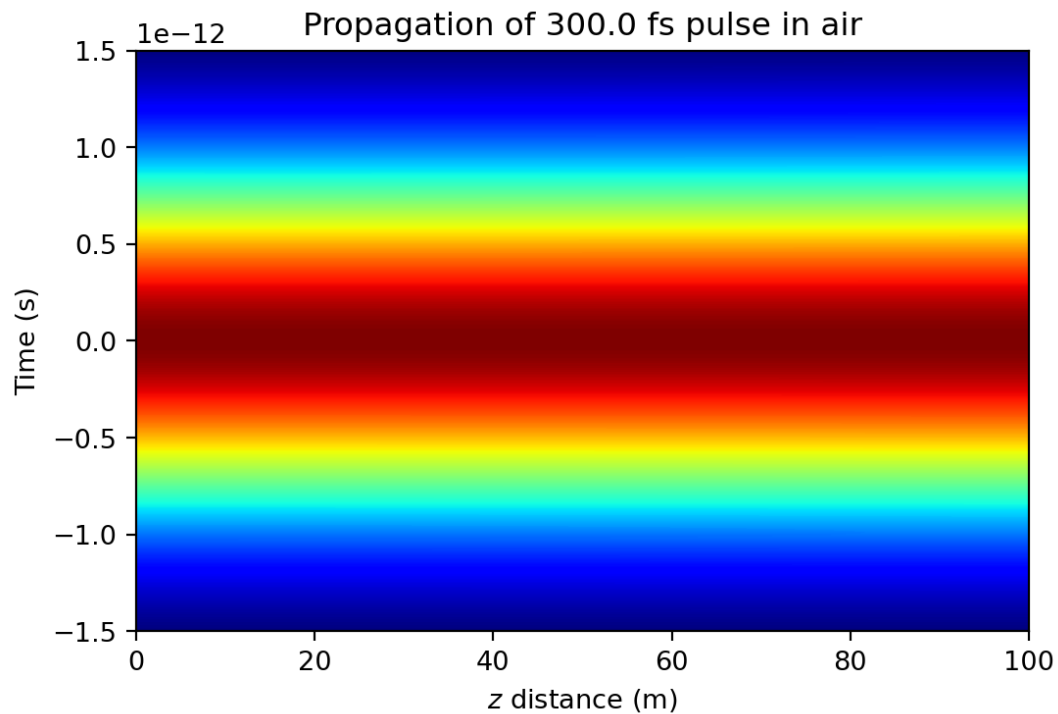
$$GDD = \frac{d^2\varphi}{d\omega}$$



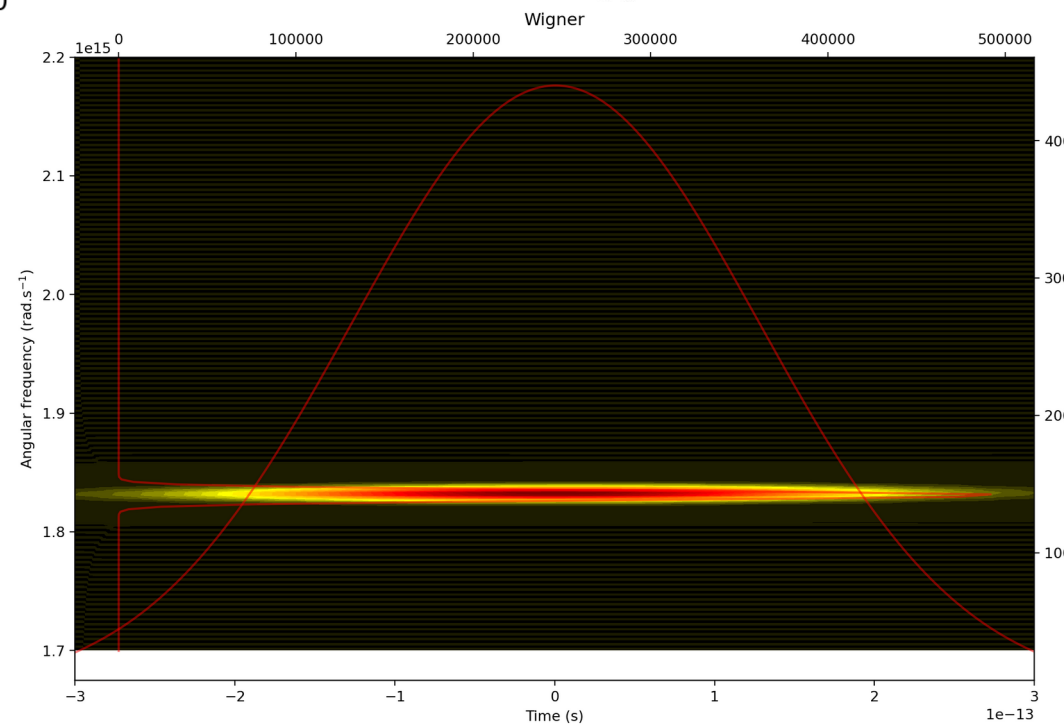
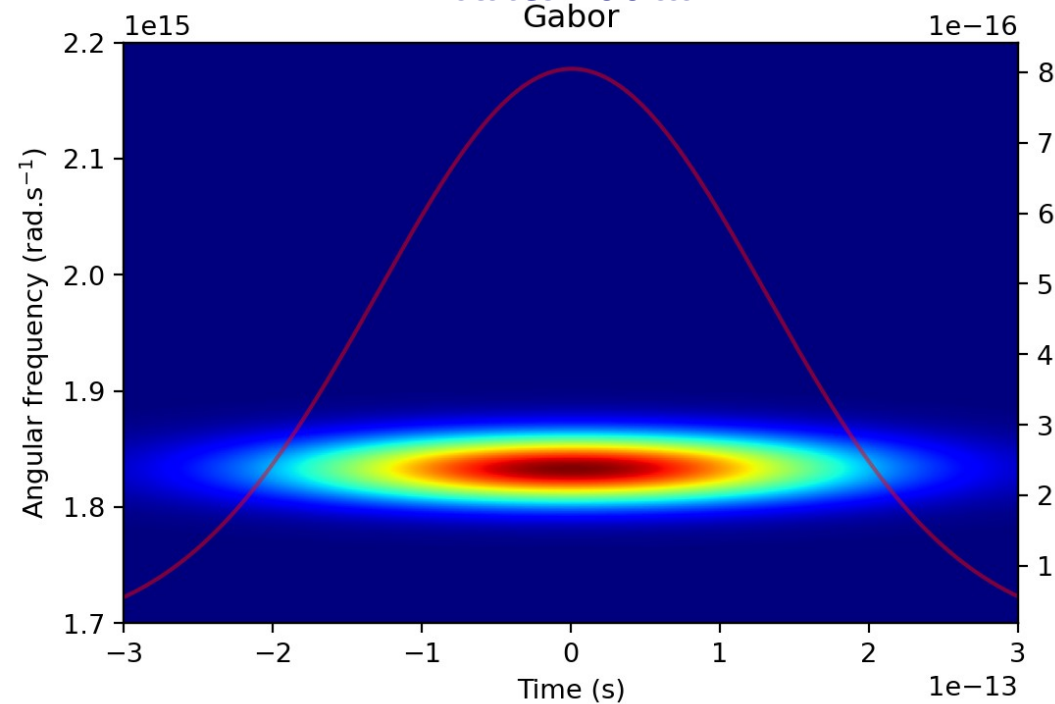
$$E_{\text{in}}(t) \rightarrow E_{\text{in}}(\omega) \rightarrow E_{\text{out}}(\omega) = E_{\text{in}}(\omega) \exp(i\varphi(\omega)) \rightarrow E_{\text{out}}(t)$$

Propagation in air

300 fs pulse at 1030 nm from Yb amplifier

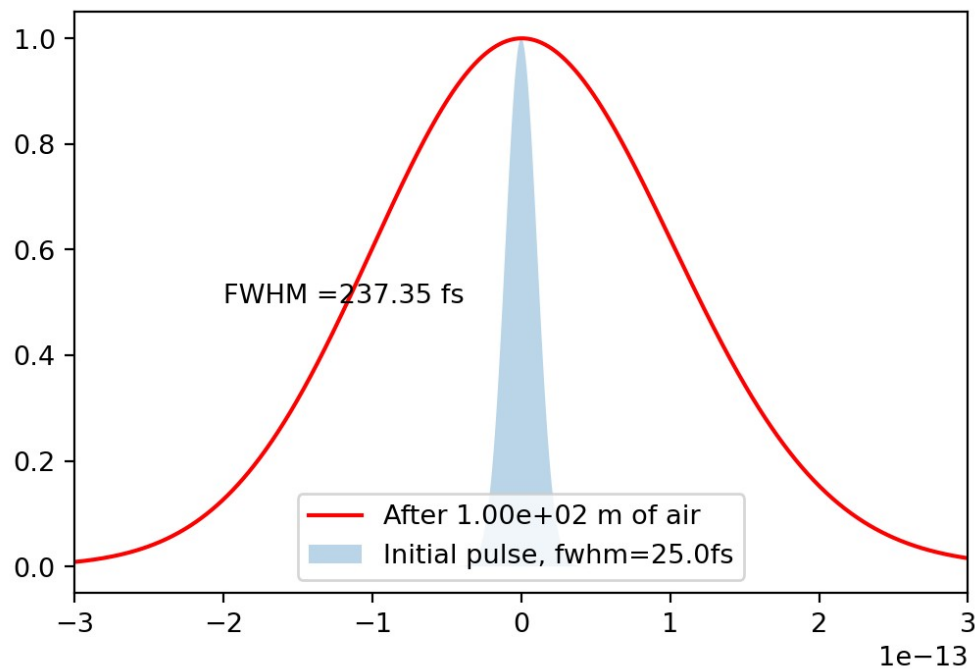
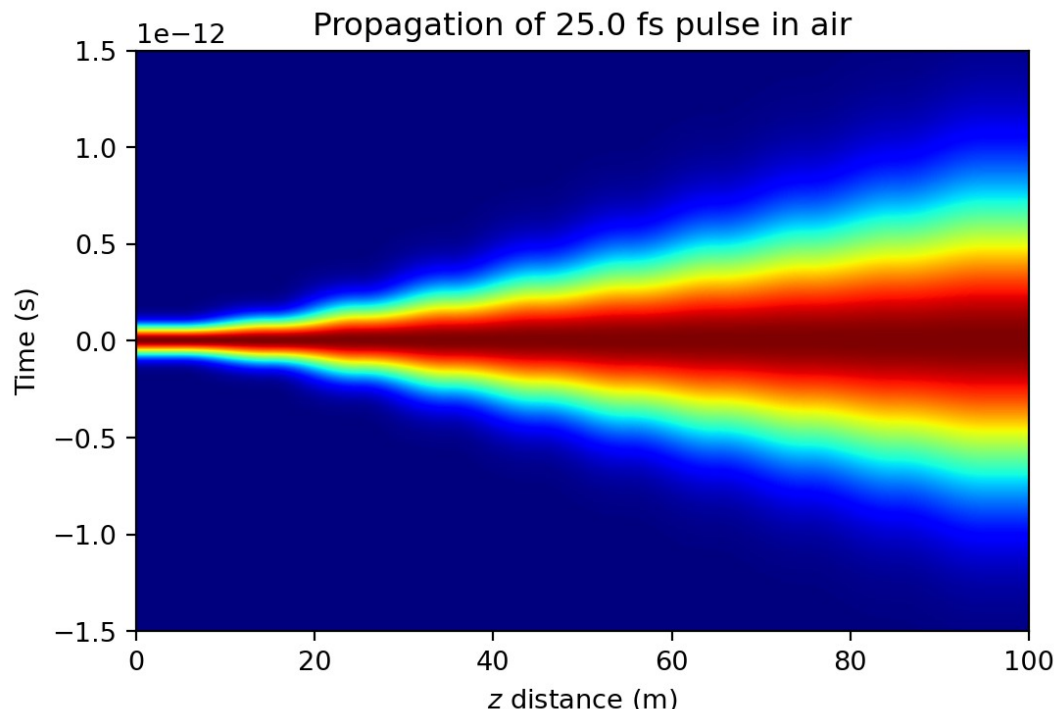


After 100 m

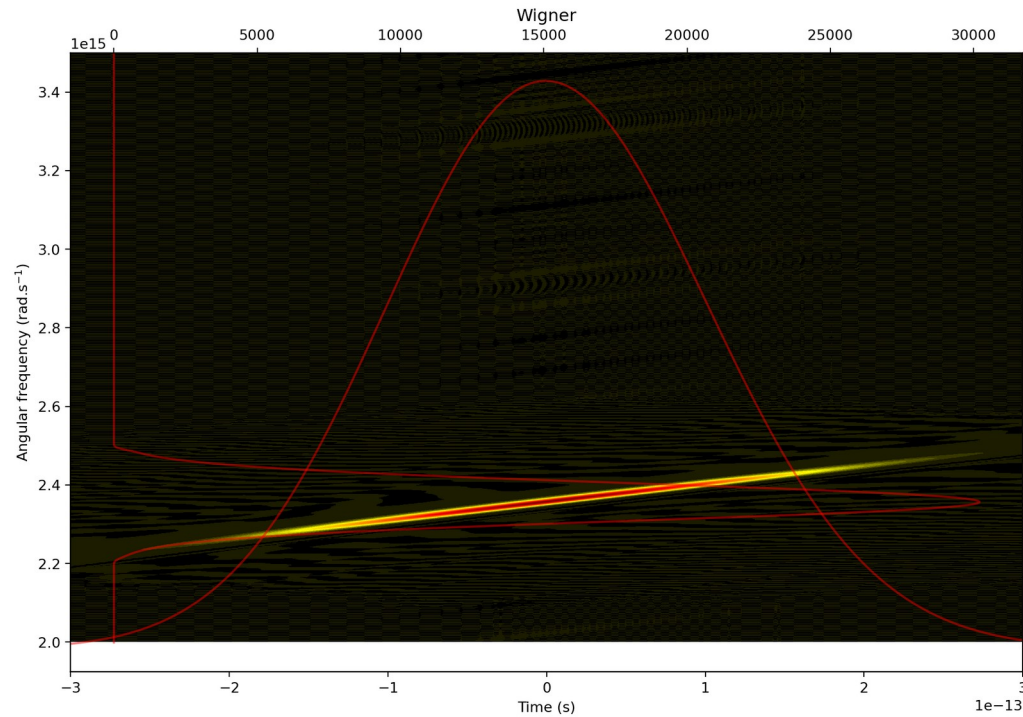
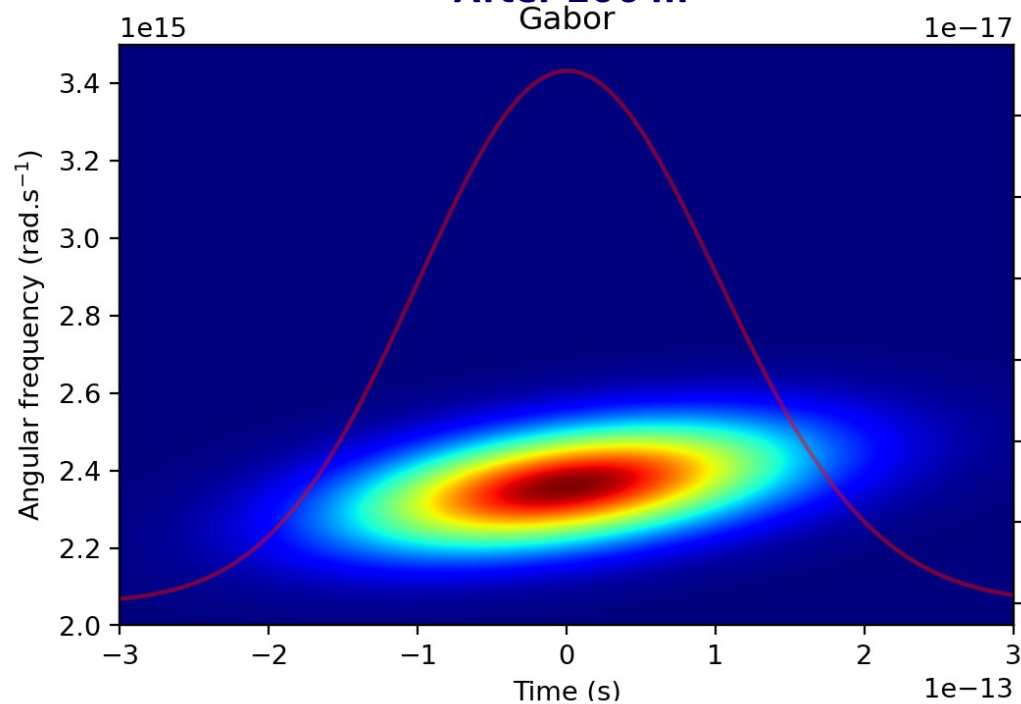


Propagation in air

25 fs pulse at 800 nm from Ti:Sa amplifier



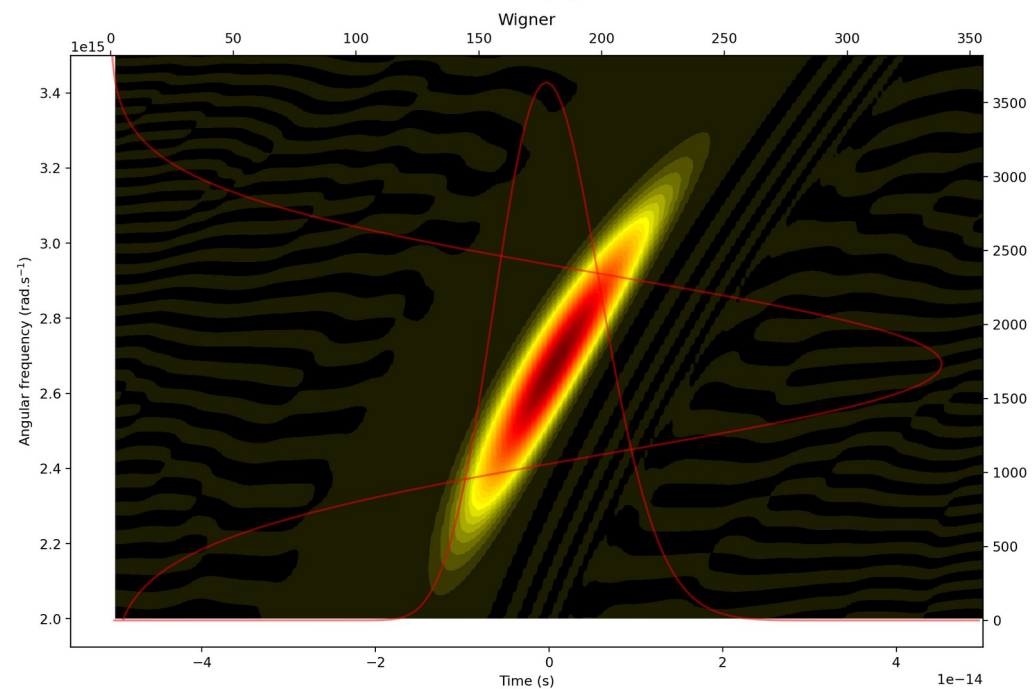
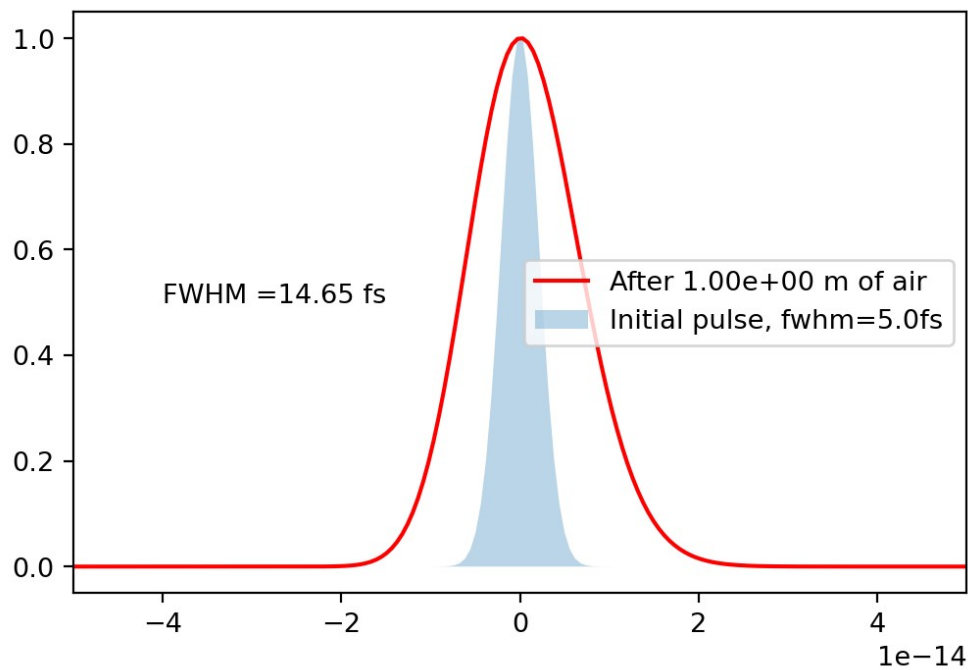
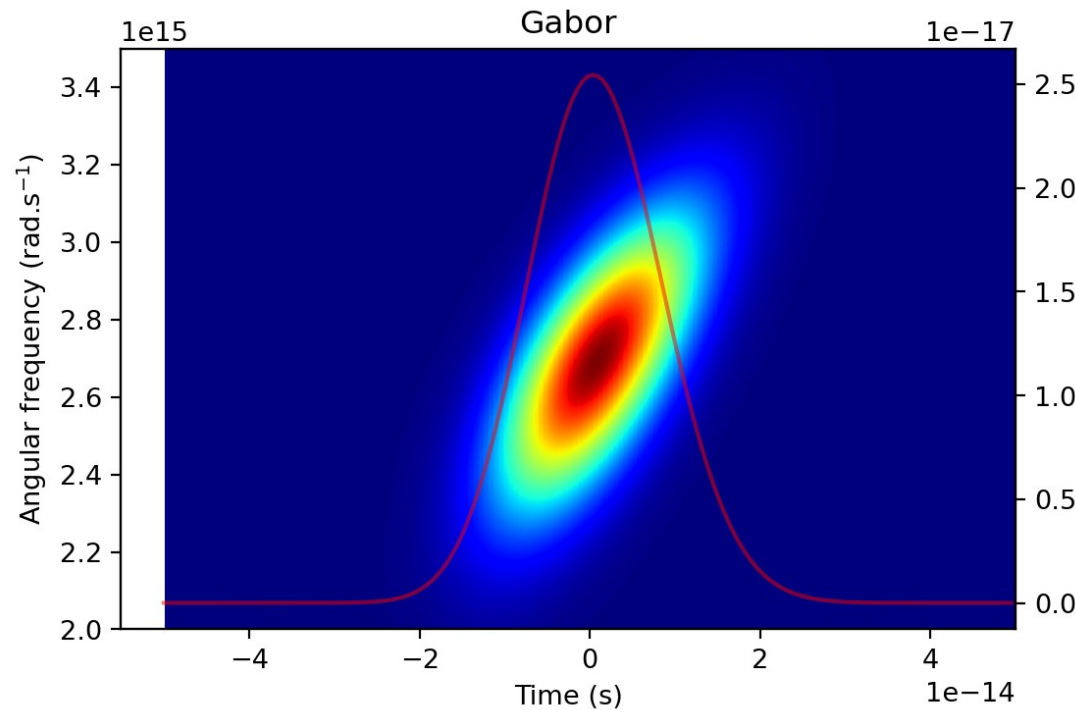
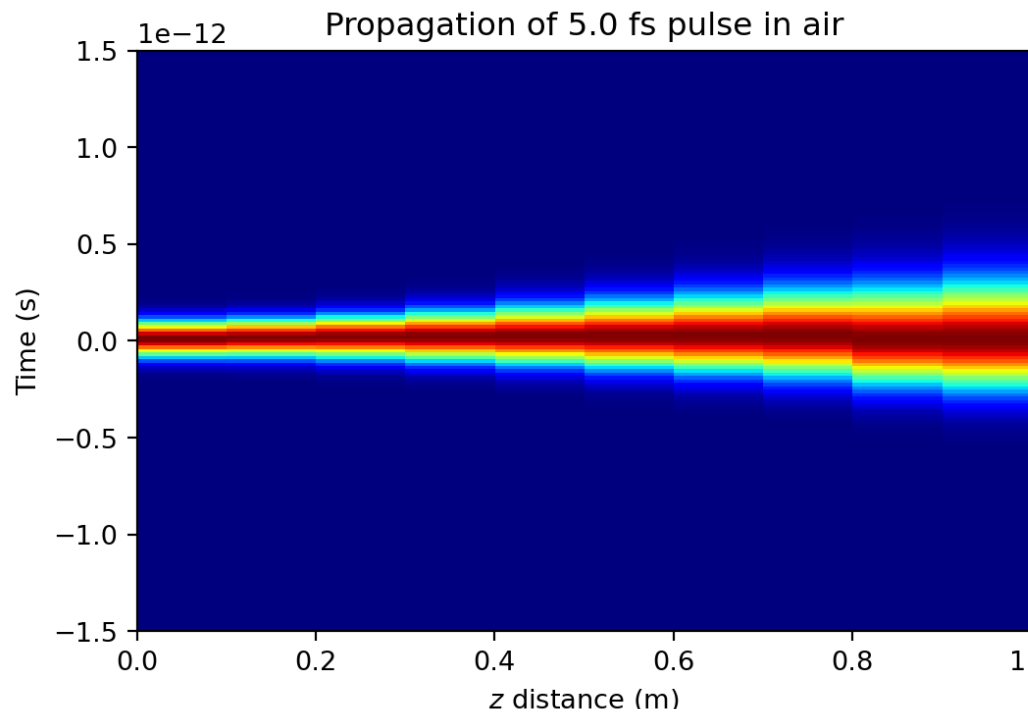
After 100 m



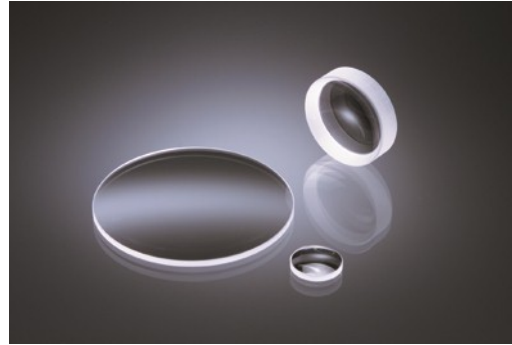
Propagation in air

5 fs pulse at 700 nm from postcompressed Ti:Sa amplifier

After 1m



Propagation in fused silica



RefractiveIndex.INFO
Refractive index database

[about]

ENHANCED BY Google



Shelf

MAIN - simple inorganic materials
ORGANIC - organic materials
GLASS - glasses
OTHER - miscellaneous materials
3D - selected data for 3D artists

Book

Fused silica (fused quartz) ▼

Page

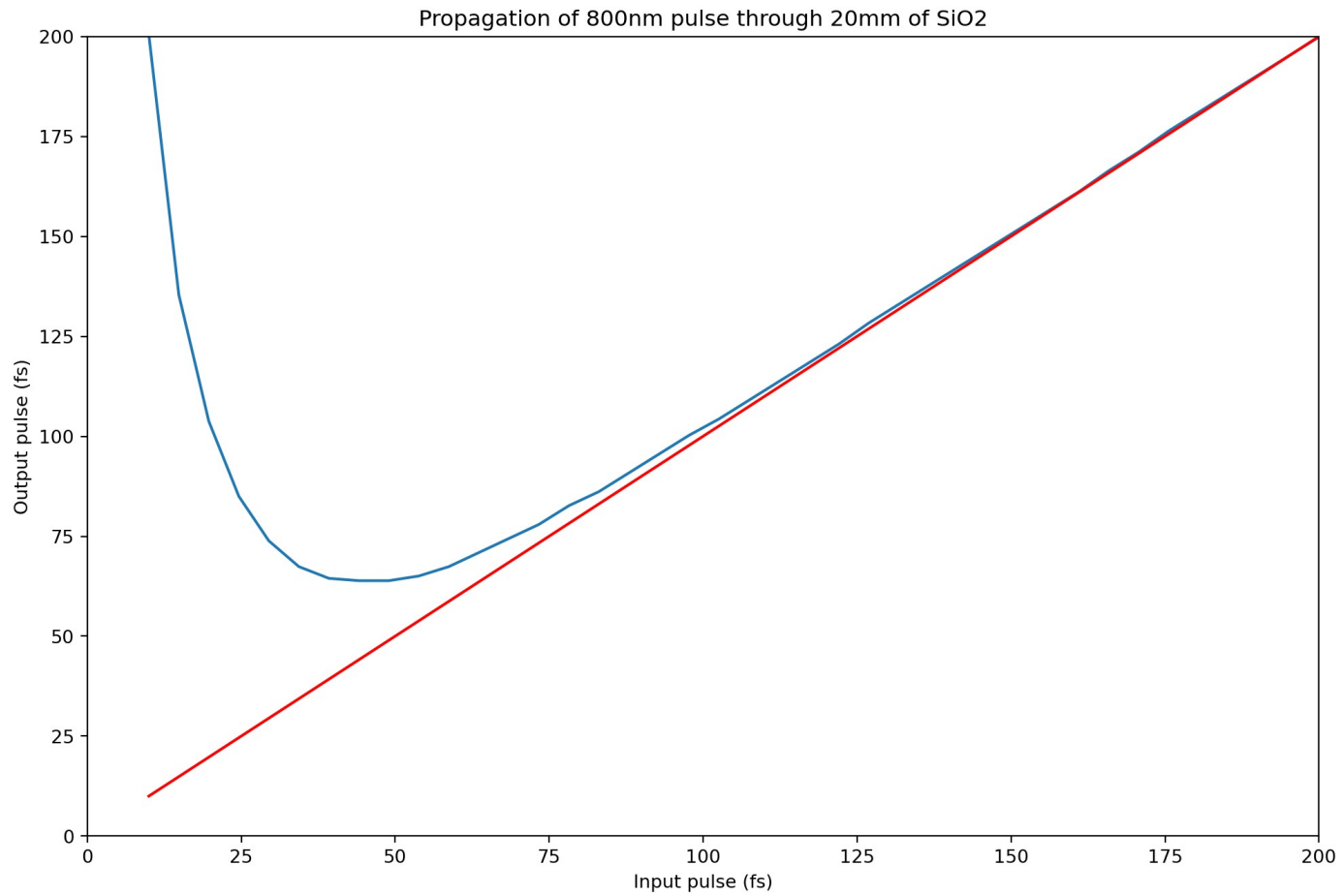
Malitson 1965: n 0.21-3.71 μm ▼

$$n^2 - 1 = \frac{0.6961663\lambda^2}{\lambda^2 - 0.0684043^2} + \frac{0.4079426\lambda^2}{\lambda^2 - 0.1162414^2} + \frac{0.8974794\lambda^2}{\lambda^2 - 9.896161^2}$$



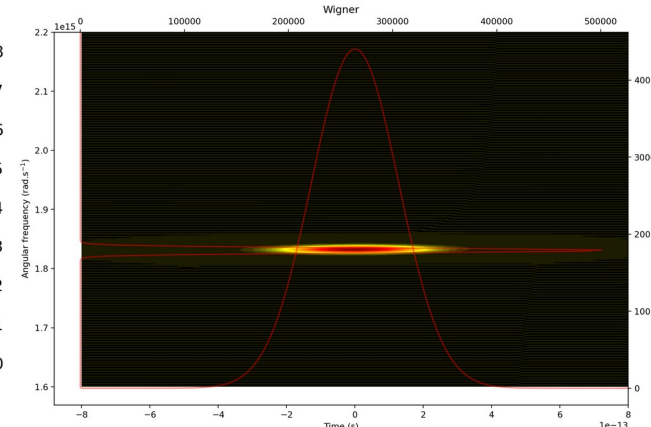
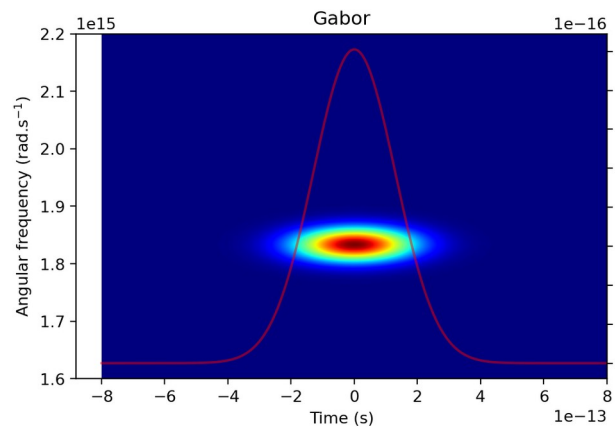
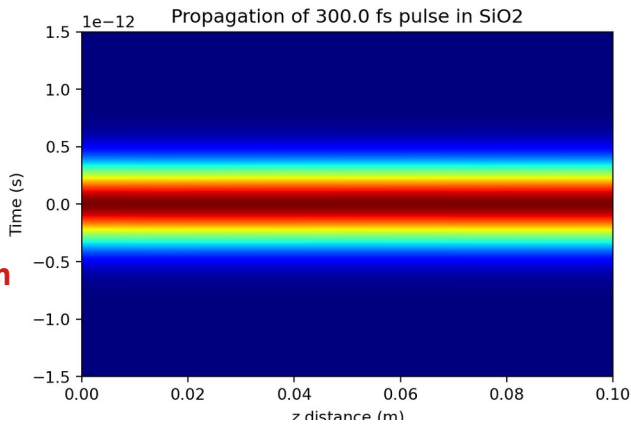
$$E_{\text{in}}(t) \rightarrow E_{\text{in}}(\omega) \rightarrow E_{\text{out}}(\omega) = E_{\text{in}}(\omega) \exp(i\varphi(\omega)) \rightarrow E_{\text{out}}(t)$$

Propagation in fused silica

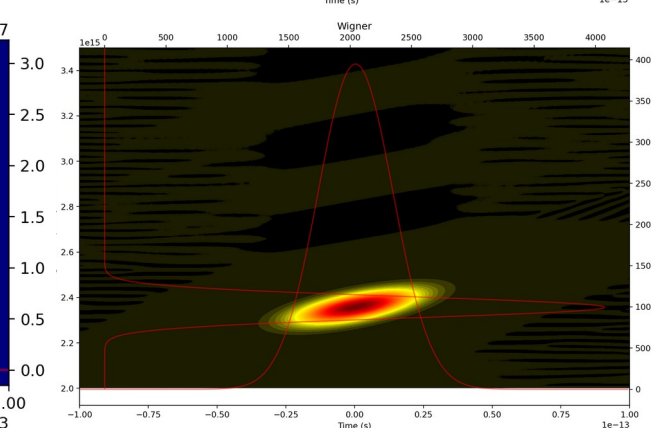
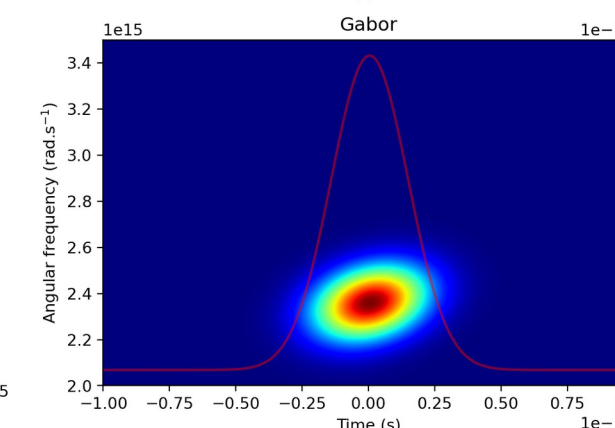
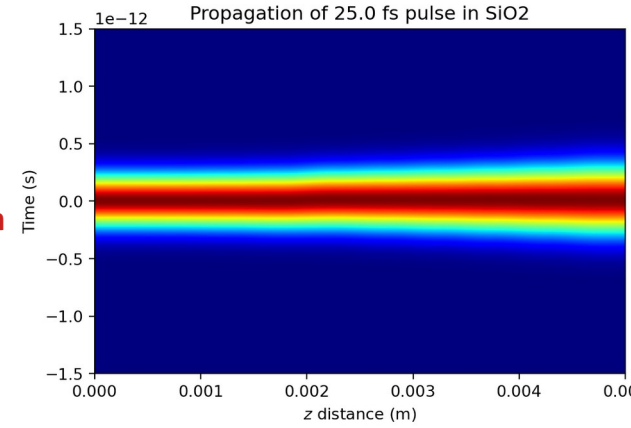


Propagation in fused silica

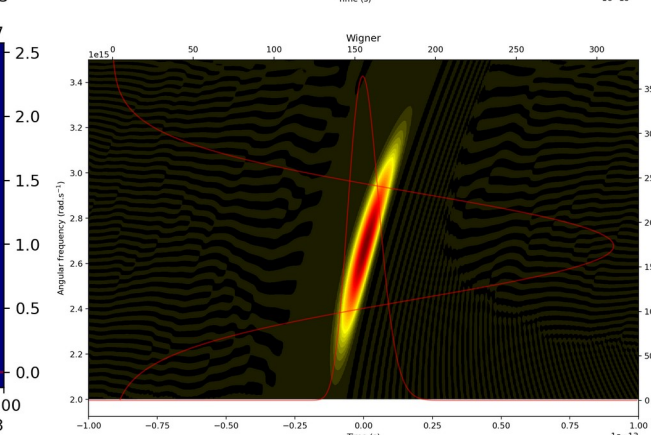
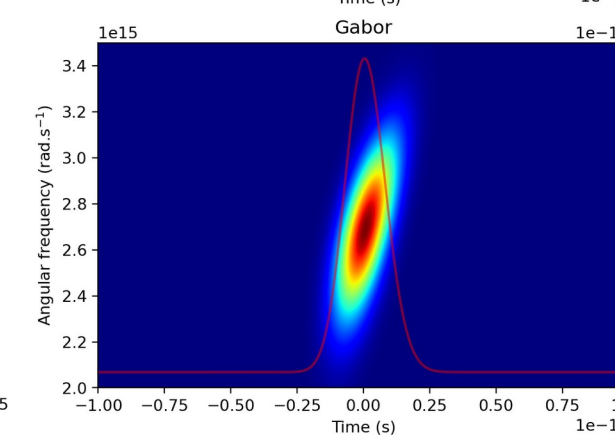
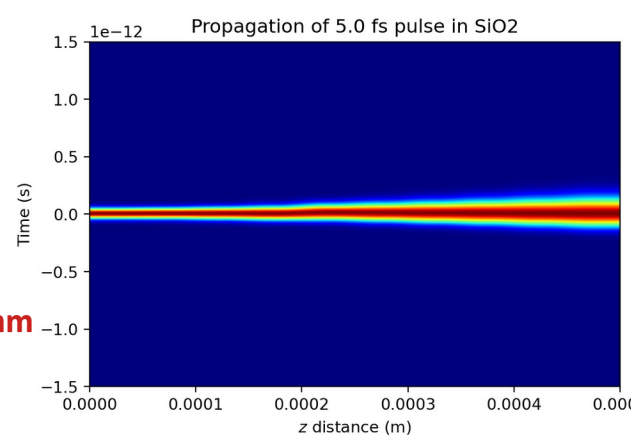
300 fs
1030nm
Up to 10cm



25 fs
800nm
Up to 5mm



5 fs
700nm
Up to 0.5mm



Mostly linear spreading of the frequency components in time

→ Linear chirp, quadratic phase

Can be compensated by introducing an opposite quadratic phase in the laser



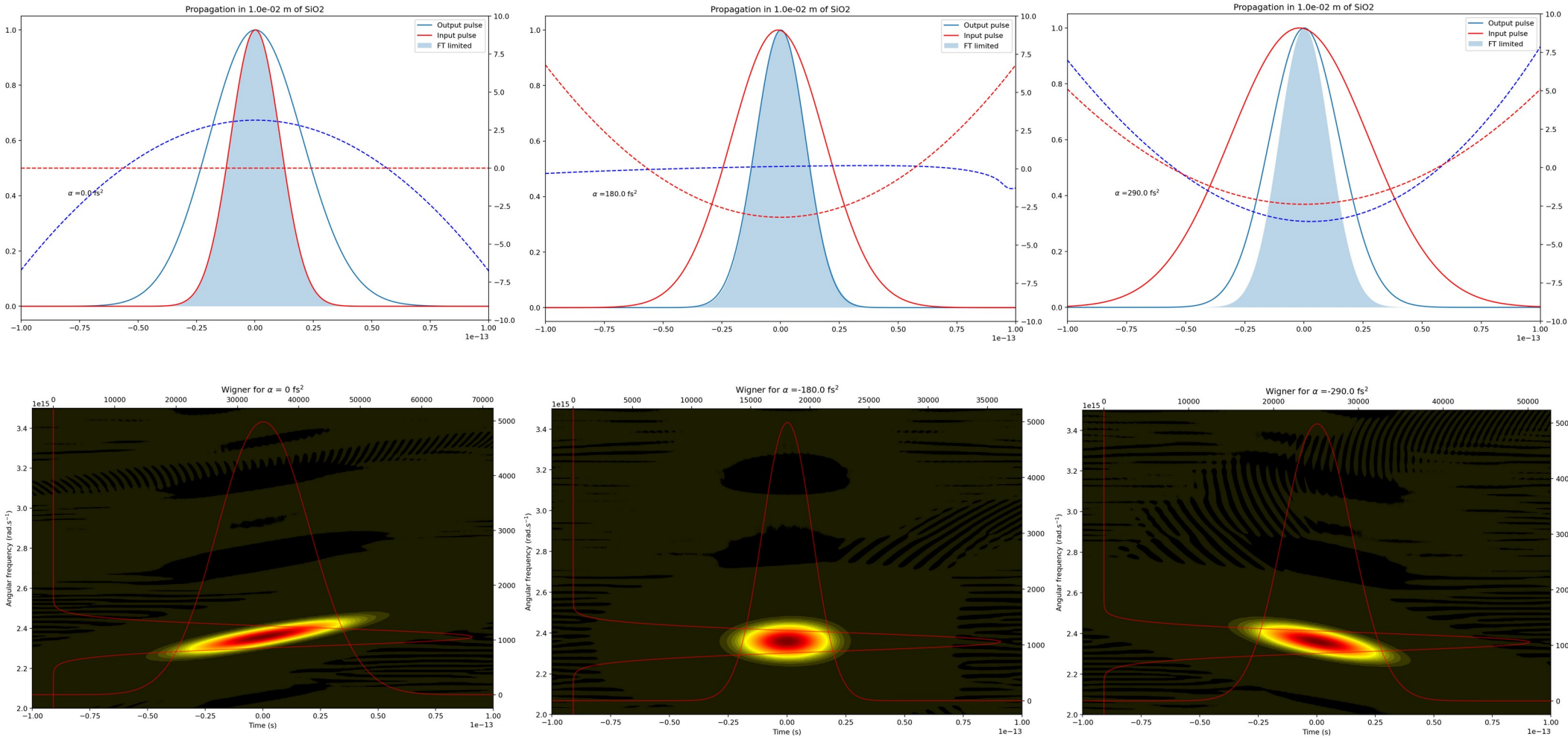
$$E_{\text{in}}(t) \rightarrow E_{\text{in}}(\omega) \rightarrow E_{\text{out}}(\omega) = E_{\text{in}}(\omega) \exp(i\varphi(\omega)) \rightarrow E_{\text{out}}(t)$$

$$E_{\text{comp}}(\omega) = E_{\text{out}}(\omega) \exp(-i \alpha (\omega - \omega_0)^2) \rightarrow E_{\text{comp}}(t)$$

α = quadratic spectral phase coefficient

Dispersion compensation

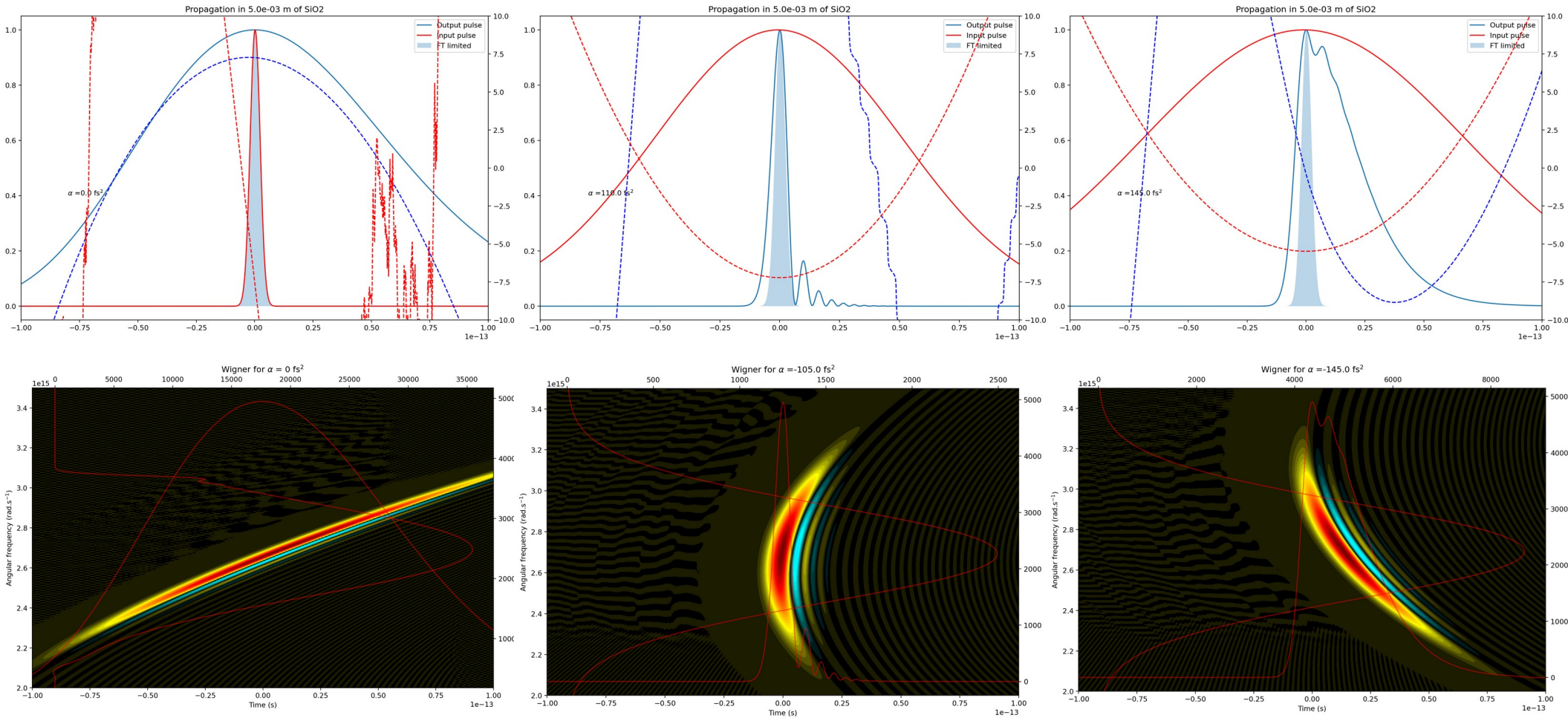
25 fs, 800nm, 1cm of SiO2



Small residual deviation from Fourier Limit: higher order spectral phase, uncompensated in the compressor

Dispersion compensation

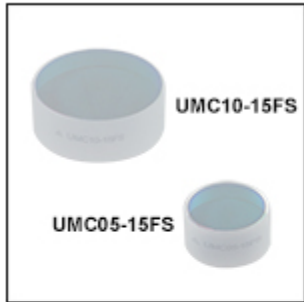
5 fs, 700nm, 5mm of SiO₂



**Clear signature of third order spectral phase
→ For very short pulses, we need better compensation**

Chirped mirrors

Chirped Mirrors for Fused Silica Compensation, Ø1/2" or Ø1"



[Zoom](#)

- ▶ >99.5% Absolute Reflectance from 650 to 1050 nm
- ▶ Group Delay Dispersion (GDD) per Reflection: -1.5 mm of Fused Silica (-54 fs² at 800 nm)
- ▶ Clear Aperture: >80% of Diameter
- ▶ 10° AOI

Thorlabs' UMC05-15FS and UMC10-15FS chirped mirrors feature >99.5% absolute reflectance over the 650 - 1050 nm wavelength range. The coating is engineered such that each reflection compensates for the dispersion introduced by 1.5 mm of fused silica over the entire range. The 10° AOI allows these mirrors to perform similarly for both s- and p-polarized light, and is ideal for a compact setup where multiple reflections are needed.

Mounting Options

The Ø1/2" mirror is 6.35 mm thick, while the Ø1" mirror is 9.5 mm thick. These mirrors can be mounted by any mirror mount that accepts these optic thicknesses. To maximize the clear edge, we recommend mounting the UMC105-15FS in a [POLARIS-C05G](#) glue-in mirror mount, which features a 180° clear edge, and the UMC10-15FS in a [POLARIS-C1G](#) glue-in mirror mount, which features a 252° clear edge.

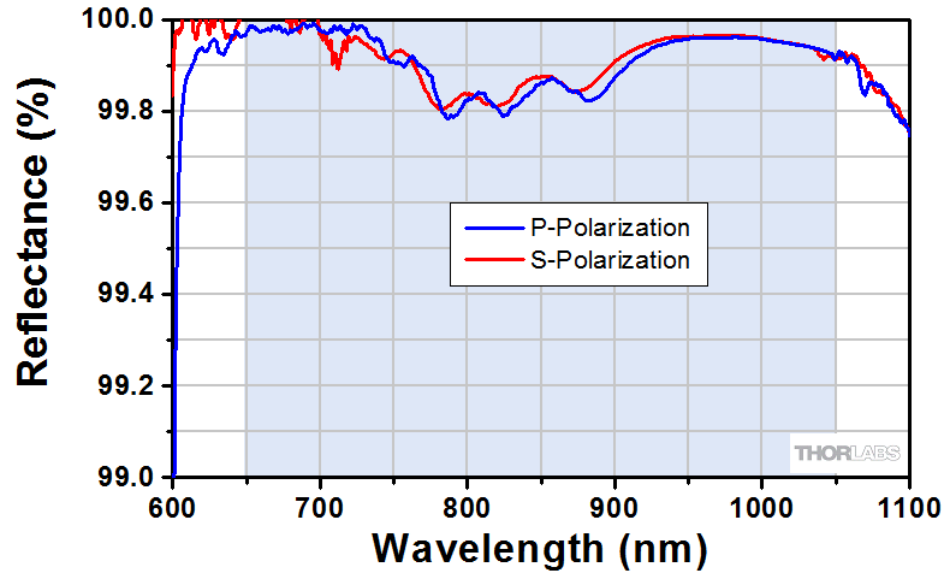
+1	Quantité	Docs	Produit - Universel	Total HT	Disponibilité
<input type="text" value="+1"/>	<input type="text"/>		UMC05-15FS Ø1/2" Dispersion-Compensating Mirror, 650 nm - 1050 nm, 10° AOI, Qty. 1	€ 173,58	Today
<input type="text" value="+1"/>	<input type="text"/>		UMC10-15FS Ø1" Dispersion-Compensating Mirror, 650 nm - 1050 nm, 10° AOI, Qty. 1	€ 284,49	Today

Multilayer dielectric coatings

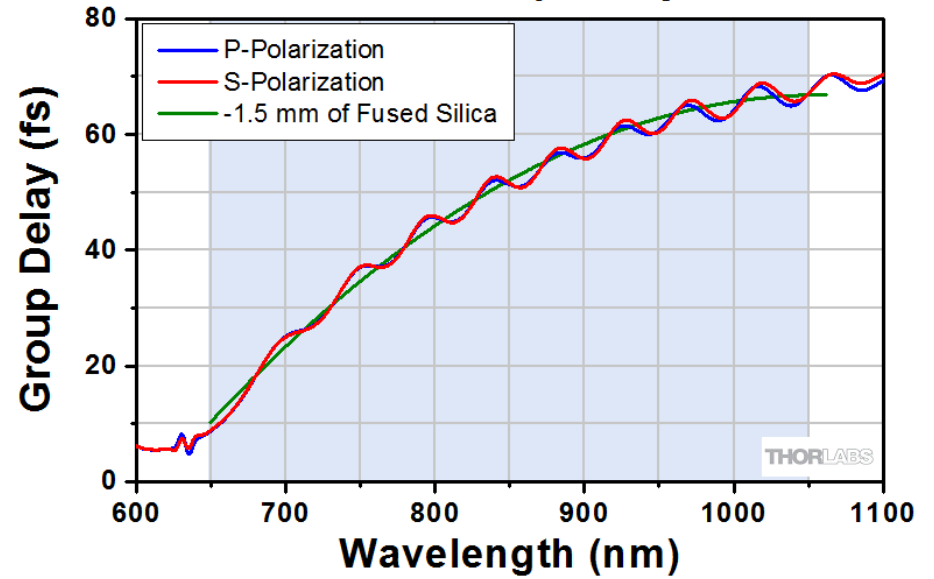
Designed to optimize broadband reflectivity and introduce a well controlled Group Delay Dispersion
Chirped mirrors compensating the dispersion of fused silica can be bought

Chirped mirrors

UMCxx-15FS Reflectance, 10° AOI



UMCxx-15FS Group Delay, 10° AOI

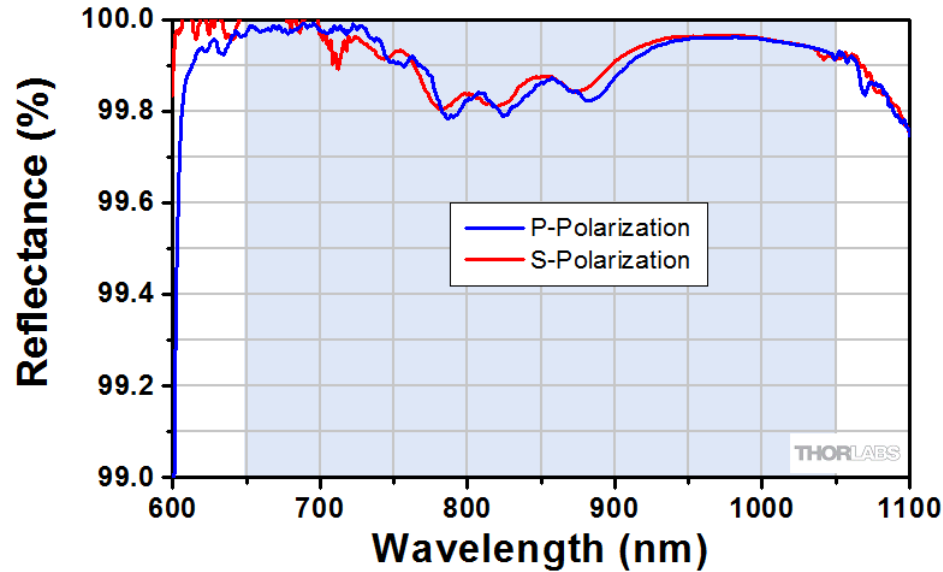


Good average dispersion compensation

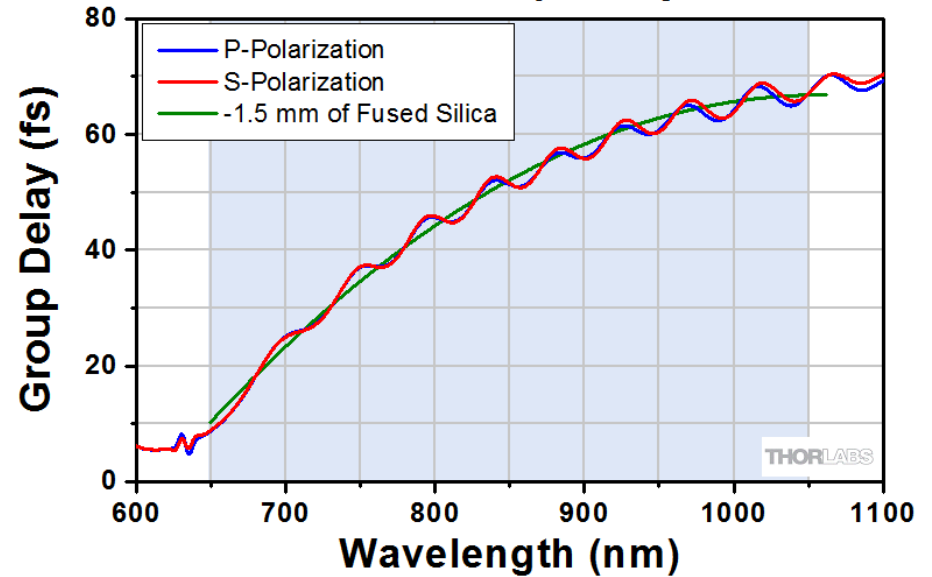
Oscillations in the GDD → Will create replicas in the temporal profile of the beam. This is bad.

Chirped mirrors

UMCxx-15FS Reflectance, 10° AOI



UMCxx-15FS Group Delay, 10° AOI



Good average dispersion compensation

Oscillations in the GDD → Will create replicas in the temporal profile of the beam. This is bad.

Avoided by matching two mirrors (different designs or different angles of incidence)

Chirped Mirror Set for Multiphoton Microscopy, 53.0 mm x 12.0 mm x 12.0 mm



- ▶ >99% Average Reflectance from 700 to 1000 nm
- ▶ Group Delay Dispersion (GDD) per Reflection: -175 fs^2 at 800 nm
- ▶ Coated Surface Dimensions: 50 mm x 8 mm
- ▶ 8° AOI
- ▶ Designed for Pulses with Spectral Bandwidth >50 nm FWHM
- ▶ Sold in Packs of 2

The DCMP175 consists of a pair of rectangular optics with >99% average reflectance over the 700 - 1000 nm wavelength range. These mirrors are designed to integrate with multiphoton microscopy setups, which typically include long path lengths through highly dispersive glass. The 8° AOI allows these mirrors to perform similarly for both s- and p-polarized light, and is ideal for a compact setup where multiple reflections are needed.

[Zoom](#)

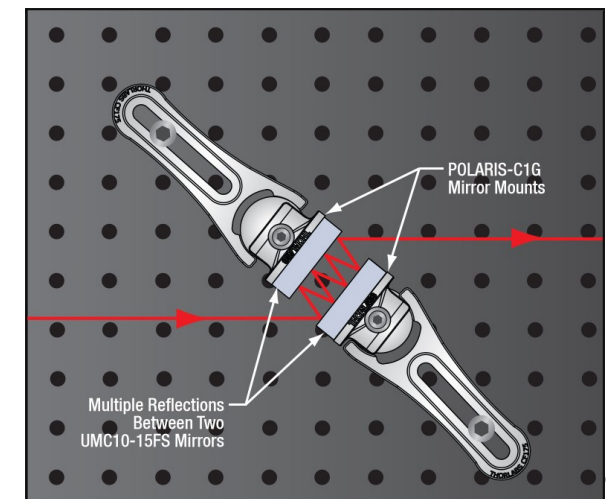
Mounting Option

As shown in the figure to the right, these mirrors can be mounted in the Kinematic Grating Mount Adapter, which is compatible with Ø1", front-loading, unthreaded mirror mounts, such as our Polaris Ultrastable Kinematic Mirror Mount.



Single DCMP175 Mirror Mounted Using a Mount Adapter

[Click to Enlarge](#)
[View Imperial Product List](#)
[View Metric Product List](#)

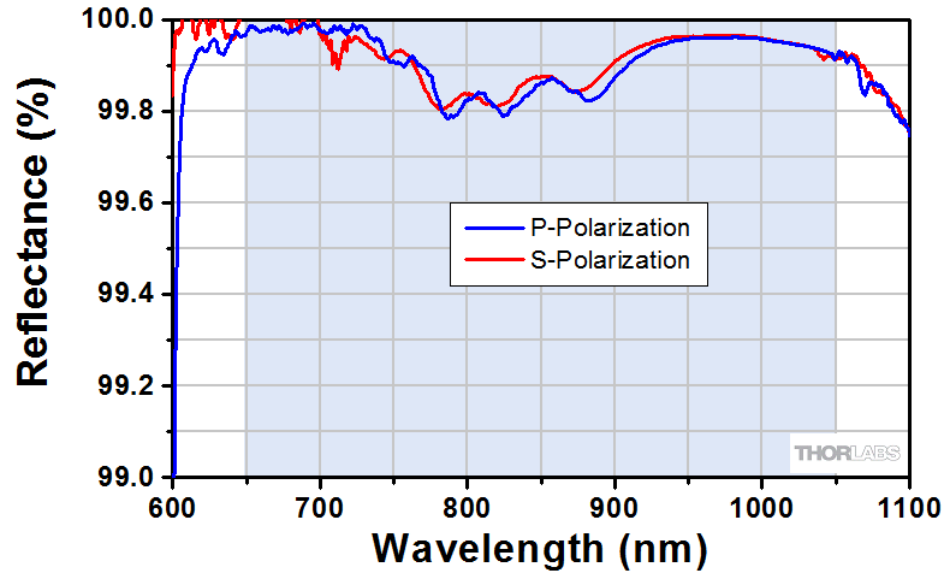


Multiple Reflections Between Two UMC10-15FS Mirrors

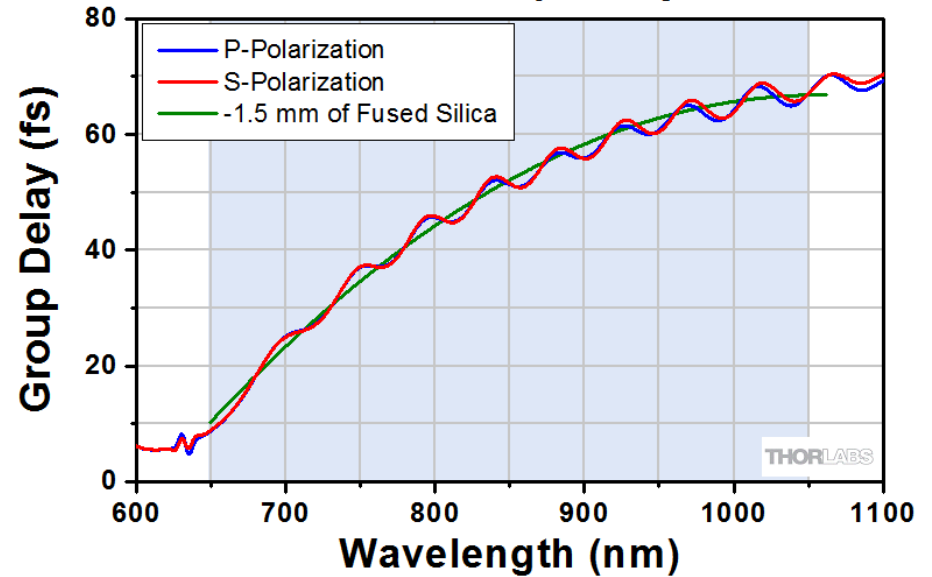
+1	Quantité	Docs	Produit - Universel	Total HT	Disponibilité
	<input type="text"/>		DCMP175 Dispersion-Compensating Mirror Set, 700 nm - 1000 nm, 8° AOI, Qty. 2	€ 2.424,68	5-8 Days

Chirped mirrors

UMCxx-15FS Reflectance, 10° AOI



UMCxx-15FS Group Delay, 10° AOI

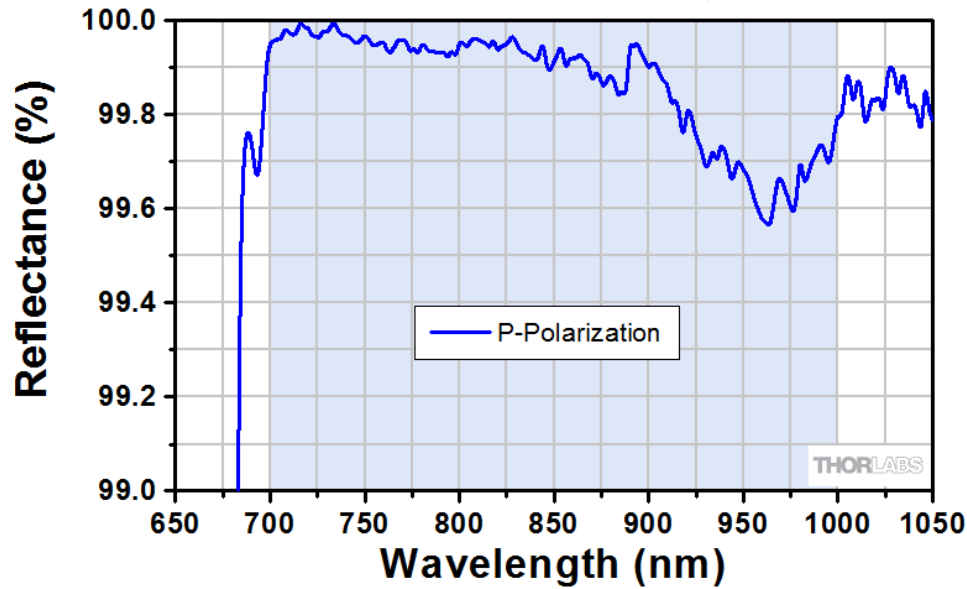


Good average dispersion compensation

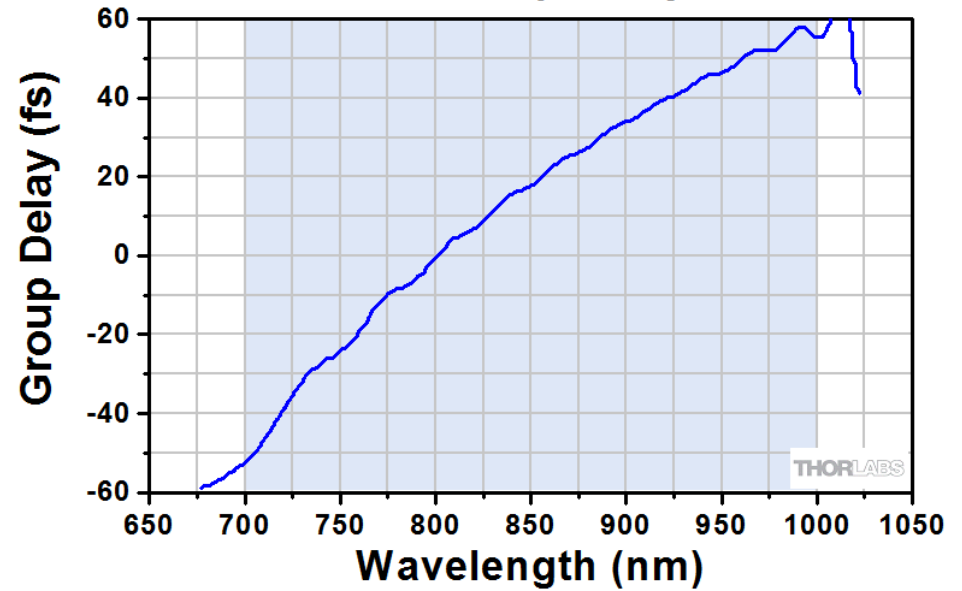
Oscillations in the GDD → Will create replicas in the temporal profile of the beam. This is bad.

Avoided by matching two mirrors (different designs or different angles of incidence)

DCMP175 Reflectance, 8° AOI



DCMP175 Group Delay, 8° AOI



Introduction: time-frequency travel

Keeping ultrashort pulses ultrashort

Self-phase modulation – the enemy within

Mirror mirror

Producing circularly polarized pulses – a perfect circle

Focus

High intensity → Non-linear dispersion

Kerr effect: the refractive index is modulated by the laser intensity:

$$n(x,y,z,t) = n_0 + n_2 \cdot I(x,y,z,t)$$

Already seen in Adeline's talk: Kerr lens modelocking – spatial effect

Already seen in Clara's talk: spectral/temporal effect

Self phase modulation

What is the effect of a Gaussian phase on a Gaussian pulse?



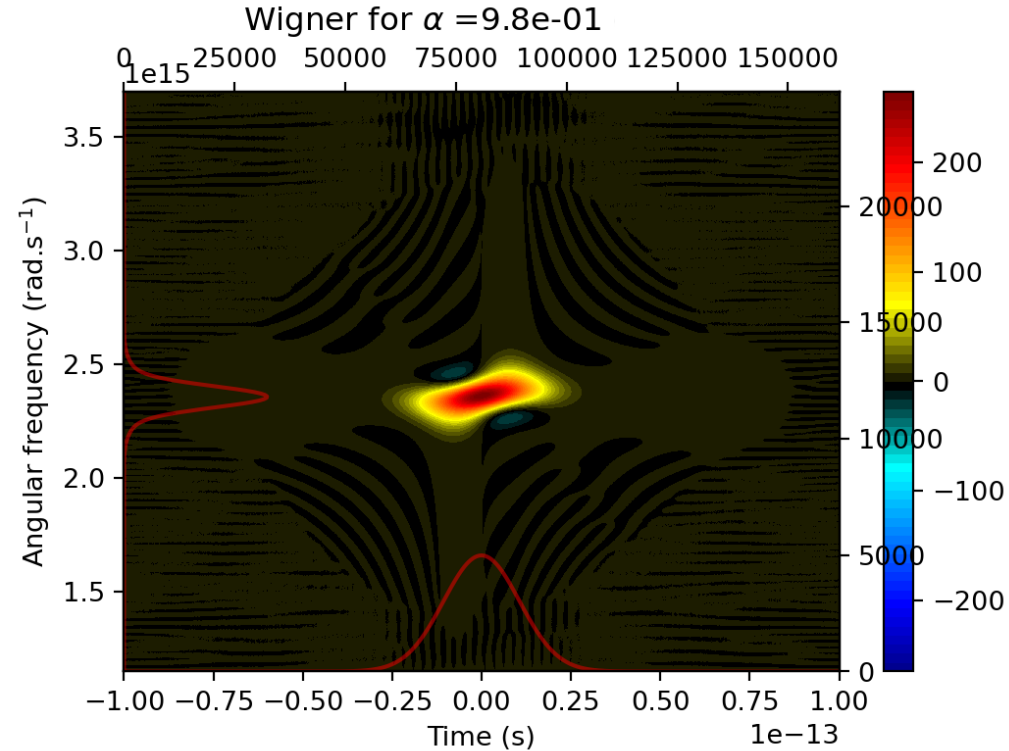
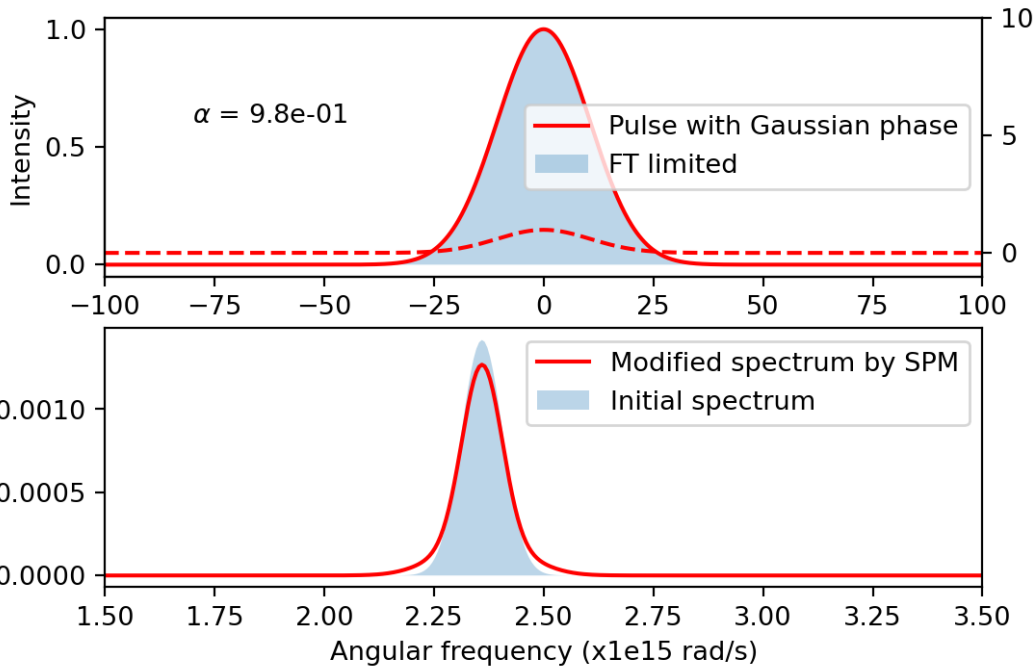
$$E_{\text{in}}(t) \rightarrow E_{\text{out}}(t) = E_{\text{in}}(t) \exp(i \sigma I_{\text{in}}(t)) \rightarrow E_{\text{out}}(\omega)$$

σ = magnitude factor of the SPM

Self phase modulation

What is the effect of a Gaussian phase on a Gaussian pulse?

Parabolic approximation \rightarrow quadratic temporal phase \rightarrow spectral broadening

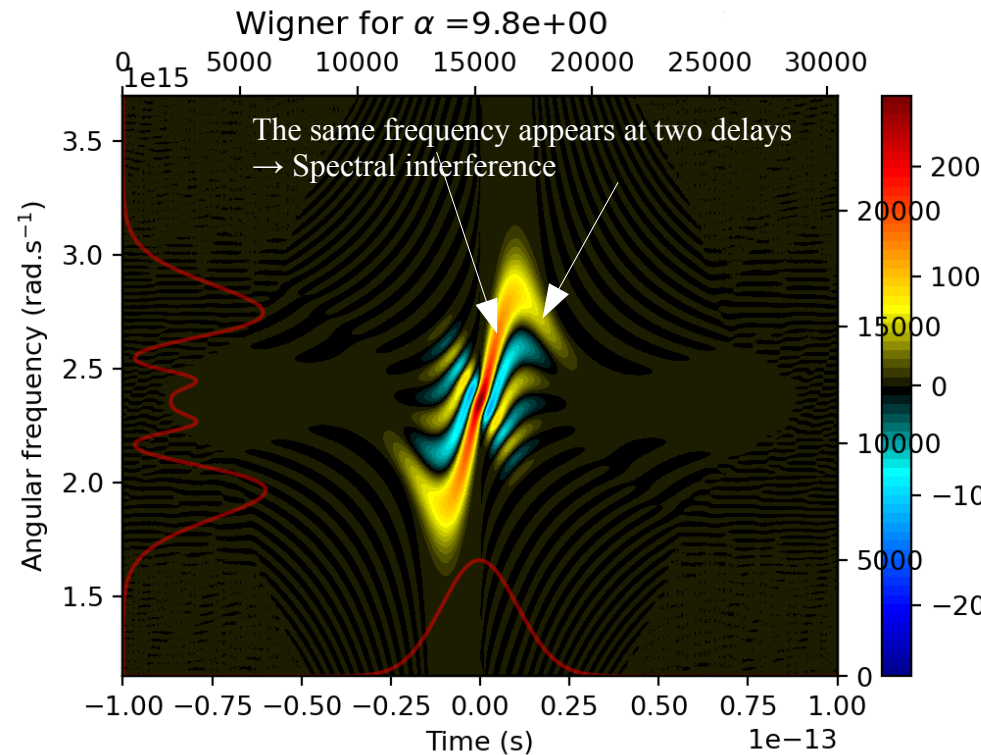
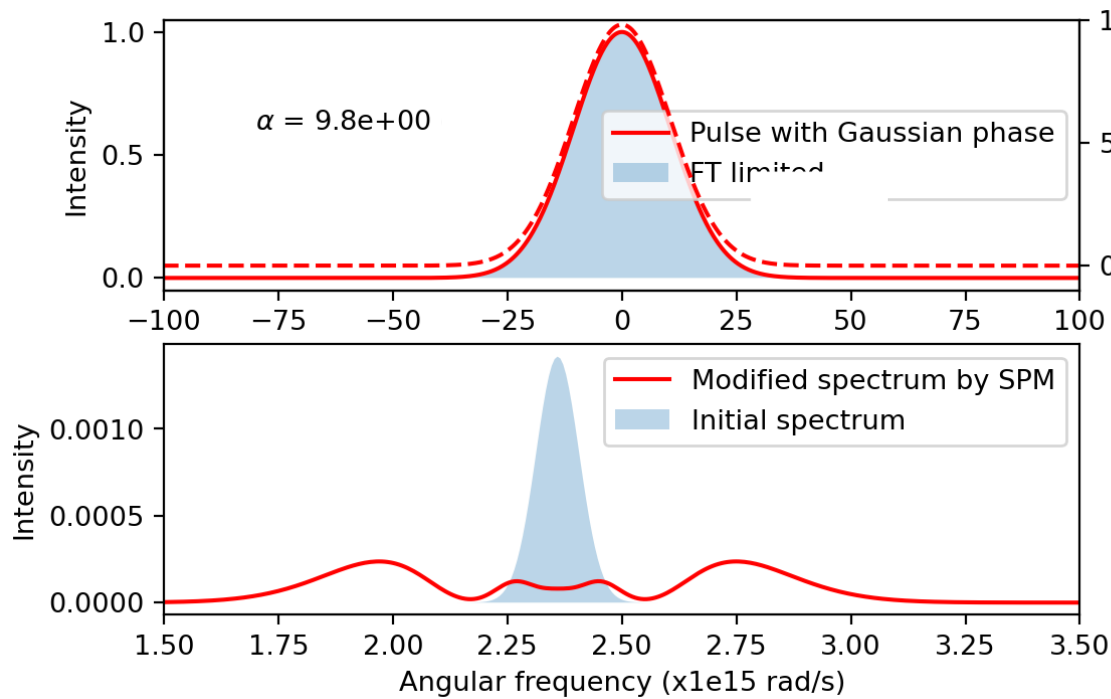


Self phase modulation

What is the effect of a Gaussian phase on a Gaussian pulse?

Parabolic approximation \rightarrow quadratic temporal phase \rightarrow spectral broadening

Strong SPM: fringes appear in the spectrum



When does SPM become a problem?

$$B = \frac{2\pi}{\lambda} \int n_2 I(z) dz \quad = \text{Accumulated non-linear phase shift}$$

Depends on the laser intensity

Energy per pulse, pulse duration, beam diameter

Is accumulated along the whole beam path

Air, glass windows, waveplates, lenses...

Can be avoided

- by increasing the beam diameter
- by shortening the optical path and avoiding transmissions
- by stretching the pulses to propagate them, and compress them as late as possible
(for instance in postcompression, do the final compression under vacuum to avoid SPM in windows)

SPM depends $x,y,z,t \rightarrow$ inhomogeneities in the beam

The spectrum depends on position

The spectral phase depends on position

\rightarrow The dispersion affects differently the various parts of the beam

\rightarrow The temporal profile becomes inhomogeneous

+ spatial phase \rightarrow focusing



When does SPM become a problem?

<http://toolbox.lightcon.com/tools/>

Optics Toolbox CONVERTERS BEAM PROPERTIES GEOMETRICAL OPTICS DISPERSION NONLINEAR OPTICS OTHER ⓘ

Pulse peak intensity and fluence

Peak fluence ⓘ
7639.437 $\mu\text{J}/\text{cm}^2$

Peak intensity Gaussian pulse ⓘ
1435.354 GW/cm^2

Peak intensity sech² pulse ⓘ
1346.64 GW/cm^2

Pulse energy
3000 μJ

Pulse length FWHM
5 fs

Beam diameter (mm)
at e⁻²: 10
at FWHM: 5.887

Super-Gaussian coefficient ⓘ
1 deg

Optics Toolbox CONVERTERS BEAM PROPERTIES GEOMETRICAL OPTICS DISPERSION NONLINEAR OPTICS OTHER ⓘ

B-integral ⓘ

B_o 0.738 B_e

fused_silica, Fused quartz/silica (FS)

Wavelength [nm] 1030 Intensity I_{max} [GW/cm²] 0.44 Distance z [mm] 1000

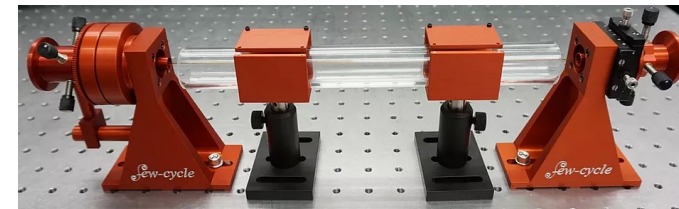
Wavelength [nm]	n ₂ [cm ² /W]
351	3.6e-16
527	3e-16
1053	2.74e-16

A few examples:

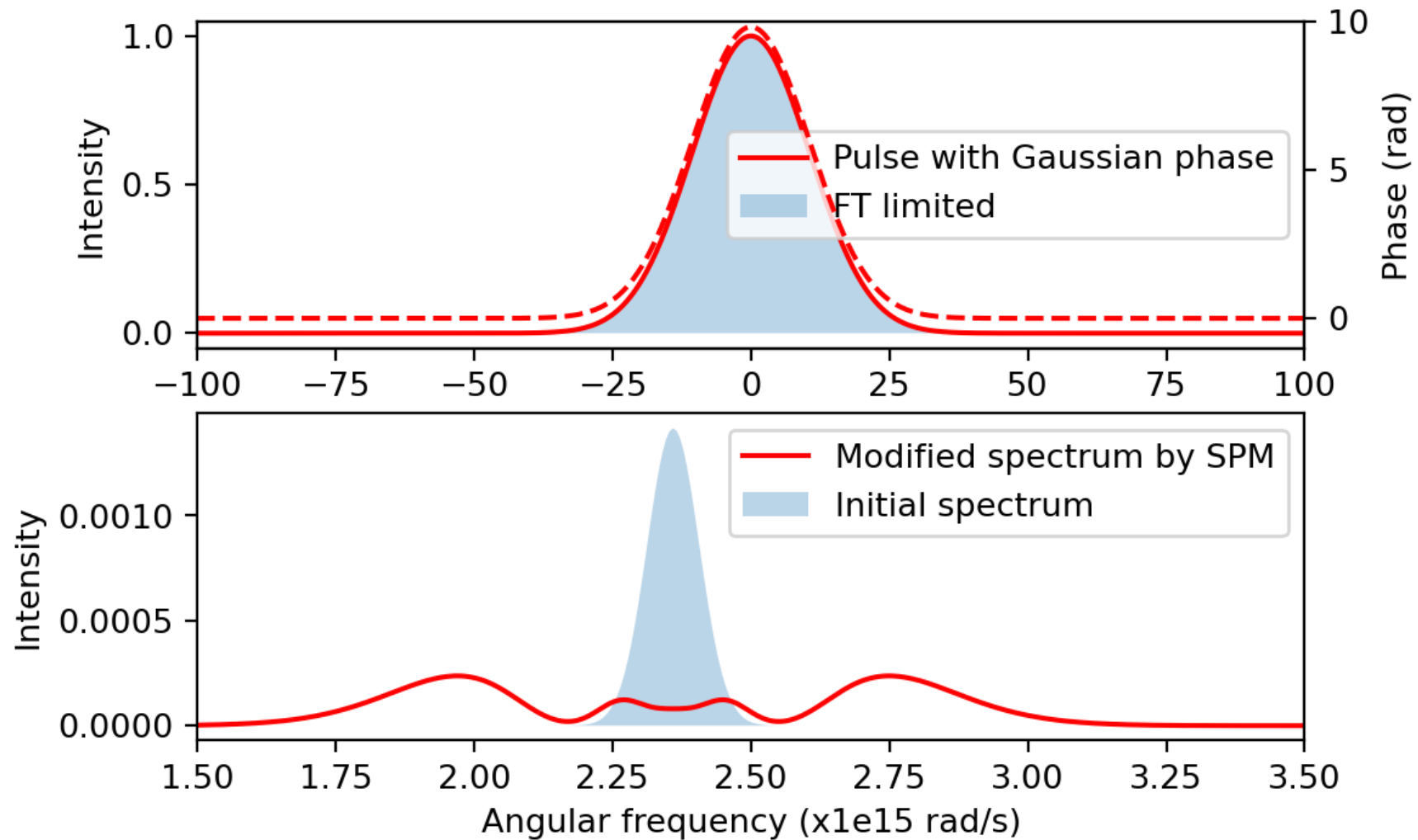
- Yb: fiber laser, waist=2mm, 300 fs, 500 μJ
 $\rightarrow I_{\text{max}} = 0,44 \text{ GW}/\text{cm}^2 \rightarrow B=5$ in 7m of SiO₂

- Ti:Sa laser, waist=20mm, 25 fs, 10 mJ
 $\rightarrow I_{\text{max}} = 240 \text{ GW}/\text{cm}^2 \rightarrow B=5$ in 10 mm of SiO₂

- Postcompressed pulse, waist = 10 mm, 5fs, 3mJ
 $\rightarrow I_{\text{max}} = 1350 \text{ GW}/\text{cm}^2 \rightarrow B=5$ in 1.7 mm of SiO₂



Using SPM to compress fs pulses



SPM induces spectral broadening → reduces the Fourier Limit duration that can be reached

Can we compensate the spectral phase?

Parabolic approximation of the phase → can be compensated by opposite second order phase

How can we introduce a negative chirp?

Mid Infrared: use negative GVD (eg in fused silica)

UV-Vis-IR: use chirped mirrors

Chirped mirrors

Chirped Mirror Set for Multiphoton Microscopy, 53.0 mm x 12.0 mm x 12.0 mm



- ▶ >99% Average Reflectance from 700 to 1000 nm
- ▶ Group Delay Dispersion (GDD) per Reflection: -175 fs^2 at 800 nm
- ▶ Coated Surface Dimensions: 50 mm x 8 mm
- ▶ 8° AOI
- ▶ Designed for Pulses with Spectral Bandwidth >50 nm FWHM
- ▶ Sold in Packs of 2

The DCMP175 consists of a pair of rectangular optics with >99% average reflectance over the 700 - 1000 nm wavelength range. These mirrors are designed to integrate with multiphoton microscopy setups, which typically include long path lengths through highly dispersive glass. The 8° AOI allows these mirrors to perform similarly for both s- and p-polarized light, and is ideal for a compact setup where multiple reflections are needed.

[Zoom](#)

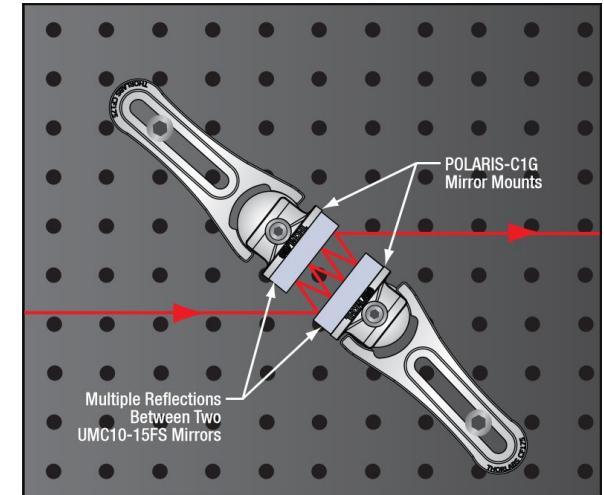
Mounting Option

As shown in the figure to the right, these mirrors can be mounted in the Kinematic Grating Mount Adapter, which is compatible with $\varnothing 1"$, front-loading, unthreaded mirror mounts, such as our Polaris Ultrastable Kinematic Mirror Mount.



Single DCMP175 Mirror Mounted Using a Mount Adapter

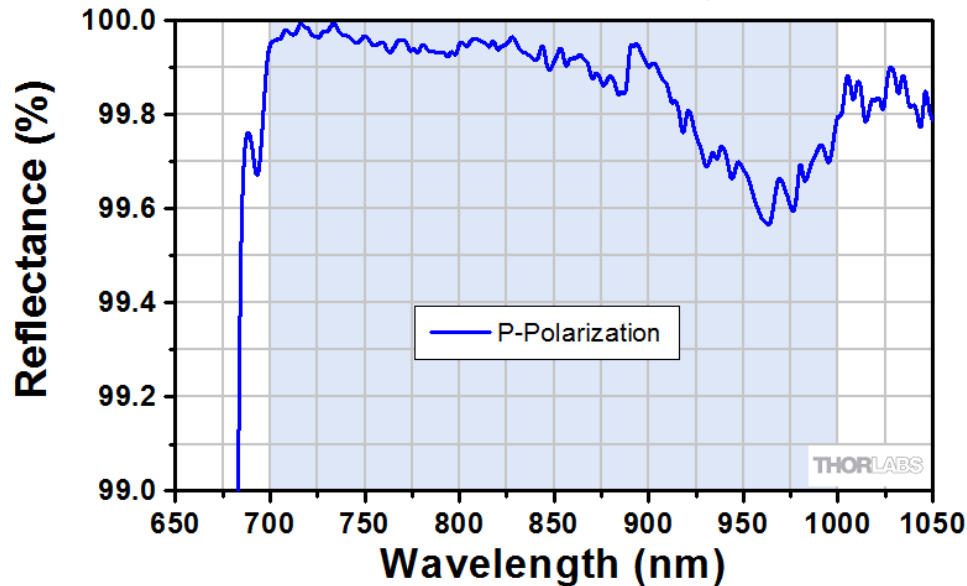
[Click to Enlarge](#)
[View Imperial Product List](#)
[View Metric Product List](#)



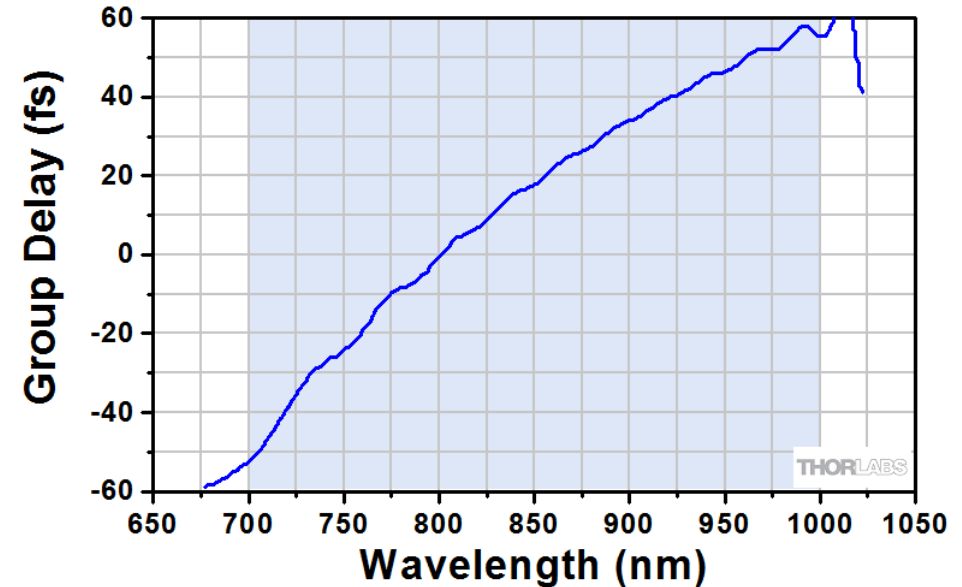
Multiple Reflections Between Two UMC10-15FS Mirrors

+1	Quantité	Docs	Produit - Universel	Total HT	Disponibilité
	<input type="text"/>		DCMP175 Dispersion-Compensating Mirror Set, 700 nm - 1000 nm, 8° AOI, Qty. 2	€ 2.424,68	5-8 Days

DCMP175 Reflectance, 8° AOI



DCMP175 Group Delay, 8° AOI



-175 fs^2 / bounce. How does it compare with the phase introduced by SPM?

→ Let's introduce a negative chirp to compensate the quadratic phase of our SPM modulated pulse

Introduce a quadratic spectral phase to compensate for the positive chirp of the pulses

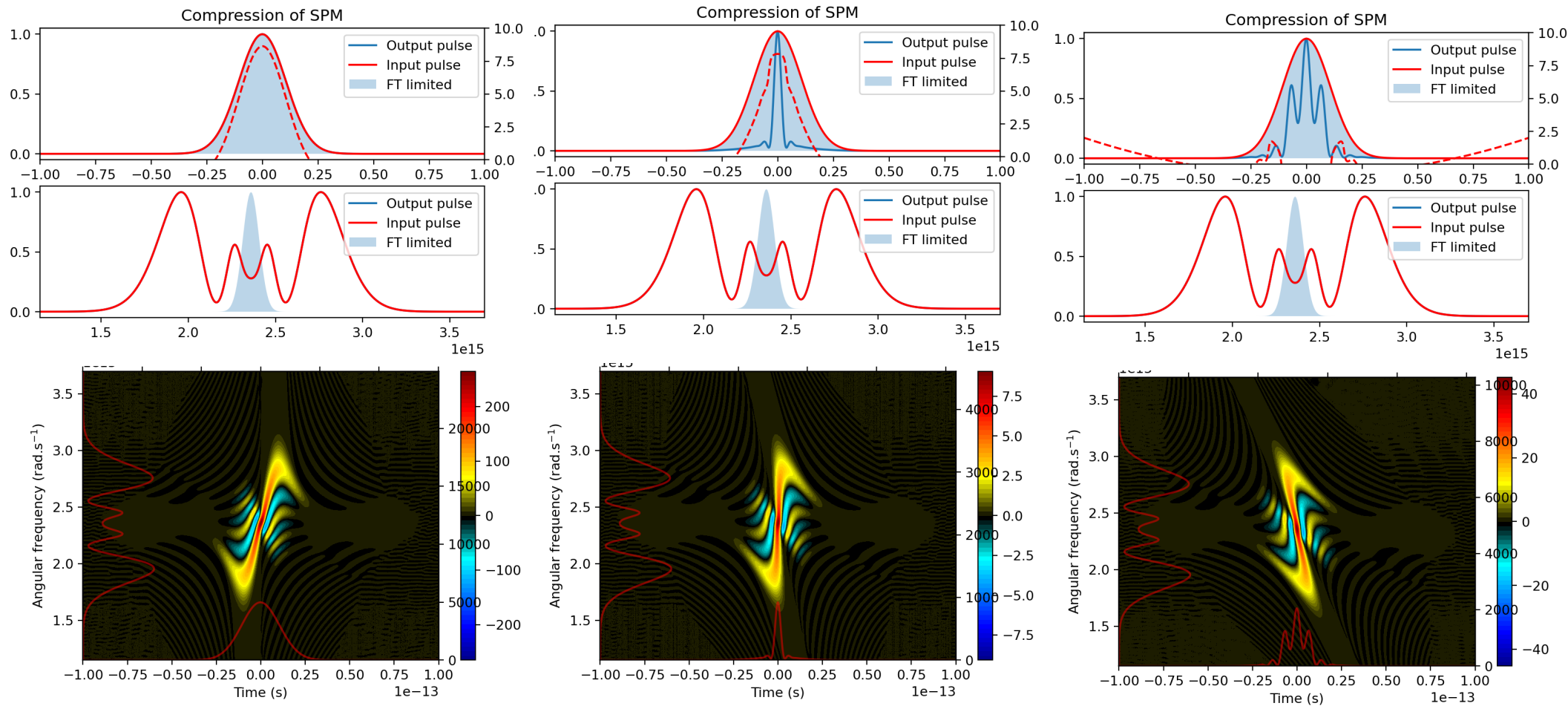


$$E_{\text{in}}(t) \rightarrow E_{\text{out}}(t) = E_{\text{in}}(t) \exp(i \sigma I_{\text{in}}(t)) \rightarrow E_{\text{out}}(\omega)$$

$$E_{\text{comp}}(\omega) = E_{\text{out}}(\omega) \exp(i \alpha (\omega - \omega_0)^2) \rightarrow E_{\text{comp}}(t)$$

Using SPM to compress fs pulses

Increasing quadratic phase compensation



Note: Characterization of ultrashort electromagnetic pulses

Ian A. Walmsley¹ and Christophe Dorrer²

¹Department of Physics, University of Oxford, Clarendon Laboratory, Parks Road, Oxford, OX1 3PU, UK, walmsley@physics.ox.ac.uk

²Laboratory for Laser Energetics, University of Rochester, 250 East River Road, Rochester, New York 14623, USA. cdorrer@le.rochester.edu

Advances in Optics and Photonics 1, 308–437 (2009) doi:10.1364/AOP.1.000308

The Wigner functions of a pulse before and after quadratic spectral phase modulation $\phi^{(2)}\omega^2/2$ are related by

$$W_{\text{OUTPUT}}(t, \omega) = W_{\text{INPUT}}(t - \phi^{(2)}\omega, \omega). \quad (2.39)$$

This corresponds to a shear of the chronocyclic Wigner function, as shown in Fig. 11(b), which encodes the spectrum of the input pulse onto the temporal intensity of the output pulse.

Postcompression in a bulk plate

Optics Communications 472 (2020) 126035

2.3-cycle mid-infrared pulses from hybrid thin-plate post-compression at 7 W average power

Mate Kurucz^{a,*}, Roland Flender^a, Ludovit Haizer^a, Roland S. Nagymihaly^a, Wosik Cho^{b,c}, Kyung T. Kim^{b,c}, Szabolcs Toth^a, Eric Cormier^{d,e}, Balint Kiss^a

^a ELI-ALPS Research Institute, Dugonics tér 13, 6720 Szeged, Hungary

^b Center for Relativistic Laser Science, Institute for Basic Science, 61005, Gwangju, Republic of Korea

^c Department of Physics and Photon Science, Gwangju Institute of Science and Technology, 61005, Gwangju, Republic of Korea

^d Laboratoire Photonique, Numérique et Nanoscience, Université Bordeaux-IOGS-CNRS (UMR 5298), rue F. Mitterrand, 33400, Talence, France

^e Institut Universitaire de France, 1 rue Descartes, 75231 Paris, France

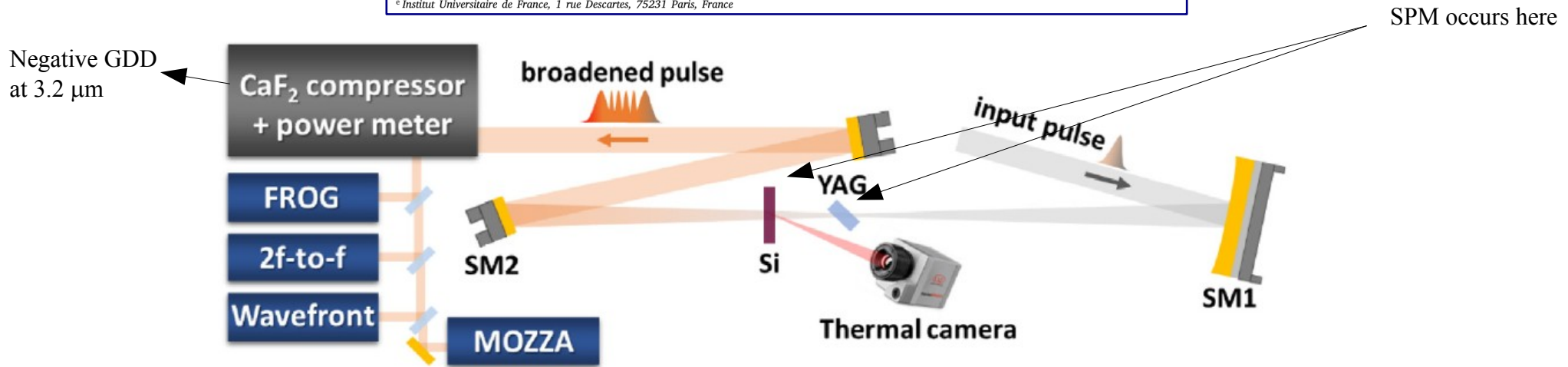


Fig. 1. Schematic view of the experimental arrangement. SM1 and SM2 are concave spherical mirrors.

Why using two plates (Si and YAG)?

Efficient spectral broadening from a single bulk plate is limited by plasma formation due to ionization, which results in nonlinear losses and degradation of the beam profile at higher input intensities [18]. To overcome the limitations of single-plate compression of MIR pulses, different material thin plates of opposite group velocity dispersion (GVD) could be employed in alternating order, in a hybrid setup. Having the appropriate parameters for these plates, such as n_2 , GVD and thickness, may allow to compensate the spectral phase (up to the second order phase) on the subsequent plate, resulting in sufficient intensity to drive the nonlinear broadening efficiently.

Semiconductors: positive GVD at 3.2 μm , high n_2

Semiconductors as silicon and germanium were the prime candidates as they have the highest nonlinear refractive index of $3.79 \cdot 10^{-14} \text{ cm}^2/\text{W}$ and $3.68 \cdot 10^{-13} \text{ cm}^2/\text{W}$ respectively [22].

Dielectrics: negative GVD at 3.2 μm , but low n_2 :

YAG has the highest nonlinearity of $7 \cdot 10^{-16} \text{ cm}^2/\text{W}$.

Postcompression in a bulk plate

Optics Communications 472 (2020) 126035

2.3-cycle mid-infrared pulses from hybrid thin-plate post-compression at 7 W average power

Mate Kurucz^{a,*}, Roland Flender^a, Ludovit Haizer^a, Roland S. Nagymihaly^a, Wosik Cho^{b,c}, Kyung T. Kim^{b,c}, Szabolcs Toth^a, Eric Cormier^{d,e}, Balint Kiss^a

^a ELI-ALPS Research Institute, Dugonics tér 13, 6720 Szeged, Hungary

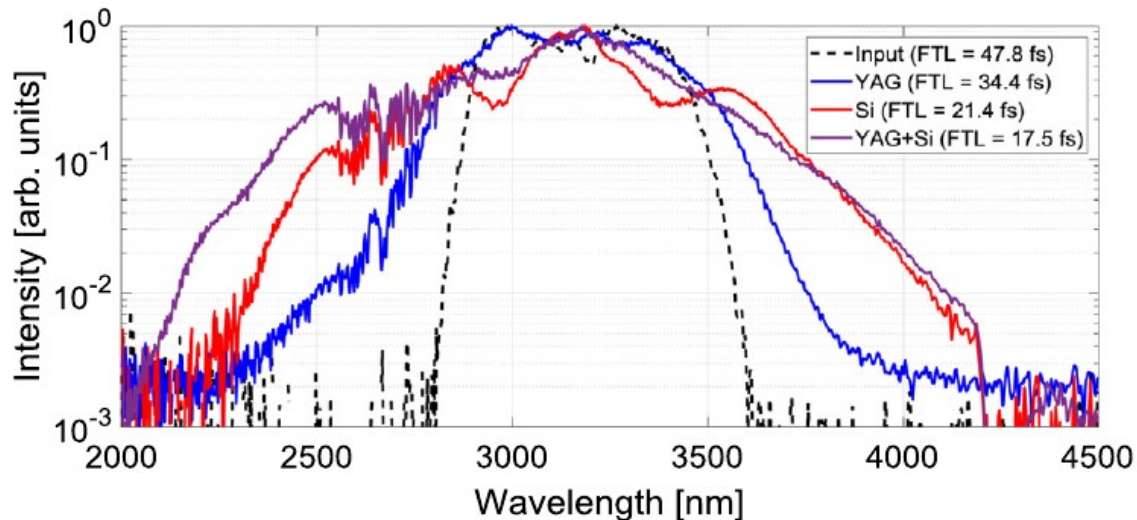
^b Center for Relativistic Laser Science, Institute for Basic Science, 61005, Gwangju, Republic of Korea

^c Department of Physics and Photon Science, Gwangju Institute of Science and Technology, 61005, Gwangju, Republic of Korea

^d Laboratoire Photonique, Numérique et Nanoscience, Université Bordeaux-IOGS-CNRS (UMR 5298), rue F. Mitterrand, 33400, Talence, France

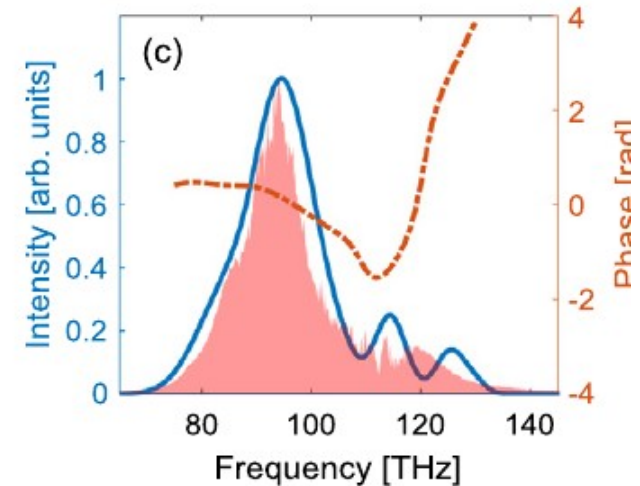
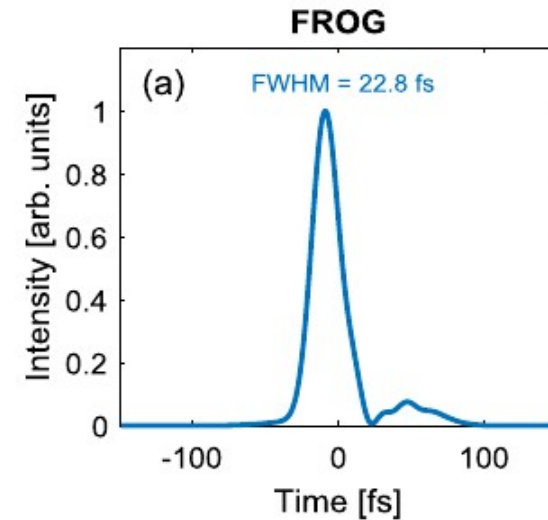
^e Institut Universitaire de France, 1 rue Descartes, 75231 Paris, France

Spectral measurements



Efficient postcompression scheme
Inherent spatial inhomogeneity
due to the intensity distribution in the plate?
Can be mitigated by using multiple plates

Temporal characterization (see next course)

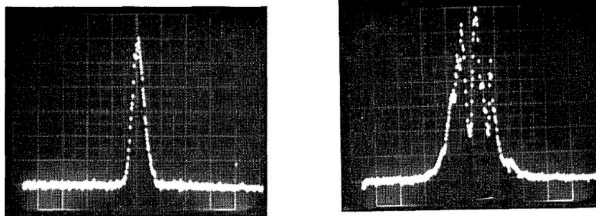


Postcompression in bulk plates – more references

Compression of high-power optical pulses

Claude Rolland and P. B. Corkum

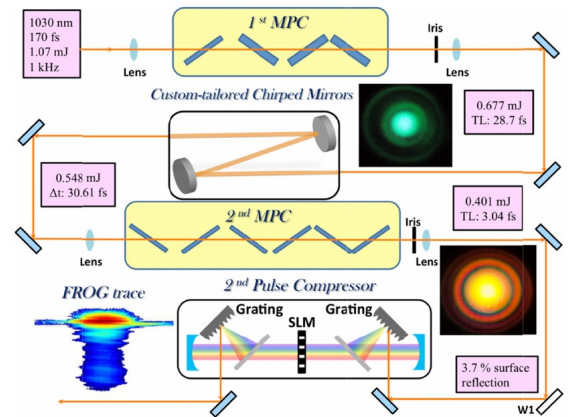
Division of Physics, National Research Council of Canada, Ottawa, Ontario K1A 0R6, Canada



Greater than 50 times compression of 1030 nm Yb:KGW laser pulses to single-cycle duration

CHIH-HSUAN LU,^{1,2,5} WEI-HSIN WU,¹ SHIANG-HE KUO,¹ JHAN-YU GUO,¹ MING-CHANG CHEN,^{1,3,4} SHANG-DA YANG,¹ AND A. H. KUNG^{1,2,6}

¹Institute of Photonics Technologies, National Tsing Hua University, Hsinchu, Taiwan
²Institute of Atomic and Molecular Sciences, Academia Sinica, Taipei, Taiwan
³Department of Physics, National Tsing Hua University, Hsinchu, Taiwan
⁴Frontier Research Center on Fundamental and Applied Sciences of Matters, National Tsing Hua University, Hsinchu, Taiwan

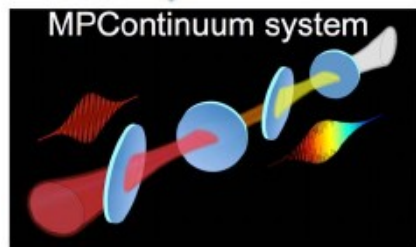


Generation of intense supercontinuum in condensed media

CHIH-HSUAN LU,¹ YU-JUNG TSOU,¹ HONG-YU CHEN,¹ BO-HAN CHEN,¹ YU-CHEN CHENG,² SHANG-DA YANG,¹ MING-CHANG CHEN,¹ CHIA-CHEN HSU,³ AND A. H. KUNG^{1,2,*}

¹Institute of Photonics Technologies, National Tsing Hua University, Hsinchu 30013, Taiwan
²Institute of Atomic and Molecular Sciences, Academia Sinica, Taipei 10617, Taiwan
³Department of Physics, National Chung Cheng University, Chiayi 62102, Taiwan
 *Corresponding author: akung@pub.iam.s.sinica.edu.tw

Received 2 September 2014; revised 16 October 2014; accepted 29 October 2014 (Doc. ID 222144); published 10 December 2014



Efficient nonlinear compression of a mode-locked thin-disk oscillator to 27 fs at 98 W average power

CHIA-LUN TSAI,^{1,*} FRANK MEYER,² ALAN OMAR,² YICHENG WANG,² AN-YUAN LIANG,¹ CHIH-HSUAN LU,¹ MARTIN HOFFMANN,² SHANG-DA YANG,¹ AND CLARA J. SARACENO²

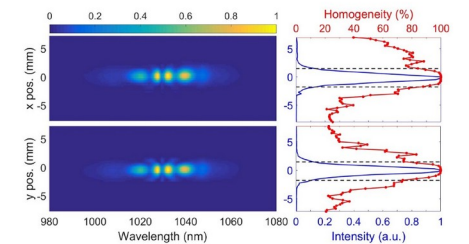


Fig. 5. Homogeneity measurement performed after multiple-plate stage supporting sub-30 fs. Dashed lines indicate $1/e^2$ level of intensity.

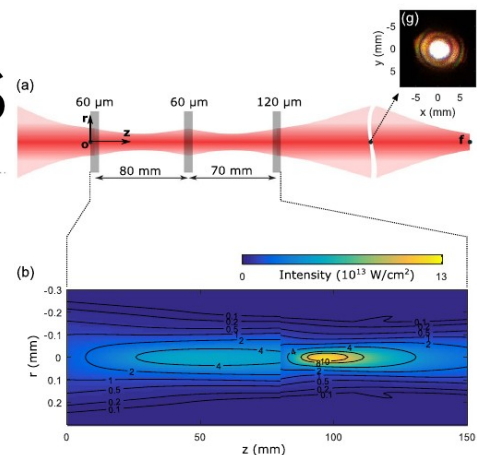
SCIENTIFIC REPORTS

OPEN

Generation of a single-cycle pulse using a two-stage compressor and its temporal characterization using a tunnelling ionization method

Received: 30 April 2018
 Accepted: 19 December 2018
 Published online: 07 February 2019

Sung In Hwang¹, Seung Beom Park¹, Jehoi Mun¹, Wosik Cho^{1,2}, Chang Hee Nam^{1,2} & Kyung Taec Kim^{1,2}



Postcompression in a hollow core fiber

Generation of high power sub-15 fs pulses at 515 nm through nonlinear compression of an Yb-doped ultrafast fiber amplifier

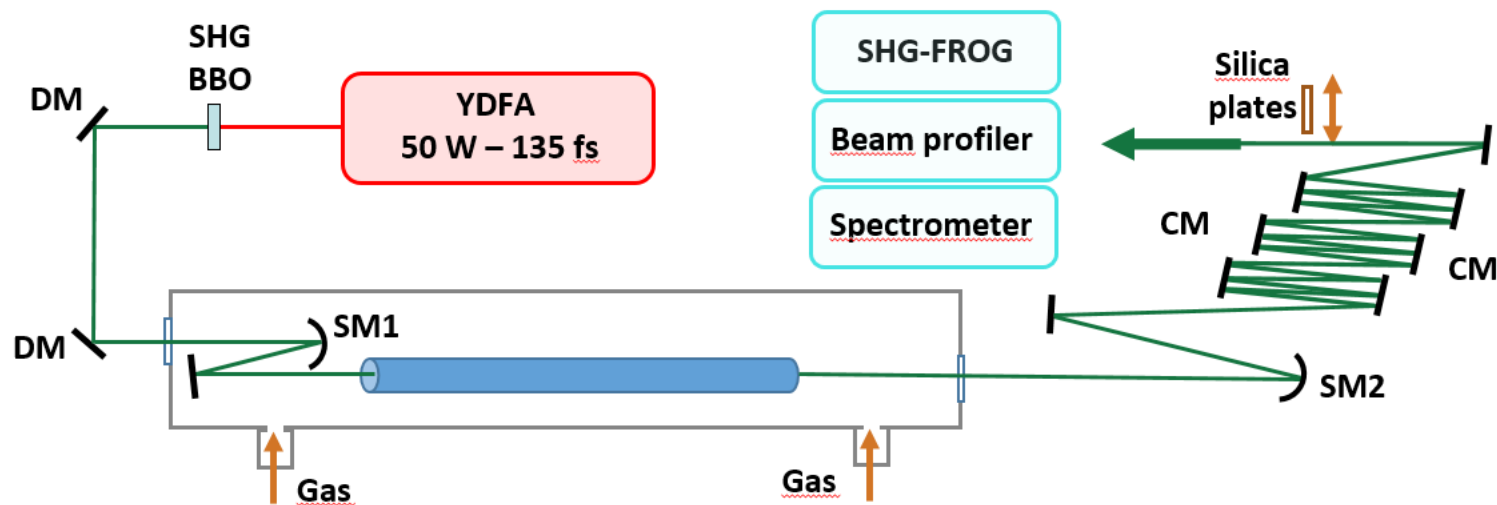
DOMINIQUE DESCAMPS,^{1,*} FLORENT GUICHARD,² STÉPHANE PETIT,¹ SANDRA BEAUVARLET, ANTOINE COMBY,¹ LOÏC LAVENU,² AND YOANN ZAOUTER,²

¹Université Bordeaux- CNRS- CEA, CELIA, UMR 5107, F33405 Talence, France

²Amplitude Laser Group, 33600 Pessac, France

*Corresponding author: dominique.descamps@u-bordeaux.fr

Received XX Month XXXX; revised XX Month, XXXX; accepted XX Month XXXX; posted XX Month XXXX (Doc. ID XXXXX); published XX Month XXXX



Propagation in hollow-core fiber : homogeneous effect of SPM

Handwaving: Propagation mixes the different parts of the beam, leading to homogeneity

Nonlinear medium? Rare gas introduced at controlled pressure, ~ changing medium optical thickness

Recompression:

Set of chirped mirrors. 18 bounces \rightarrow -1000 fs^2

Additional silica plates \rightarrow fine tune the dispersion, adding positive GDD.

Optimal dispersion: -850 fs^2

Postcompression in a hollow core fiber

Generation of high power sub-15 fs pulses at 515 nm through nonlinear compression of an Yb-doped ultrafast fiber amplifier

DOMINIQUE DESCAMPS,^{1,*} FLORENT GUICHARD,² STÉPHANE PETIT,¹ SANDRA BEAUVARLET, ANTOINE COMBY,¹ LOÏC LAVENU,² AND YOANN ZAOUTER,²

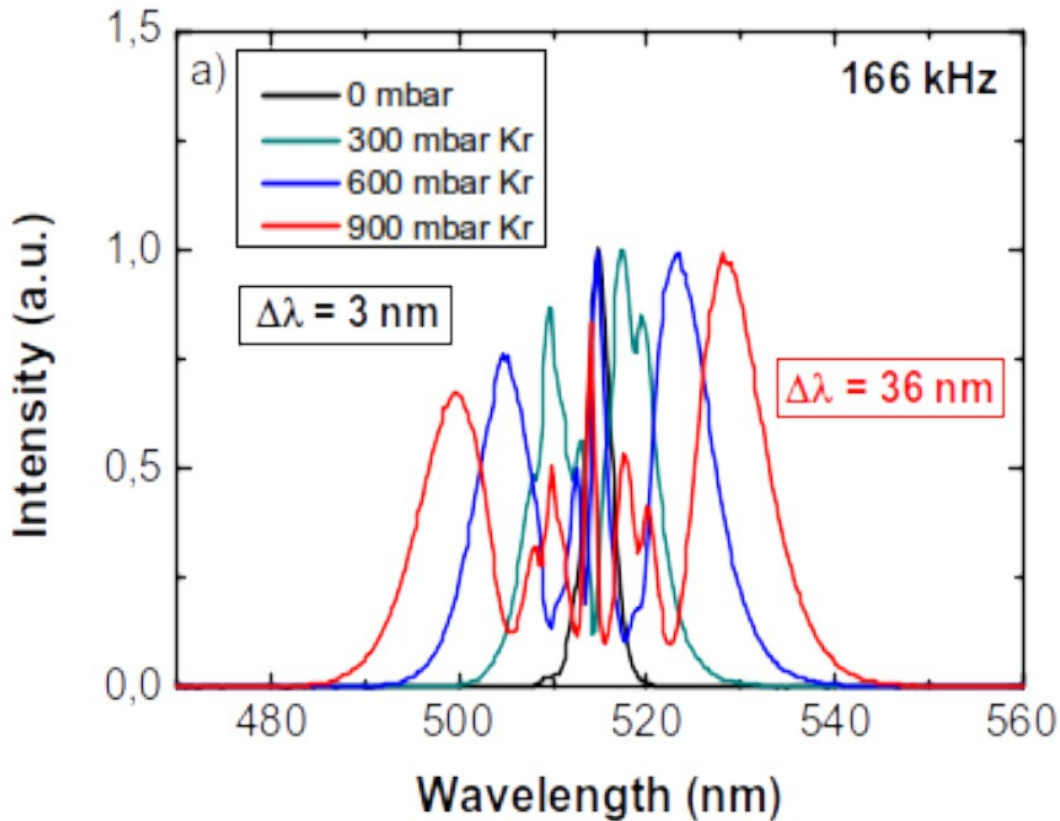
¹Université Bordeaux- CNRS- CEA, CELIA, UMR 5107, F33405 Talence, France

²Amplitude Laser Group, 33600 Pessac, France

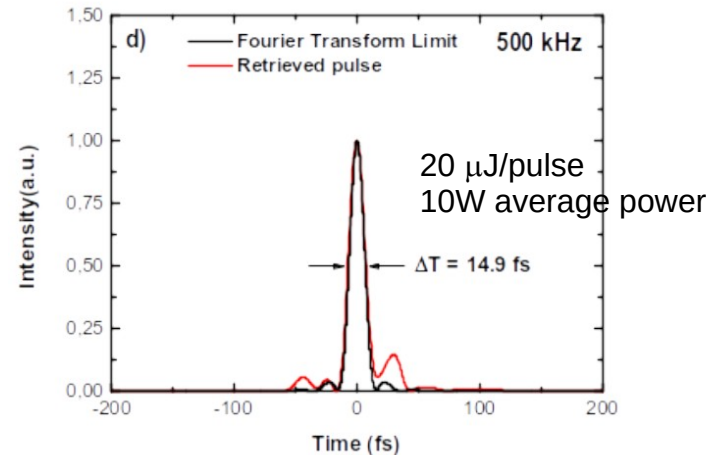
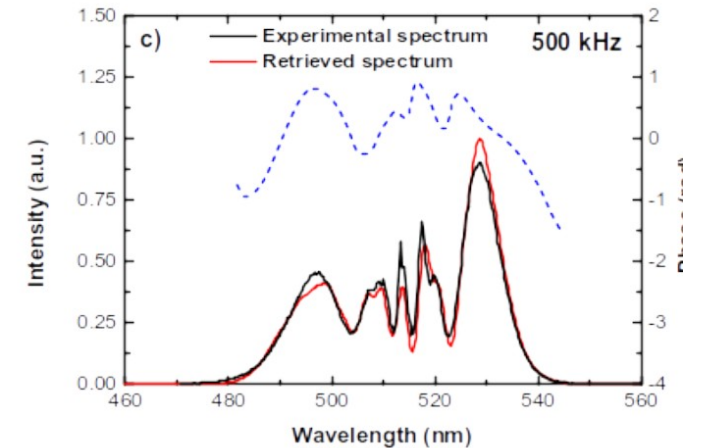
*Corresponding author: dominique.descamps@u-bordeaux.fr

Received XX Month XXXX; revised XX Month, XXXX; accepted XX Month XXXX; posted XX Month XXXX (Doc. ID XXXXX); published XX Month XXXX

Spectral measurements



Temporal characterization (see next course)



Efficient postcompression scheme: 15fs, 20 μJ , 500kHz (10W)
Some losses due to coupling to higher order modes in the capillary. Transmission = 78%

Generation of high energy 10 fs pulses by a new pulse compression technique

M. Nisoli, S. De Silvestri, and O. Svelto
 Centro di Elettronica Quantistica e Strumentazione Elettronica–CNR, Dipartimento di Fisica, Politecnico,
 Piazza L. da Vinci 32, 20133 Milano, Italy

(Received 12 January 1996; accepted for publication 11 March 1996)

Applied Physics Letters **68**, 2793 (1996); doi: 10.1063/1.116609

5224 OPTICS LETTERS / Vol. 39, No. 17 / September 1, 2014

53 W average power few-cycle fiber laser system generating soft x rays up to the water window

Jan Rothhardt,^{1,2,*} Steffen Hädrich,^{1,2} Arno Klenke,^{1,2} Stefan Demmler,¹ Armin Hoffmann,¹ Thomas Gotschall,¹
 Tino Eidam,¹ Manuel Krebs,¹ Jens Limpert,^{1,2} and Andreas Tünnermann^{1,2,3}

¹Institute of Applied Physics, Abbe Center of Photonics, Friedrich-Schiller University Jena, Albert-Einstein-Straße 15, 07745 Jena, Germany

²Helmholtz-Institute Jena, Fröbelstieg 3, 07743 Jena, Germany

³Fraunhofer Institute of Applied Optics and Precision Engineering, Albert-Einstein-Straße 7, 07745 Jena, Germany

*Corresponding author: j.rothhardt@gsi.de

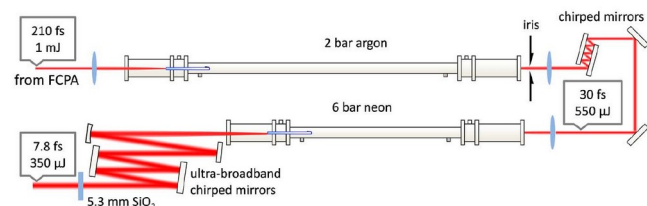


Fig. 1. Experimental setup of the two nonlinear compression stages that reduce the pulse duration from the initial 210 to 30 fs and 7.8 fs.

Ouillé et al. *Light: Science & Applications* (2020)9:47
<https://doi.org/10.1038/s41377-020-0280-5>

Official journal of the CIOMP 2047-7538
www.nature.com/lsa

ARTICLE

Open Access

Relativistic-intensity near-single-cycle light waveforms at kHz repetition rate

Marie Ouillé,^{1,2} Aline Vernier,¹ Frederik Böhle,¹ Maimouna Bocoum,¹ Aurélie Jullien,¹ Magali Lozano,¹
 Jean-Philippe Rousseau,¹ Zhao Cheng,¹ Dominykas Gustas,¹ Andreas Blumenstein,³ Peter Simon,³ Stefan Haessler,¹
 Jérôme Faure,¹ Tamas Nagy,⁴ and Rodrigo Lopez-Martens¹

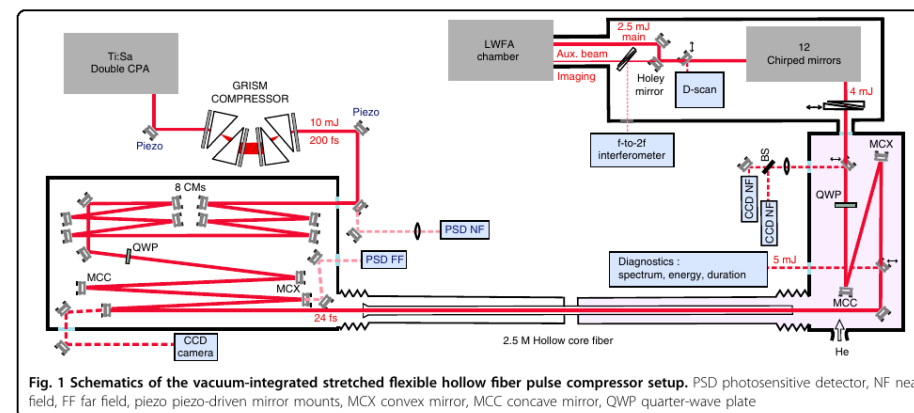
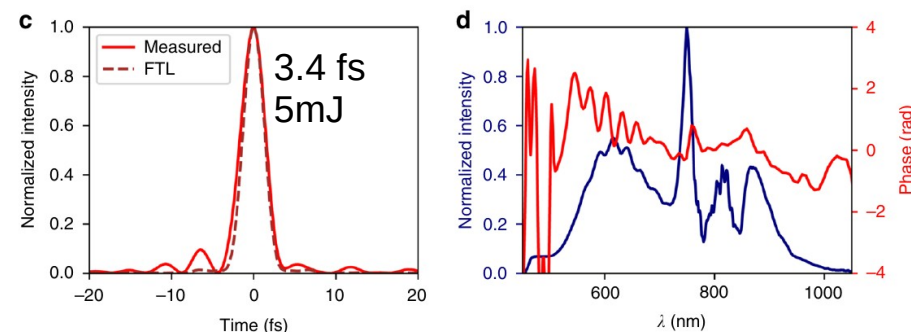


Fig. 1 Schematics of the vacuum-integrated stretched flexible hollow fiber pulse compressor setup. PSD photosensitive detector, NF near field, FF far field, piezo piezo-driven mirror mounts, MCX convex mirror, MCC concave mirror, QWP quarter-wave plate



Generation of three-cycle multi-millijoule laser pulses at 318 W average power

TAMAS NAGY,^{1,*†} STEFFEN HÄDRICH,^{2,8,†} PETER SIMON,^{3,9,†} ANDREAS BLUMENSTEIN,³ NICO WALTHER,²
 ROBERT KLAS,^{4,5} JOACHIM BULDT,⁴ HENNING STARK,⁴ SVEN BREITKOPF,² PÉTER JÓJÁRT,⁶ IMRE SERES,⁶
 ZOLTÁN VÁRALLYAY,⁶ TINO EIDAM,² AND JENS LIMPERT^{2,4,5,7}

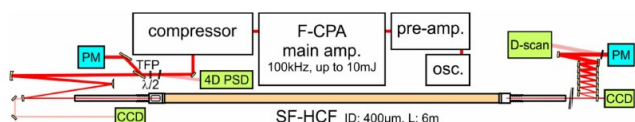
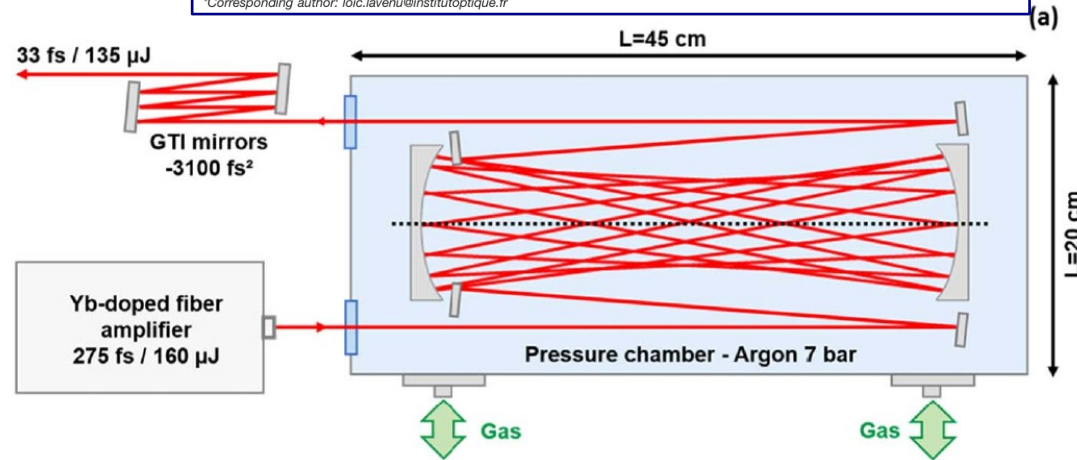
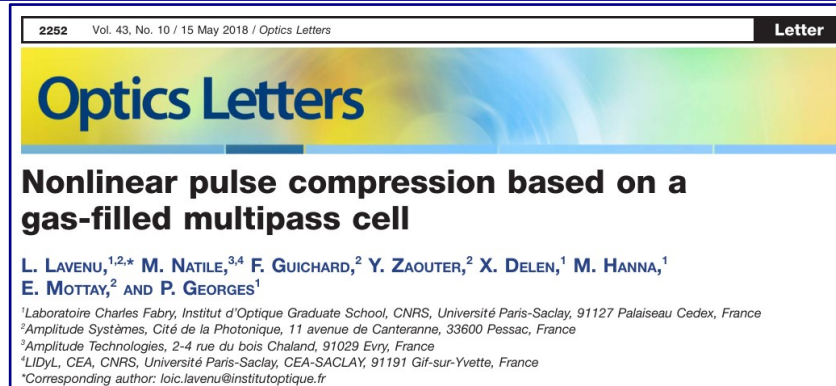


Fig. 1. Experimental layout. F-CPA, fiber chirped pulse amplifier; HCF, stretched flexible hollow-core fiber; d-scan, dispersion scan device; PM, water-cooled power meter; 4D PSD, position-sensitive detectors for near and far field; TFP, thin-film polarizer; $\lambda/2$, half-wave plate; CCD, camera.

Postcompression in a multipass cell



Propagation in cavity : homogeneous effect of SPM

Handwaving: inhomogeneities washed out by mode propagation in the cavity

34 roundtrips. Total distance 20 m

Nonlinear medium?

7 bars of argon. This gas pressure results in a nonlinear index $n_2 = 6.5 \times 10^{-23} \text{ m}^2/\text{W}$ and a group velocity dispersion $\beta_2 = 110 \text{ fs}^2/\text{m}$ [17].

Recompression:

Gires Tournoi Interferometer mirrors $\rightarrow -250 \text{ fs}^2$ per bounce + -100 fs^2 per bounce

Optimal dispersion: -3100 fs^2

What about spatial homogeneity of the beam?

Postcompression in a multipass cell

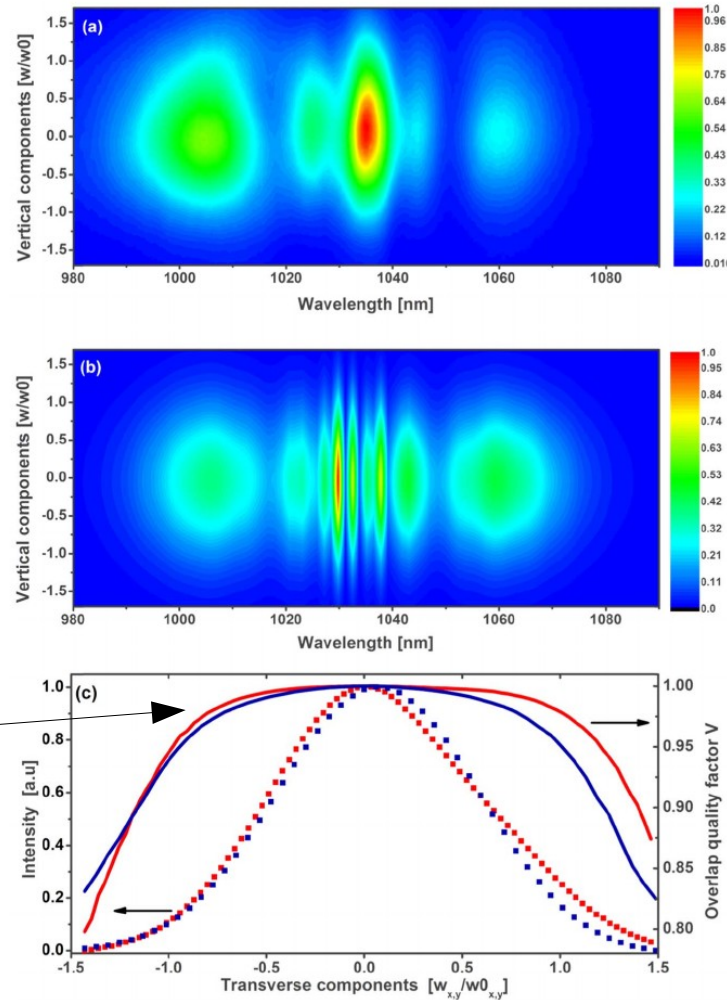
2252 Vol. 43, No. 10 / 15 May 2018 / Optics Letters Letter

Optics Letters

Nonlinear pulse compression based on a gas-filled multipass cell

L. LAVENU,^{1,2,*} M. NATILE,^{3,4} F. GUICHARD,² Y. ZAOUTER,² X. DELEN,¹ M. HANNA,¹
E. MOTTAY,² AND P. GEORGES¹

¹Laboratoire Charles Fabry, Institut d'Optique Graduate School, CNRS, Université Paris-Saclay, 91127 Palaiseau Cedex, France
²Amplitude Systèmes, Cité de la Photonique, 11 avenue de Canteranne, 33600 Pessac, France
³Amplitude Technologies, 2-4 rue du bois Chaland, 91029 Evry, France
⁴LIDyL, CEA, CNRS, Université Paris-Saclay, CEA-SACLAY, 91191 Gif-sur-Yvette, France
*Corresponding author: loic.lavenu@institutoptique.fr



Overlap integral of the spectrum at location
With the spectrum at center
>90% wherever intensity >10%

Fig. 4. Spatio-spectral couplings at the output of the cavity in the vertical axis. (a) Experimental spectro-imaging measurement. (b) Simulated spectro-imaging measurement. (c) Spatio-spectral quality factor measured with a spectro-imaging setup: vertical axis (red), horizontal axis (blue).

Good spatial homogeneity of the spectrum

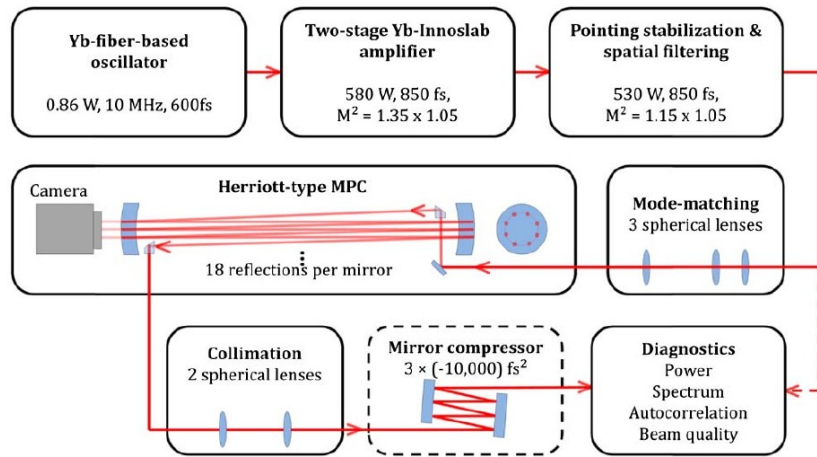
Postcompression in a multipass cell – more references

Optics Letters

Nonlinear pulse compression in a multi-pass cell

JAN SCHULTE,^{1,*} THOMAS SARTORIUS,¹ JOHANNES WEITENBERG,^{1,2} ANDREAS VERNALEKEN,² AND PETER RUSSBUEDT¹

¹Fraunhofer-Institut für Lasertechnik ILT, Steinbachstraße 15, 52074 Aachen, Germany
²Max-Planck-Institut für Quantenoptik, Hans-Kopfermann-Straße 1, 85748 Garching, Germany

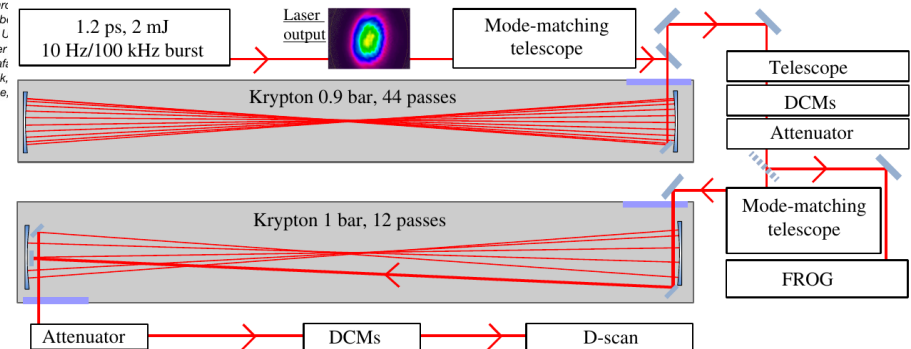


Optics Letters

Postcompression of picosecond pulses into the few-cycle regime

PRANNAY BALLA,^{1,2,1,*} AMMAR BIN WAHID,^{1,1} IVAN SYTCEVICH,³ CHEN GUO,³ ANNE-LISE VIOTTI,³ LAURA SILLETTI,^{1,4} ANDREA CARTELLA,⁵ SKIRMANTAS ALISAUSKAS,¹ HAMED TAVAKOL,¹ UWE GROSSE-WORTMANN,¹ ARTHUR SCHÖNBERG,^{1,2} MARCUS SEIDEL,¹ ANDREA TRABATTONI,^{1,4} BASTIAN MANSCHWETUS,¹ TINO LANG,¹ FRANCESCA CALEGARI,^{1,4,5,6} ARNAUD COUAIRON,⁷ ANNE L'HUILLIER,³ CORD L. ARNOLD,³ INGMAR HARTL,¹ AND CHRISTOPH M. HEYL^{1,2,8}

¹Deutsches Elektronen-Synchrotron
²Helmholtz-Institute Jena, Fröb
³Department of Physics, Lund U
⁴Center for Free-Electron Laser
⁵The Hamburg Centre for Ultraf
⁶Institut für Experimentalphysik,
⁷Centre de Physique Théorique,

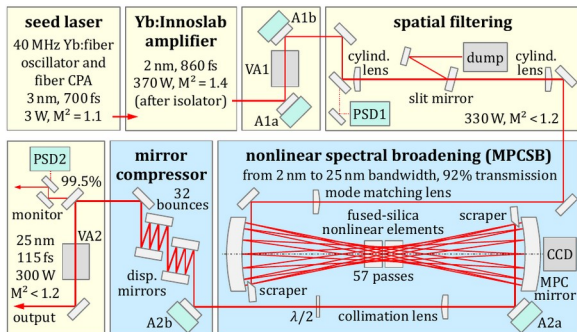


Optics EXPRESS

Multi-pass-cell-based nonlinear pulse compression to 115 fs at 7.5 μJ pulse energy and 300 W average power

JOHANNES WEITENBERG,^{1,2,*} ANDREAS VERNALEKEN,¹ JAN SCHULTE,² AKIRA OZAWA,¹ THOMAS SARTORIUS,² VLADIMIR PERVAK,¹ HANS-DIETER HOFFMANN,² THOMAS UDEM,¹ PETER RUSSBUEDT,² AND THEODOR W. HÄNSCH¹

¹Max-Planck-Institut für Quantenoptik MPQ,
²Fraunhofer-Institut für Lasertechnik ILT, Sie

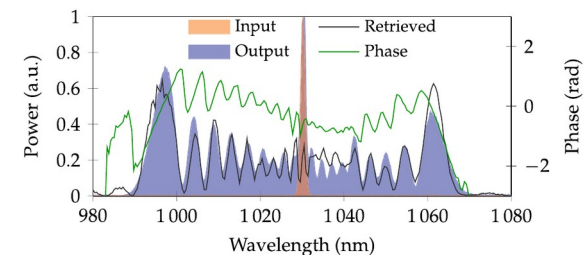
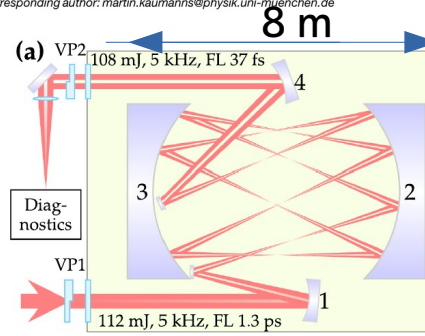


Optics Letters

Spectral broadening of 112 mJ, 1.3 ps pulses at 5 kHz in a LG₁₀ multipass cell with compressibility to 37 fs

MARTIN KAUMANN,^{1,*} DMITRII KORMIN,¹ THOMAS NUBBEMEYER,¹ VLADIMIR PERVAK,¹ AND STEFAN KARSCH^{1,2}

¹Ludwig-Maximilians-Universität München, Am Coulombwall 1, 85748 Garching, Germany
²Max-Planck-Institut für Quantenoptik, Hans-Kopfermann-Str. 1, 85748 Garching, Germany
 *Corresponding author: martin.kaumanns@physik.uni-muenchen.de



Recap on postcompression

ADVANCES IN PHYSICS: X
2020, VOL. 6, NO. 1, 10.1080/23746149.2020.1845795
<https://doi.org/10.1080/23746149.2020.1845795>



OPEN ACCESS Check for updates

High-energy few-cycle pulses: post-compression techniques

Tamas Nagy^a, Peter Simon^b and Laszlo Veisz^c

^aMax Born Institute for Nonlinear Optics and Short Pulse Spectroscopy, Berlin, Germany; ^bInstitute for Nanophotonics Göttingen e.V.*, Göttingen, Germany; ^cDepartment of Physics, Umeå University, SE-901 87, Umeå, Sweden

HC-PCF: Hollow Core Photonic Crystal Fiber
HCF: Hollow Core Fiber
SF-HCF: Stretched Hollow Core Fiber

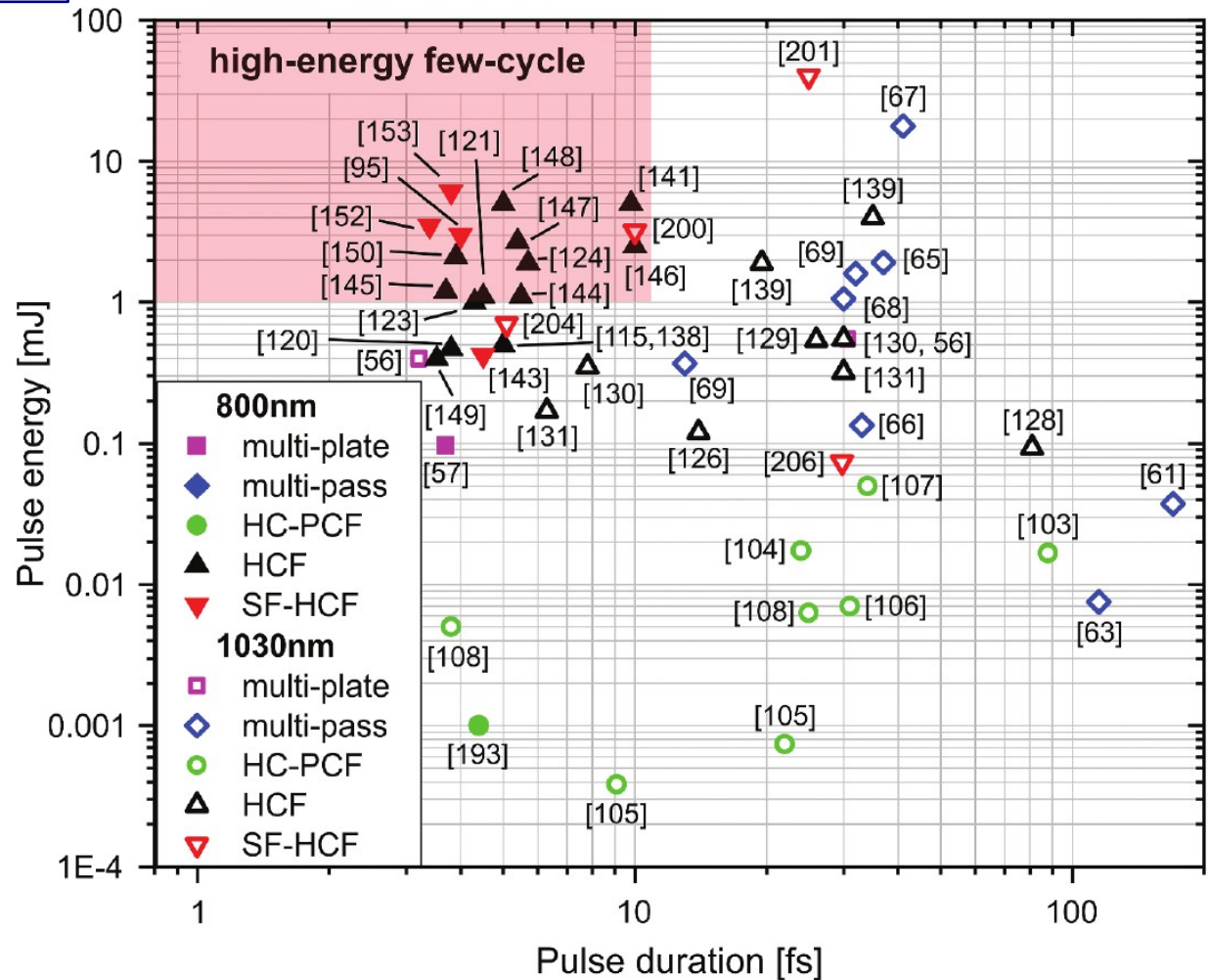


Figure 10. Pulse energy versus pulse duration in compression experiments in the near-infrared range. The red-shaded area in represents the high-energy few-cycle regime.

Attosecond nonlinear polarization and light-matter energy transfer in solids

A. Sommer^{1*}, E. M. Bothschafter^{1,2*}†, S. A. Sato³, C. Jakubeit¹, T. Latka¹, O. Razskazovskaya¹, H. Fattahi¹, M. Jobst¹, W. Schweinberger^{1,2}, V. Shirvanyan¹, V. S. Yakovlev^{1,4}, R. Kienberger⁵, K. Yabana^{3,6}, N. Karpowicz¹, M. Schultze^{1,2} & F. Krausz^{1,2}

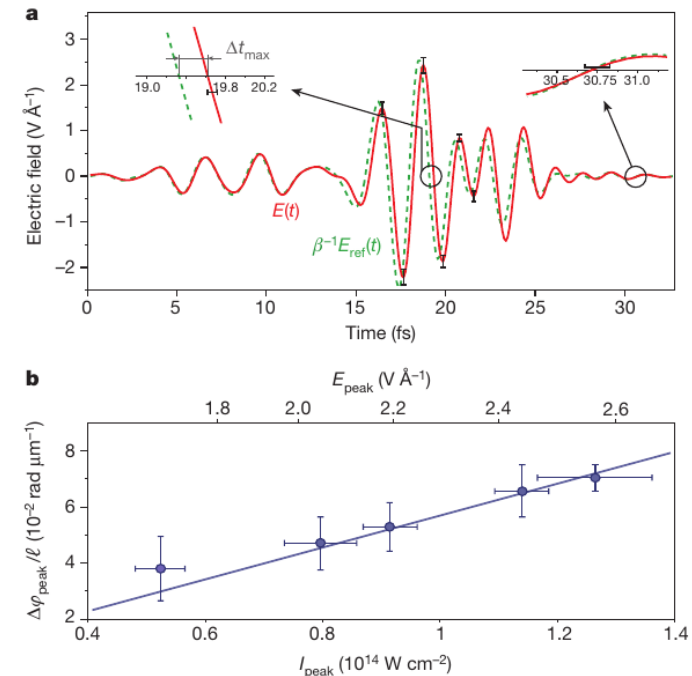
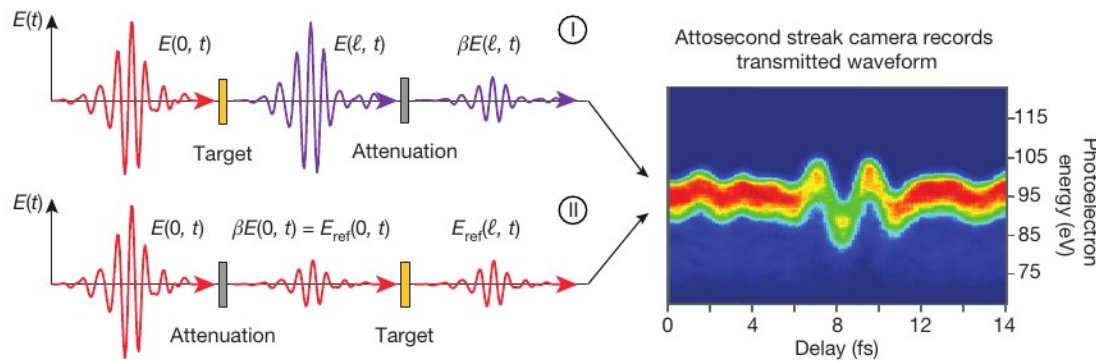


Figure 2 | Sub-femtosecond-resolved optical Kerr effect in silica.

a, After passage through a 10- μm -thick fused silica sample, the electric field $E(t)$ of the few-cycle near-infrared pulse with a peak intensity of $1.3 \times 10^{14} \text{ W cm}^{-2}$, approximately 10% below the threshold for optical damage, is modified as a result of the nonlinear light-matter interaction, as revealed by its comparison to a low-intensity ($I_{\text{peak}} = 7 \times 10^{12} \text{ W cm}^{-2}$) reference waveform $E_{\text{ref}}(t)$ (for $\beta = 0.27$). This comparison yields a transient positive phase shift induced by the strong field, as anticipated from the dynamic increase of the refractive index owing to the optical Kerr effect. The two insets show close-ups of the comparison near the centre and at the end of the pulse, revealing the full reversibility of the effect. $E(t)$ and $E_{\text{ref}}(t)$ are obtained from averaging a set of three recordings performed under identical conditions on individual samples. **b**, The phase shift $\Delta \varphi_{\text{peak}}$ evaluated at the peak of the field envelope for different peak intensities I_{peak} of $E(t)$ is found to exhibit a linear dependence on the field intensity. Each data point represents the mean value of three individual recordings under identical conditions; the error bars indicate the standard deviation.

Introduction: time-frequency travel

Keeping ultrashort pulses ultrashort

Self-phase modulation – the enemy within

Mirror mirror

Producing circularly polarized pulses – a perfect circle

Focus

Why bother about mirrors?

Ubiquitous in experimental setups

We've seen that chirped-mirrors could induce strong dispersion

What about "regular" mirrors?

Getting the dispersion of metallic mirrors

RefractiveIndex.INFO

Refractive index database

ENHANCED BY Google

The complex refractive index gives the complex reflection coefficients through Fresnel equations

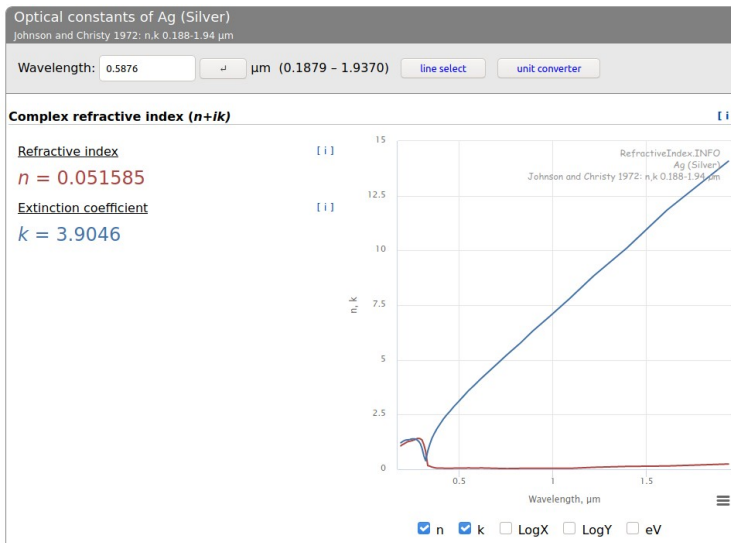


WIKIPEDIA
The Free Encyclopedia

Article Talk

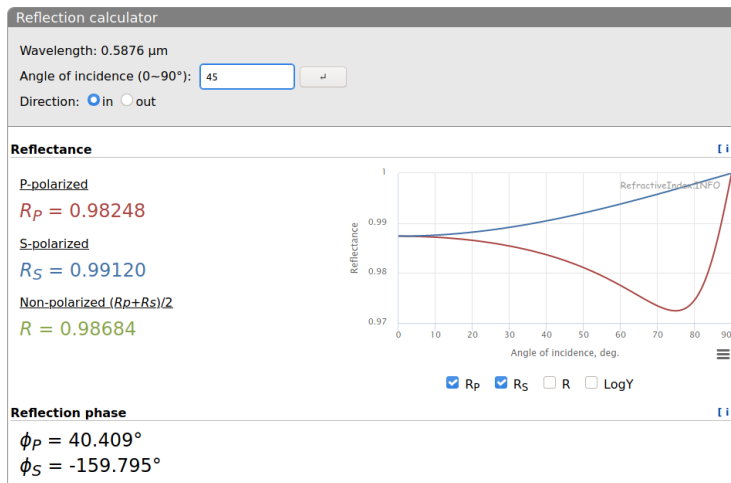
Fresnel equations

From Wikipedia, the free encyclopedia



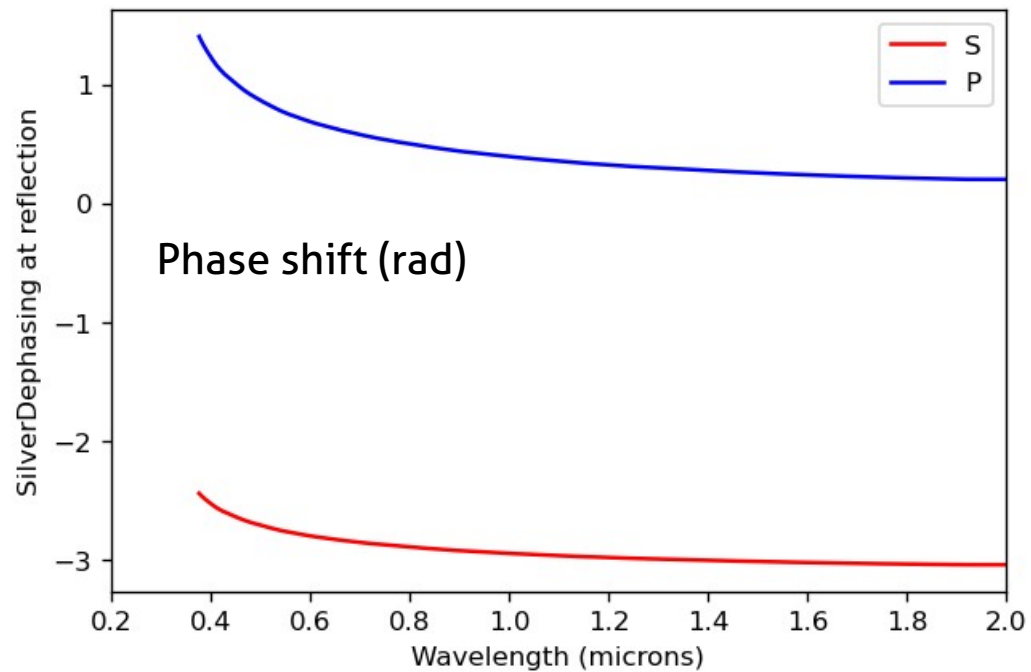
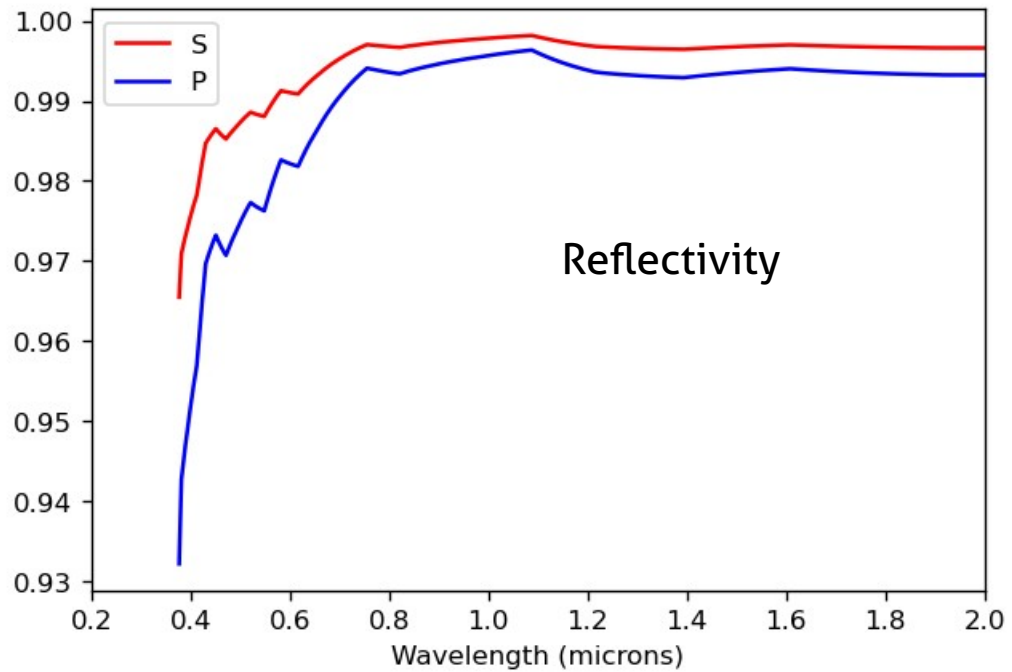
$$R_s = \left| \frac{n_1 \cos \theta_i - n_2 \cos \theta_t}{n_1 \cos \theta_i + n_2 \cos \theta_t} \right|^2 = \left| \frac{n_1 \cos \theta_i - n_2 \sqrt{1 - \left(\frac{n_1}{n_2} \sin \theta_i\right)^2}}{n_1 \cos \theta_i + n_2 \sqrt{1 - \left(\frac{n_1}{n_2} \sin \theta_i\right)^2}} \right|^2$$

$$R_p = \left| \frac{n_1 \cos \theta_t - n_2 \cos \theta_i}{n_1 \cos \theta_t + n_2 \cos \theta_i} \right|^2 = \left| \frac{n_1 \sqrt{1 - \left(\frac{n_1}{n_2} \sin \theta_i\right)^2} - n_2 \cos \theta_i}{n_1 \sqrt{1 - \left(\frac{n_1}{n_2} \sin \theta_i\right)^2} + n_2 \cos \theta_i} \right|^2$$



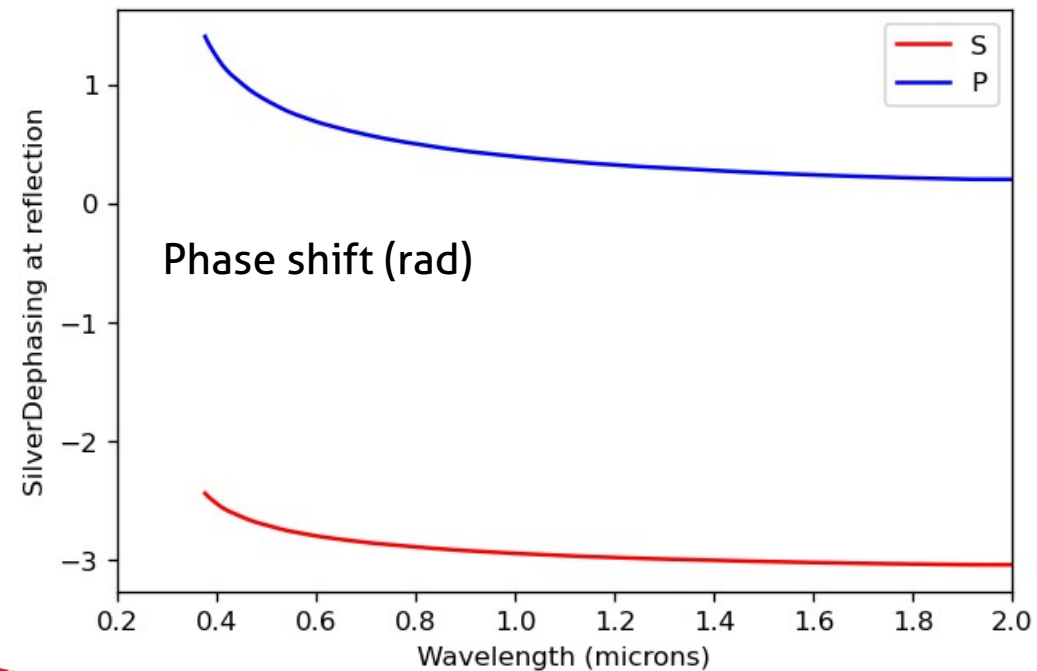
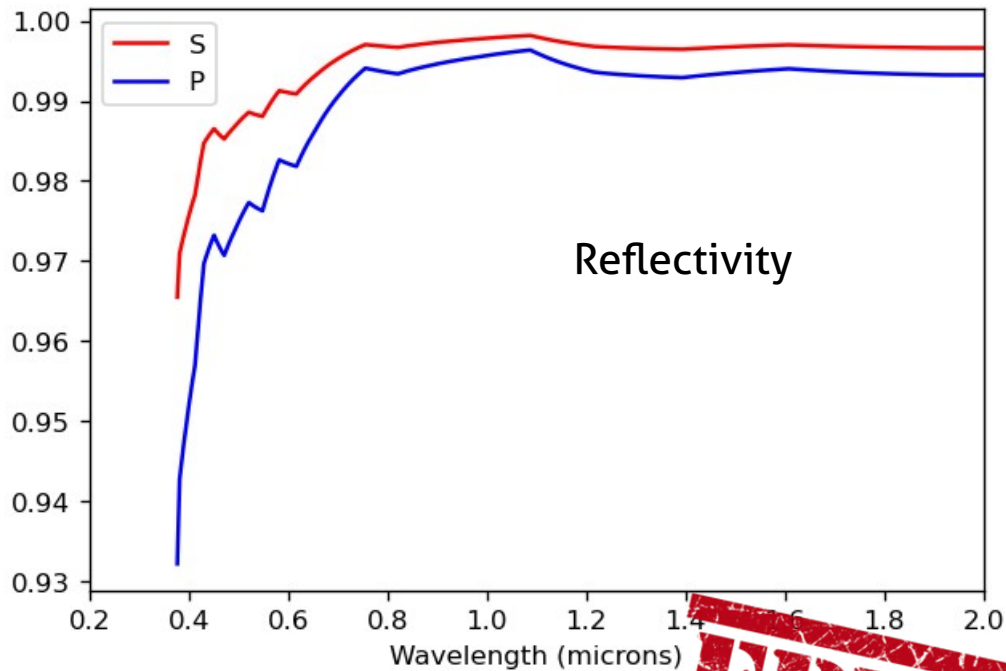
The modulus square gives the reflectivity
The phase of sqrt(R) gives the dephasing at reflection

Silver mirror reflectivity and dephasing



The phase is not linear \rightarrow GDD!

Getting the dispersion of metallic mirrors

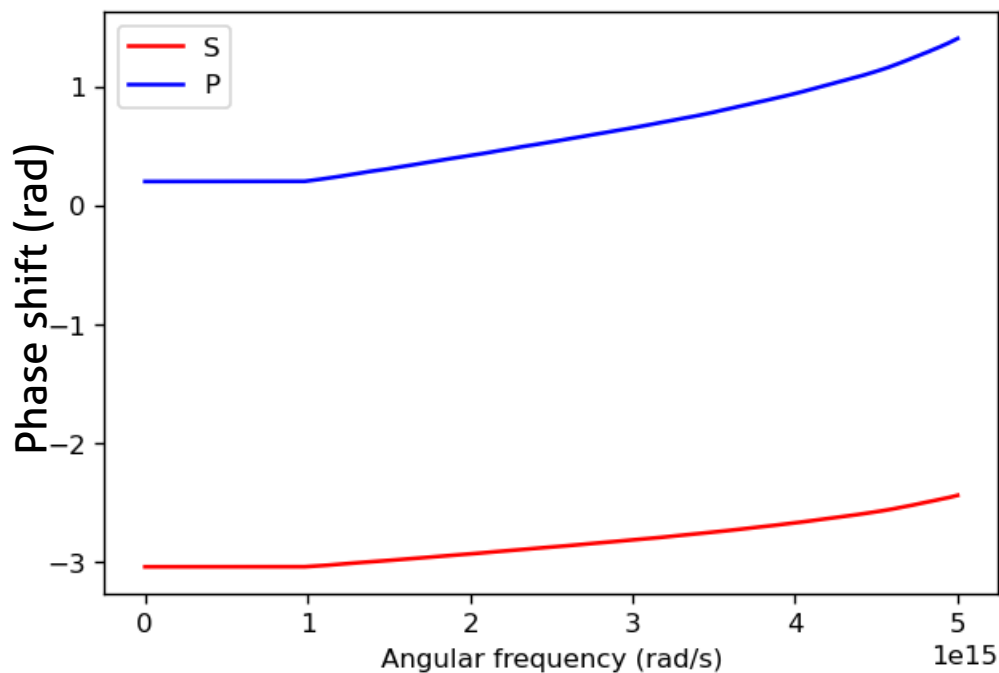
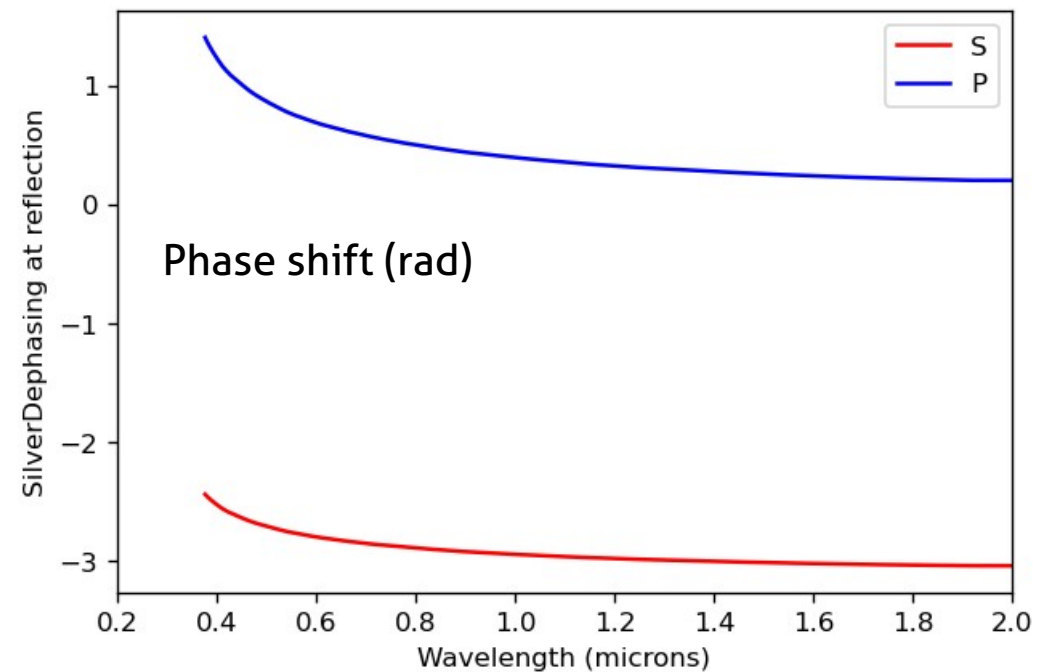
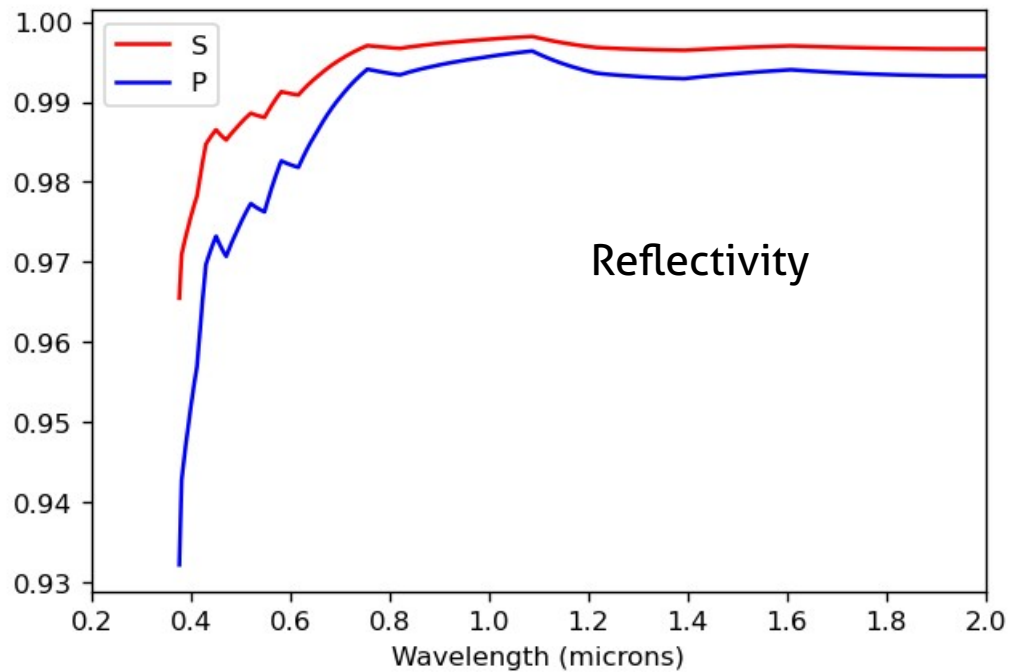


The phase is not linear → GDD!

The spectral phase is defined along the frequency / angular frequency / photon energy coordinate
Not the wavelength.

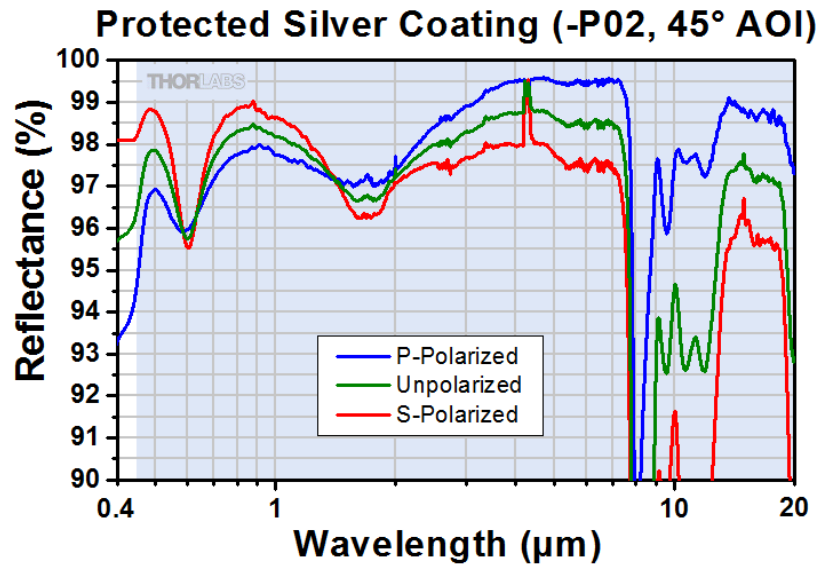
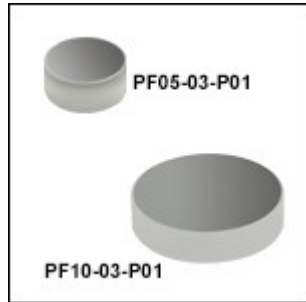
$\omega = 2\pi c / \lambda \rightarrow$ nonlinear mapping between ω and λ

Getting the dispersion of metallic mirrors

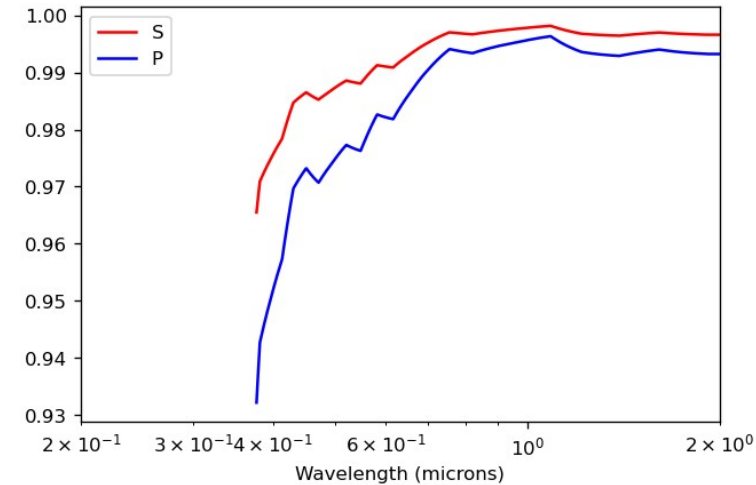


Now you can say:
The phase is not linear \rightarrow GDD!

Commercial Ag mirrors



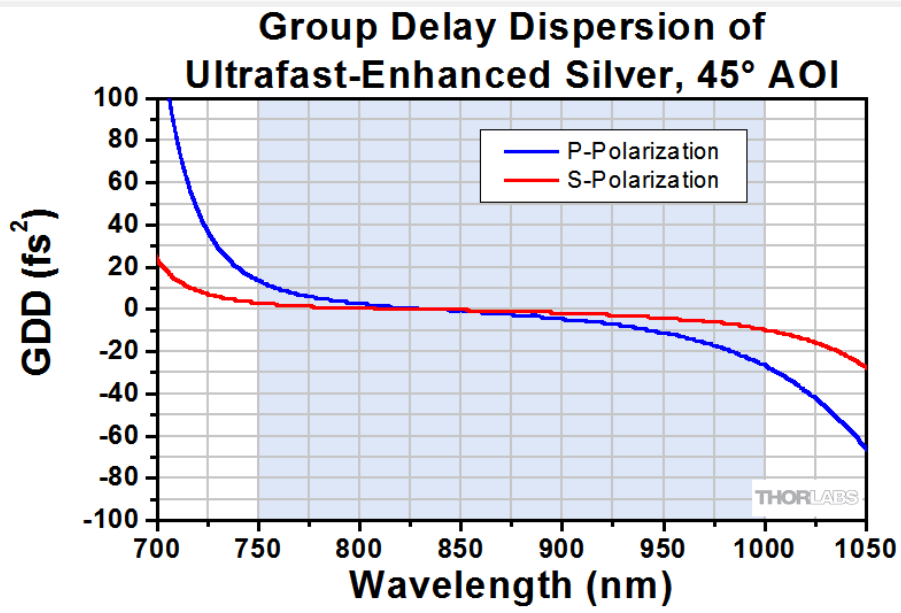
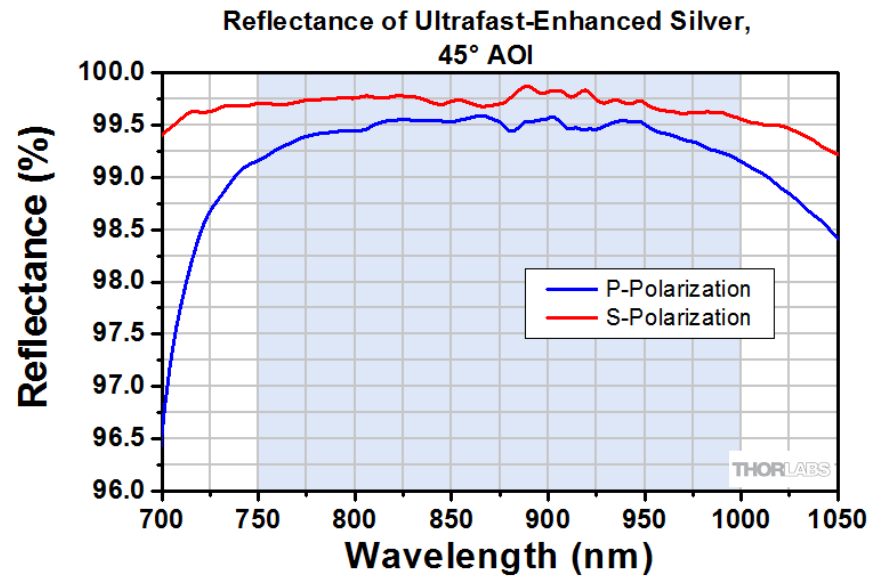
From Ag Fresnel equations



The Protected Silver mirror has a different reflectivity than the bare Ag mirror (but you can't really buy bare Ag mirrors)

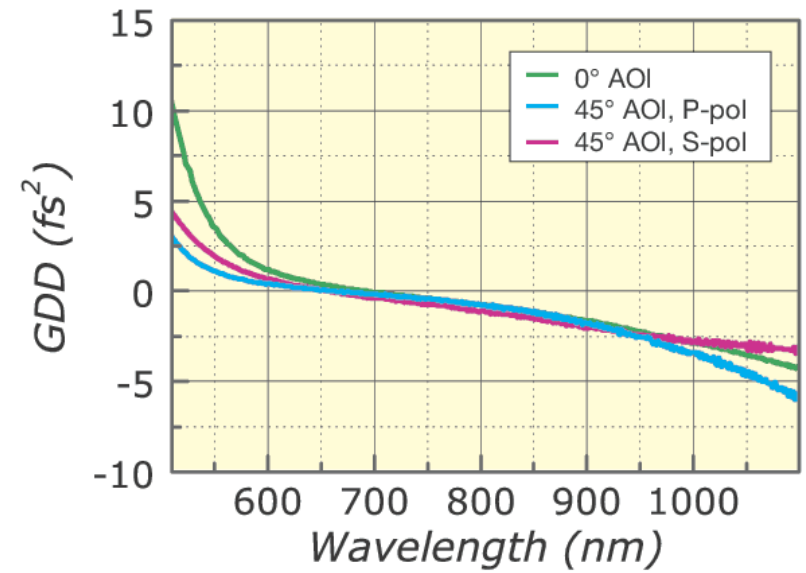
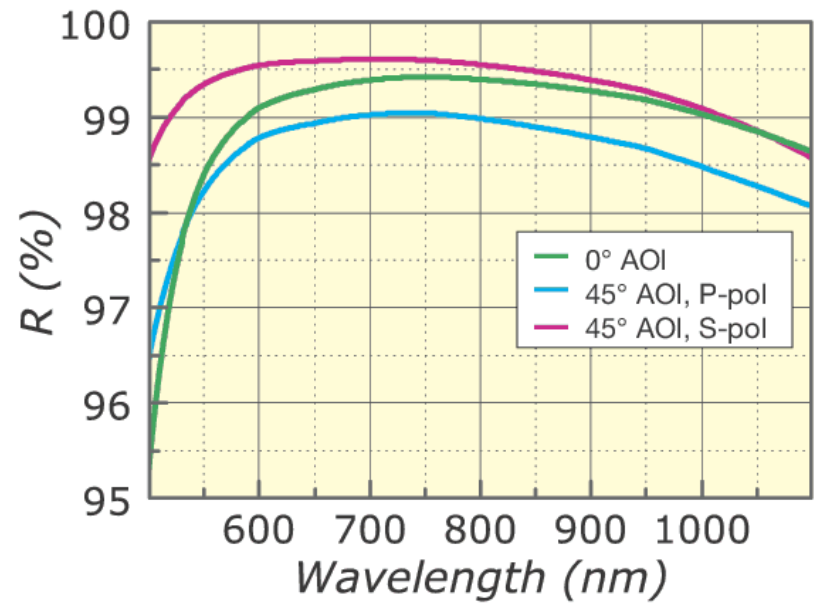
Note the different reflectivity of S and P polarizations
Dip at 600 nm: scary. Probably means high dispersion.
Dispersion not provided by company.

Ultrafast-enhanced silver mirrors

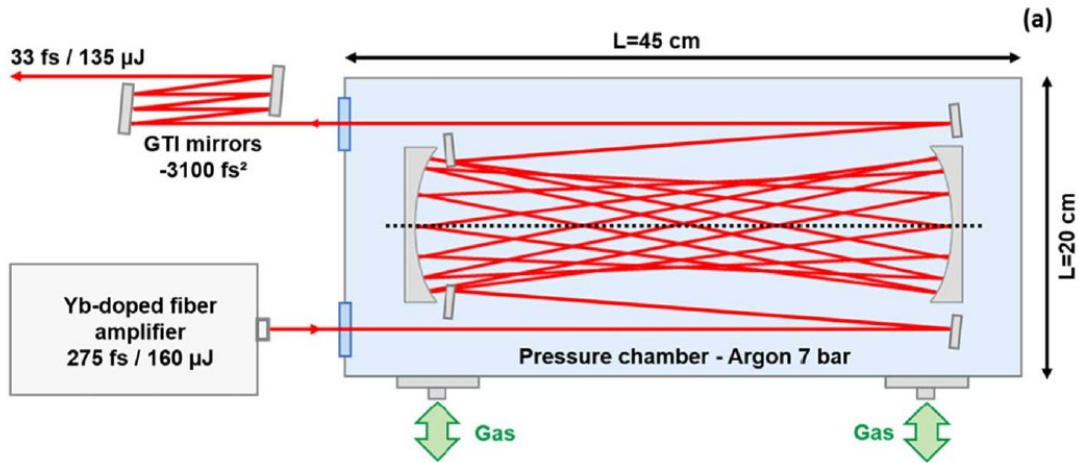


- 10B20EAG.1 Silver Mirror, fs Optimized, 0-45° AOI, 25.4 mm, 600-1000 nm
- 10B20EAG.2 Silver Mirror, fs Optimized, 0-45° AOI, 25.4 mm, 470-1000 nm

In Stock €193



Dielectric multilayer mirrors

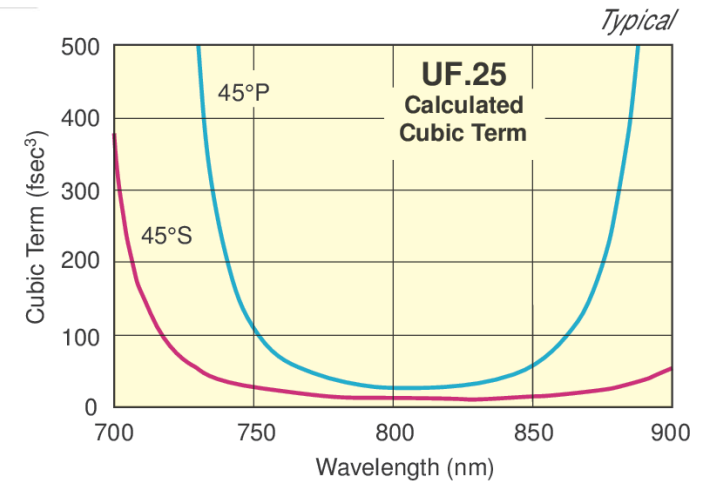
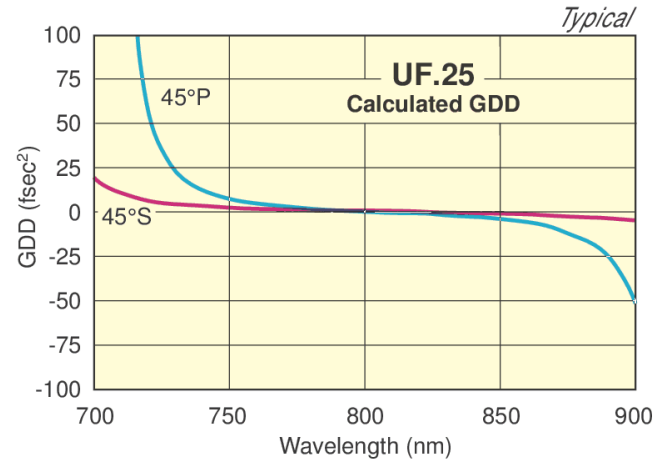
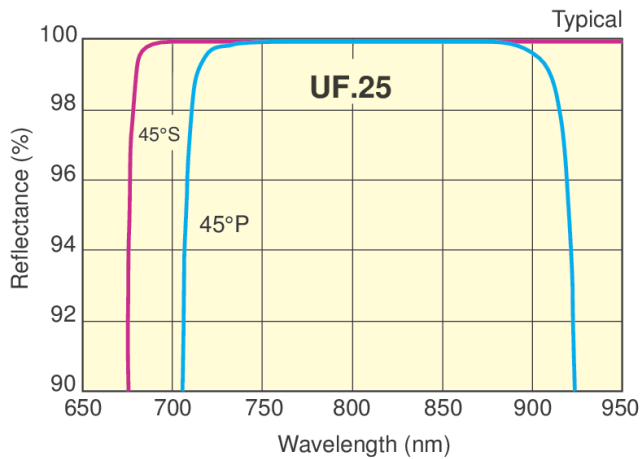


68 bounces inside cavity

$R=90\% \rightarrow \text{Cell transmission } T=0.9^{68}=0.07\%$
 $R=95\% \rightarrow T=3\%$
 $R=99\% \rightarrow T=50\%$
 $R=99.5\% \rightarrow T=71\%$
 $R=99.8\% \rightarrow T=87\%$
 $R=99.9\% \rightarrow T=93\%$

10B20UF.25
Low GDD Ultrafast Mirror, 45° AOI, 25.4 mm, 700-930 nm

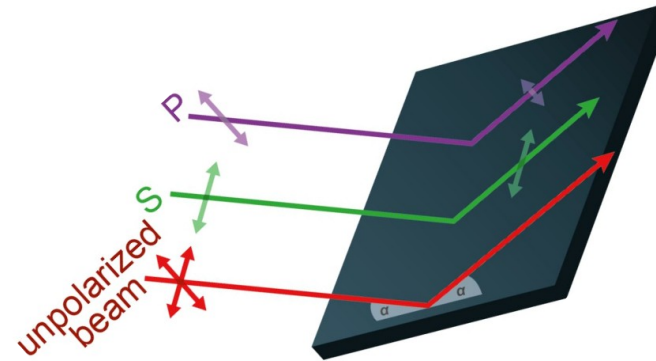
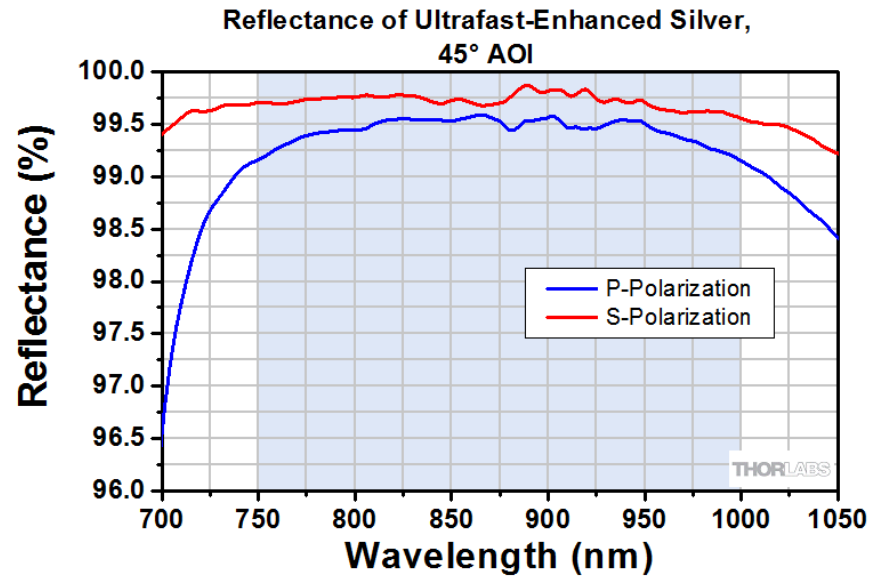
In Stock €223 1 Cart



The bandwidth of dielectric mirrors can be a limitation in cavity postcompression

More trouble: polarization state

The mirror reflectivity is defined for S and P polarizations



In general, you work with S or P polarization

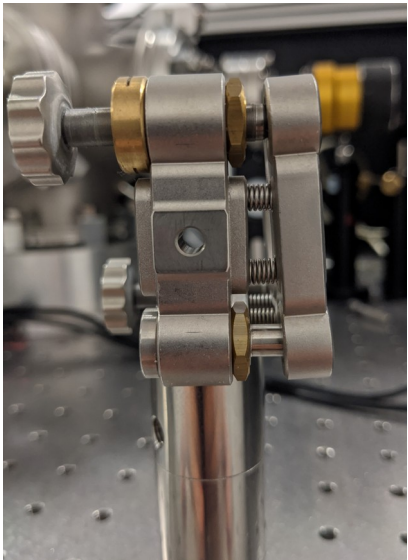
The beam is polarized at the exit of the laser
It remains in the horizontal plane
It doesn't go through birefringent optics
→ OK

More trouble: polarization state

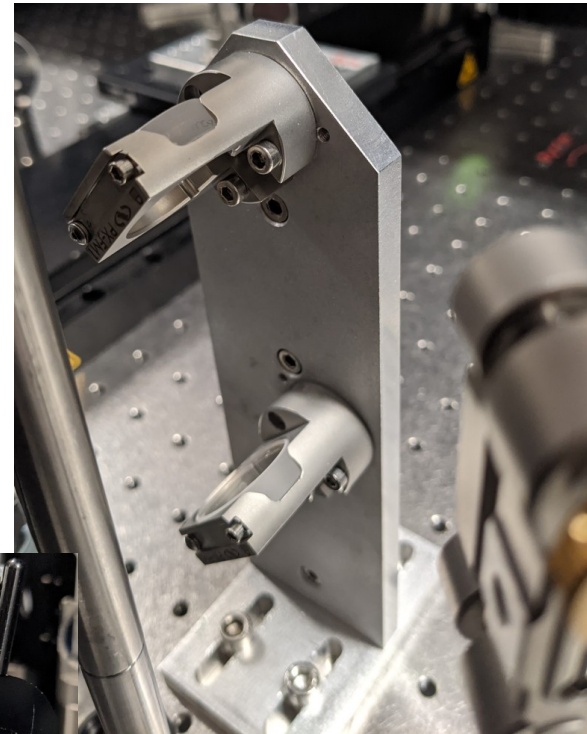
The mirror reflectivity is defined for S and P polarizations

What if :

You change beam height between two distant mirrors?



You change beam height using a periscope?



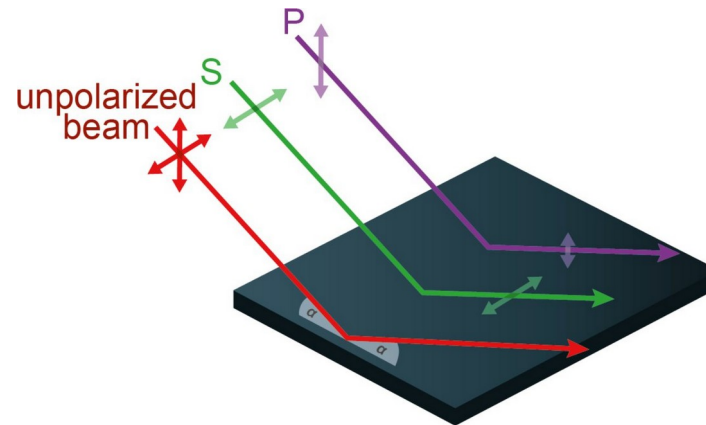
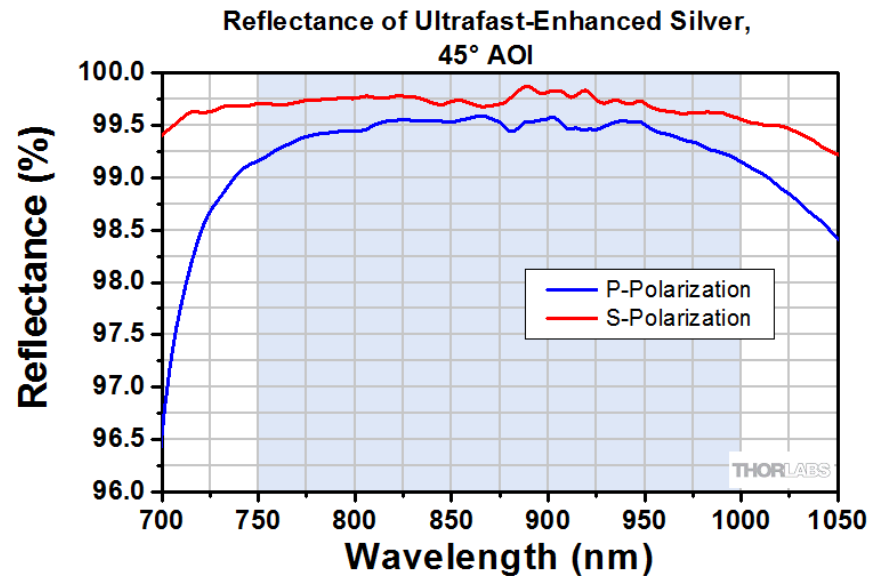
You go through a non-linear crystal for frequency conversion?



You may end up with a polarization state which is neither S or P

More trouble: polarization state

The mirror reflectivity is defined for S and P polarizations



Let us decompose the input beam along S and P directions

Different reflectivity → Rotation of the polarization angle

Phase shift between the two components → Introduces some ellipticity in the laser field

Different GDD between the two components → Complex temporal evolution of the beam polarization

Can we calculate this?

More trouble: polarization state

We send a linearly polarized laser pulse to a set of 45° incidence silver mirror, in a horizontal plane
Mirror complex reflectivity calculated from Fresnel equations
We introduce an initial rotation of the polarization direction with respect to the vertical S polarization
We calculate the resulting pulse polarization, as a function of the number of bounces on mirrors.



See practical 1

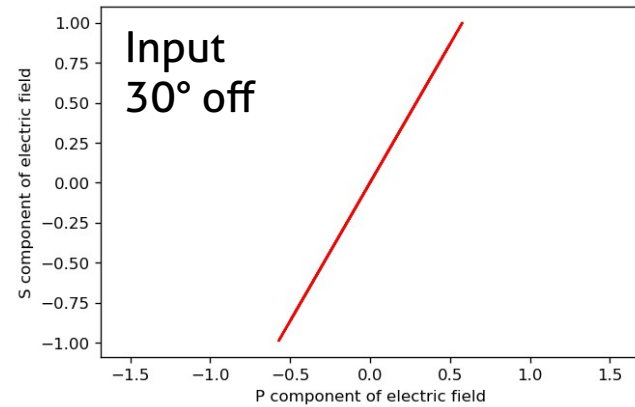
More trouble: polarization state

We send a linearly polarized laser pulse to a set of 45° incidence silver mirror, in a horizontal plane

Mirror complex reflectivity calculated from Fresnel equations

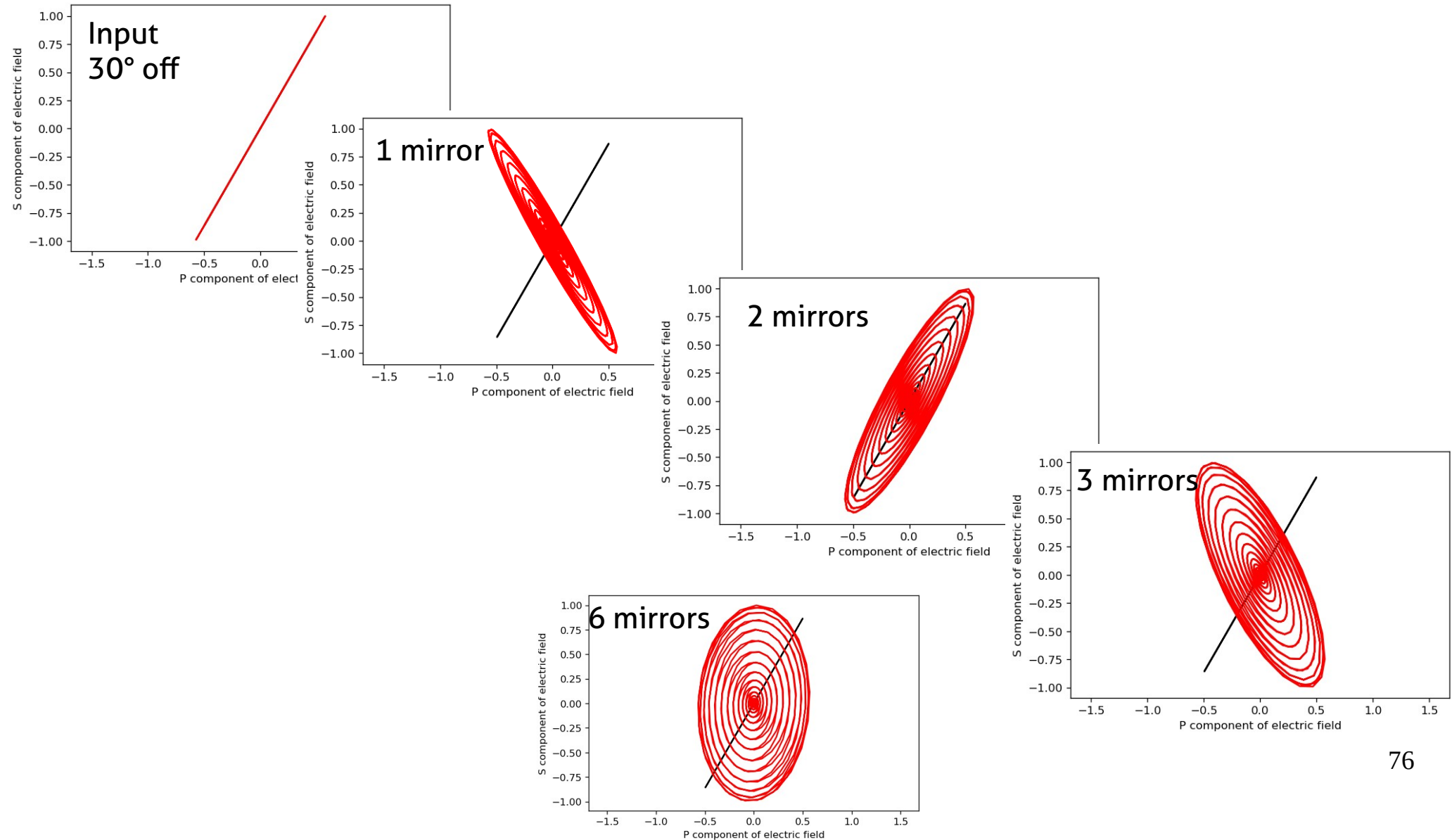
We introduce an initial rotation of the polarization direction with respect to the vertical S polarization

We calculate the resulting pulse polarization, as a function of the number of bounces on mirrors.



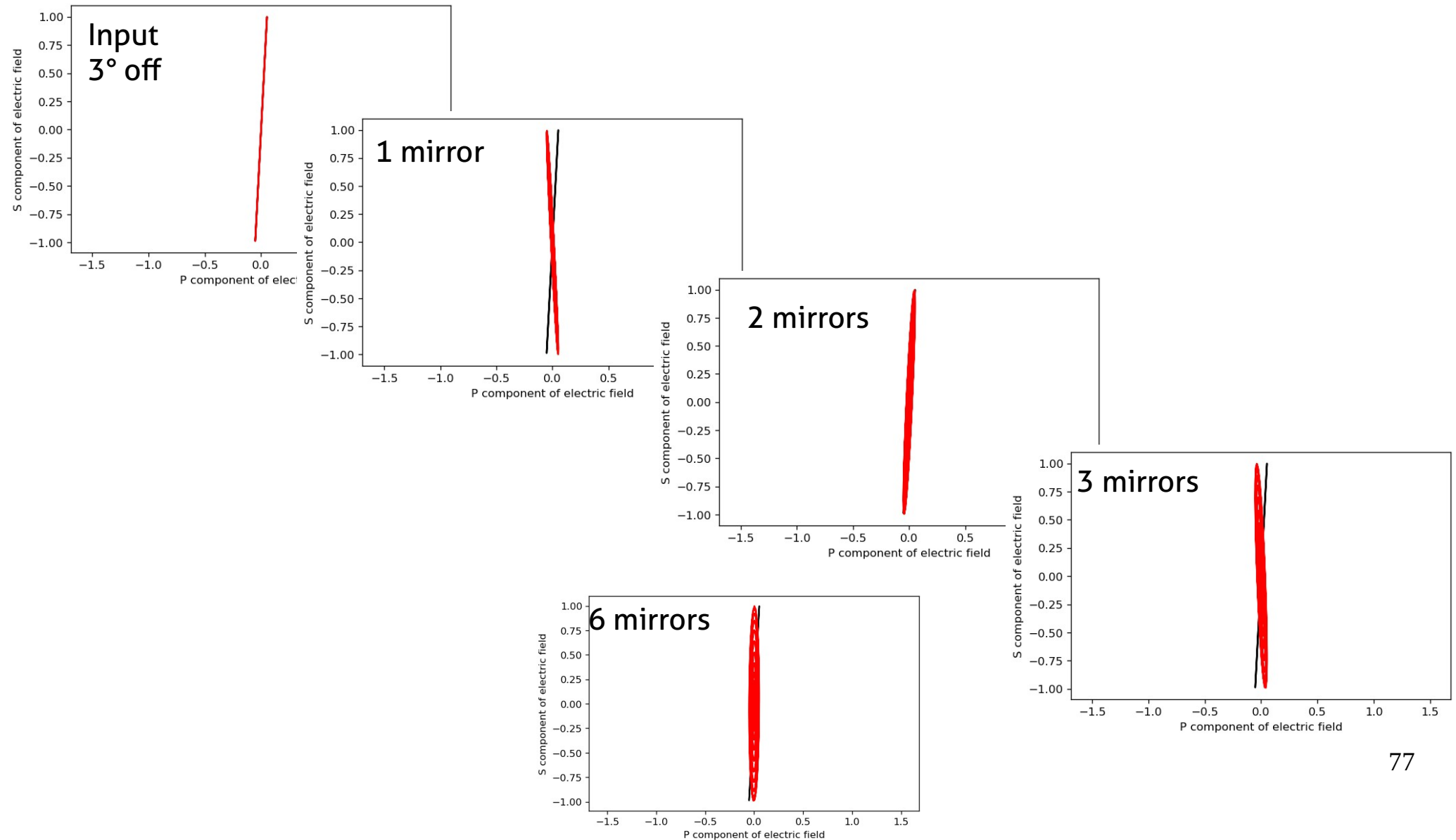
More trouble: polarization state

We send a linearly polarized laser pulse to a set of 45° incidence silver mirror, in a horizontal plane
Mirror complex reflectivity calculated from Fresnel equations
We introduce an initial rotation of the polarization direction with respect to the vertical S polarization
We calculate the resulting pulse polarization, as a function of the number of bounces on mirrors.



More trouble: polarization state

We send a linearly polarized laser pulse to a set of 45° incidence silver mirror, in a horizontal plane
Mirror complex reflectivity calculated from Fresnel equations
We introduce an initial rotation of the polarization direction with respect to the vertical S polarization
We calculate the resulting pulse polarization, as a function of the number of bounces on mirrors.



Introduction: time-frequency travel

Keeping ultrashort pulses ultrashort

Self-phase modulation – the enemy within

Mirror mirror

Producing circularly polarized pulses – a perfect circle

Focus

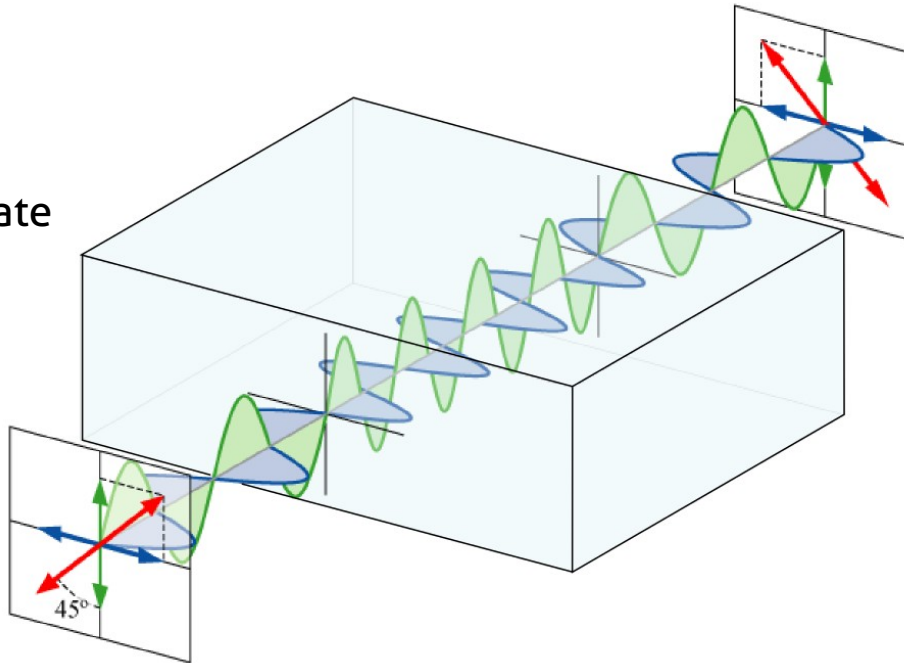
Controlling the polarization state of femto pulses

Many experiments require circularly polarized light, or well defined elliptical light
Circular Dichroisms, attoclock...

In principle, polarization manipulation is easy: use wave plates

Decompose the field in two components in a birefringent crystal
They accumulate different phases
→ The resulting polarization is modified

Ex: Half Wave Plate



Controlling the polarization state of femto pulses

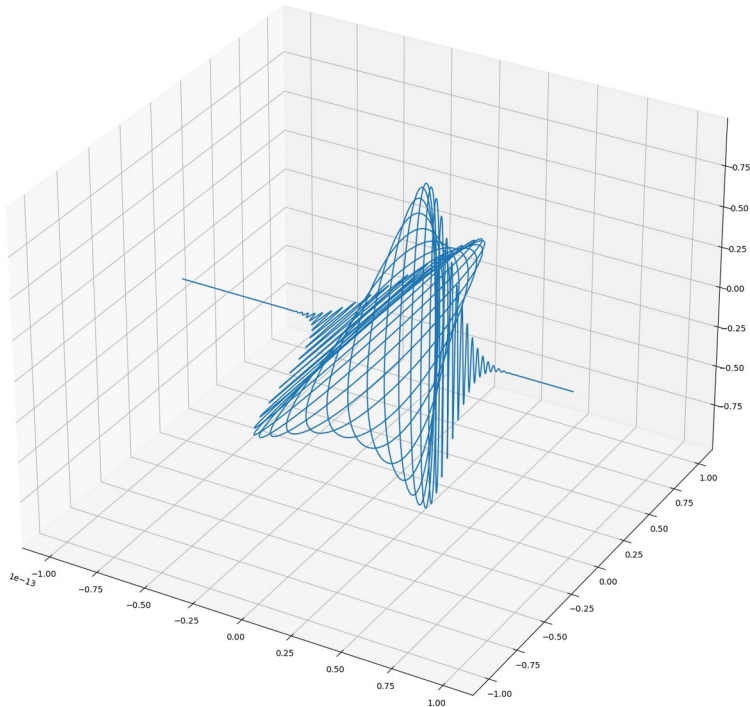
The crystal thickness can be set to achieve a phase-shift of $\lambda/4$ between the two components
→ Converts linear light into circular

First constraint : we want zero order waveplates

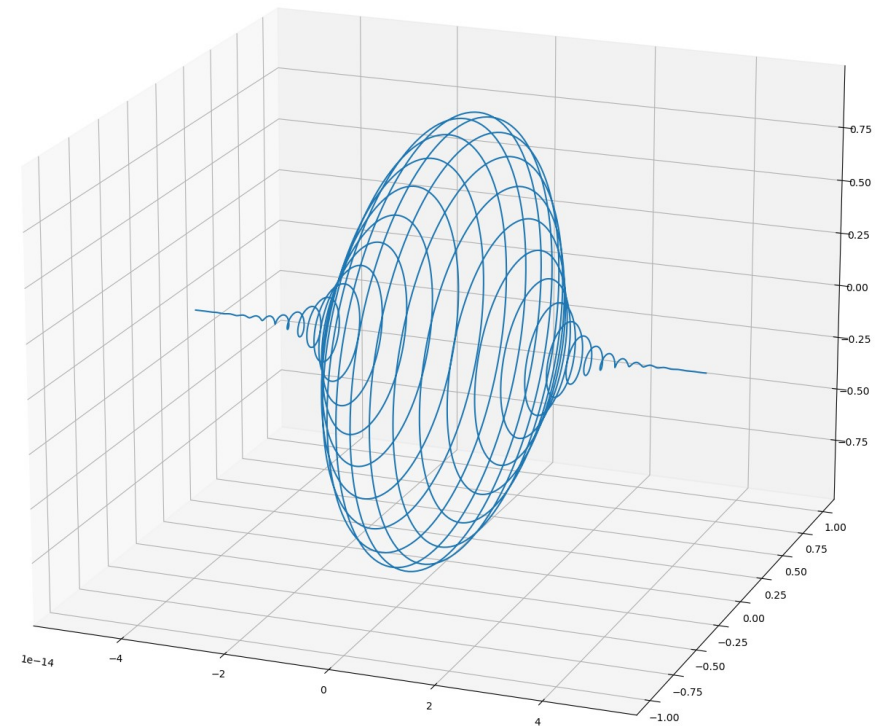
Multiple order quarter waveplate: introduces a delay of $n.T_0 + T_0/4$

$n=0$ → Zero-order quarter waveplate

20fs pulse, multiple order wp with $n=5$



20fs pulse, zero order waveplate



(can be useful for temporal shaping of polarization state, e.g. for polarization gating of attosecond pulse generation)

Controlling the polarization state of femto pulses

The crystal thickness can be set to achieve a phase-shift of $\lambda/4$ between the two components
→ Converts linear light into circular

First constraint : we want zero order waveplates

Multiple order quarter waveplate: introduces a delay of $n \cdot T_0 + T_0/4$

$n=0$ → Zero-order quarter waveplate

Technology:

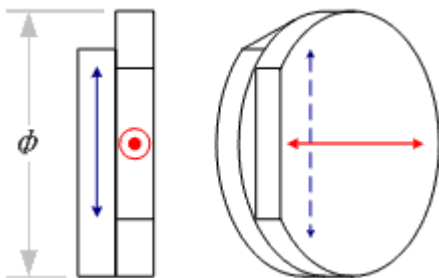
- Very thin polymer film (true zero order)
- Quartz: stack two crystals, for instance one introducing $5 \cdot T_0 + T_0/4$ and the other one $-5 \cdot T_0$

Second constraint: we sometimes need broadband waveplates

Impossible with a single dispersive birefringent medium (n_{ordinary} and $n_{\text{extraordinary}}$ vary with λ)

Use a combination of two media, with opposite dispersions: quartz and MgF_2

The bandwidth can be increased by increasing the complexity of the stacking

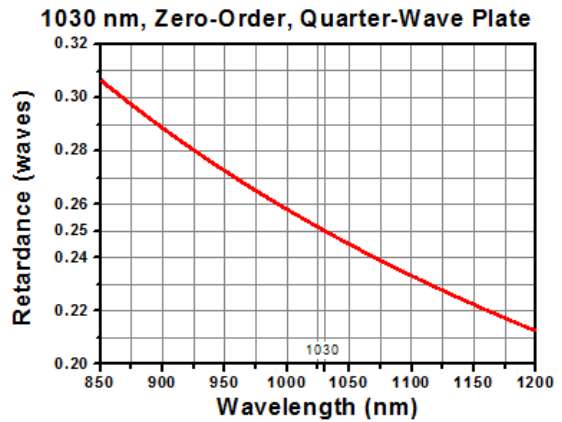


Which quarter wave plate?

Zero order

 **05RP04-50**
 Zero-Order Waveplate, Quarter-Wave, Quartz, 12.7 mm Diameter, 1030 nm

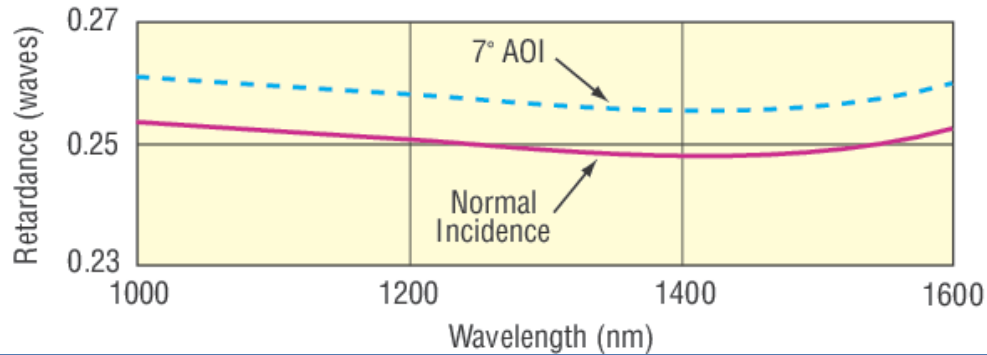
   12.7 mm 1030 nm In Stock  €410 



Achromatic

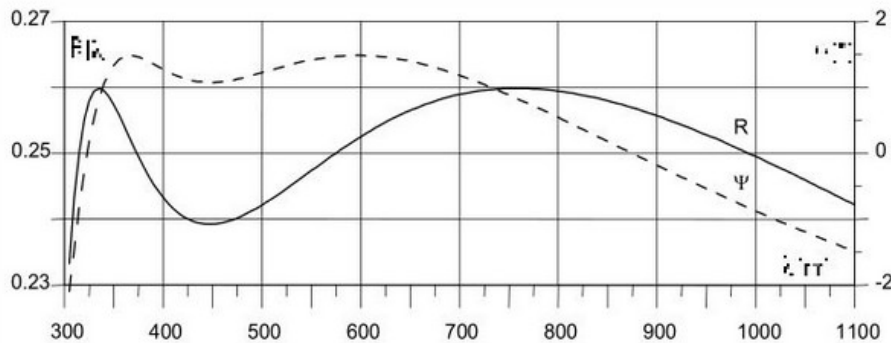
 **10RP54-4**
 Achromatic Zero-Order Quartz-MgF₂ Wave Plate, 1 in, λ/4, 650-1350 nm

   650-1350 nm 12 mm Show €861 



Super achromatic

λ/4 Wavelength variation of the retardation R and the axis direction Ψ



λ/4 superachromatic waveplates with cover plates

order no.	1 piece in €
RSU 1.4.10	2164.-
RSU 1.4.15	3429.-
order no.	1 piece in €
RSU 1.4.20	6237.-
RSU 1.4.25	7991.-

Transferring the attoclock technique to velocity map imaging

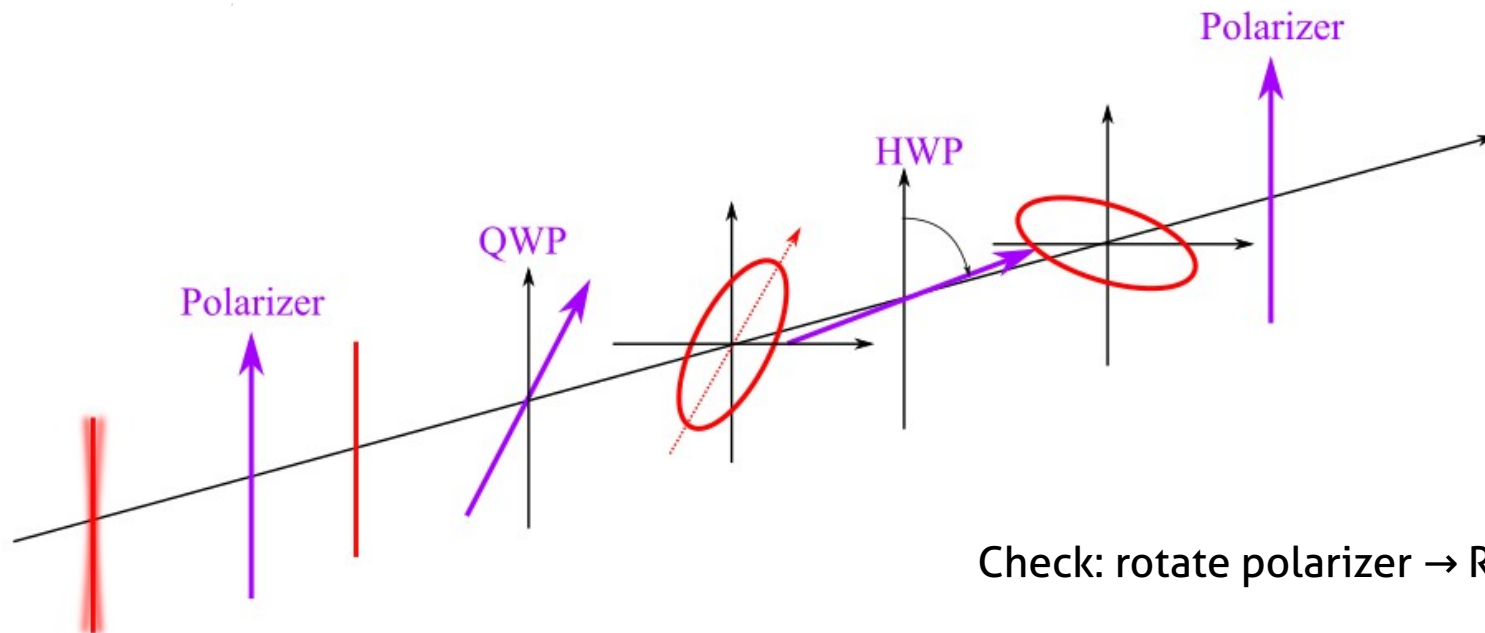
Matthias Weger, Jochen Maurer,* André Ludwig, Lukas Gallmann,
and Ursula Keller

Department of Physics, ETH Zurich, Wolfgang-Pauli-Str. 16, 8093 Zurich, Switzerland

(C) 2013 OSA 23 September 2013 | Vol. 21, No. 19 | DOI:10.1364/OE.21.021981 | OPTICS EXPRESS 21981

Goal: produce an elliptical beam, and rotate the main axis of the ellipse during the acquisition (tomographic Velocity-Map Imaging)

The pulse characterization with a SPIDER resulted in a measured pulse length of 6.1 fs at a central wavelength of 735 nm. Before the pulse entered the vacuum chamber through the entrance window it passed a polarizer, a quarter-wave plate (QWP) and a half-wave plate (HWP). The polarizer (Newport polarcor 05P109AR.16) ensured a clean linear polarization state of the beam before the pulse passes through the QWP. The desired ellipticity of 0.87 was induced by the quarter-wave plate (B.Halle Nachfl. GmbH RAC 5.4.10L



Check: rotate polarizer → Record Malus' law 83

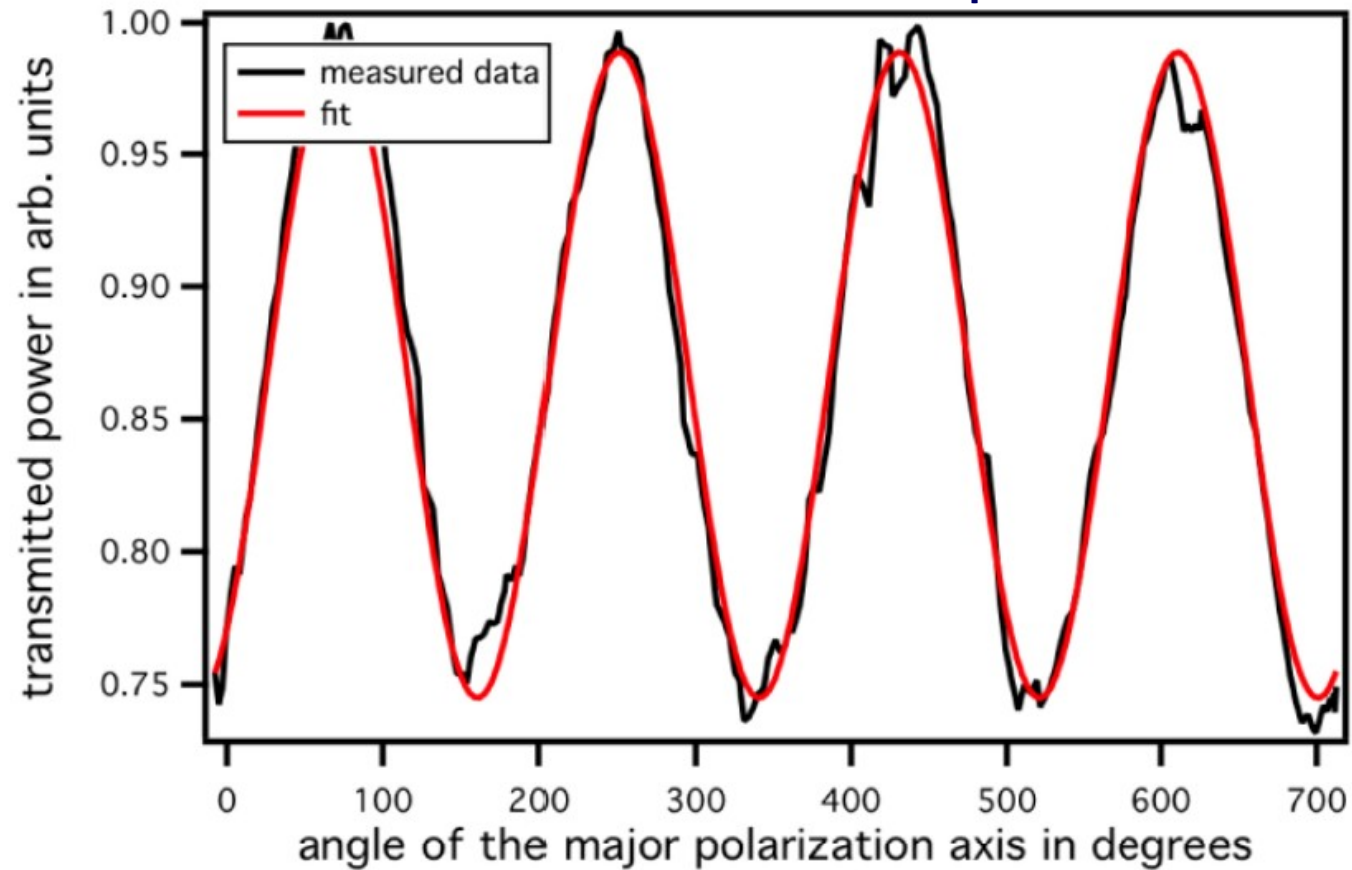
Transferring the attoclock technique to velocity map imaging

Matthias Weger, Jochen Maurer,* André Ludwig, Lukas Gallmann,
and Ursula Keller

Department of Physics, ETH Zurich, Wolfgang-Pauli-Str. 16, 8093 Zurich, Switzerland

(C) 2013 OSA 23 September 2013 | Vol. 21, No. 19 | DOI:10.1364/OE.21.021981 | OPTICS EXPRESS 21981

Superachromatic waveplate



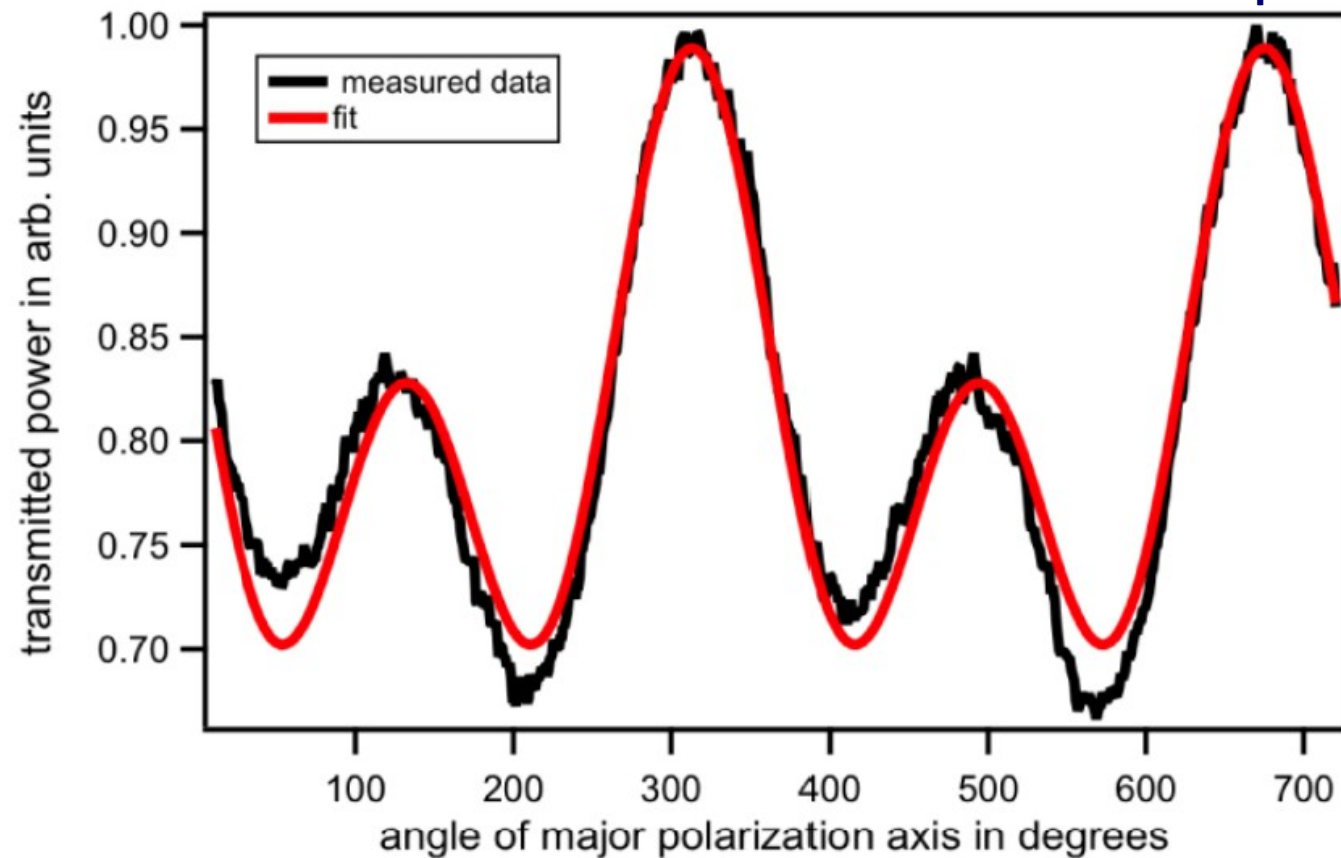
Transferring the attoclock technique to velocity map imaging

Matthias Weger, Jochen Maurer,* André Ludwig, Lukas Gallmann,
and Ursula Keller

Department of Physics, ETH Zurich, Wolfgang-Pauli-Str. 16, 8093 Zurich, Switzerland

(C) 2013 OSA 23 September 2013 | Vol. 21, No. 19 | DOI:10.1364/OE.21.021981 | OPTICS EXPRESS 21981

Achromatic waveplate



A superachromatic waveplate is necessary for this experiment

Polarization by reflections

Finding good waveplates can be difficult
In DUV-VUV-XUV → Very challenging

Fig.1 Retardation Spectrum of VUV Achromatic QWP

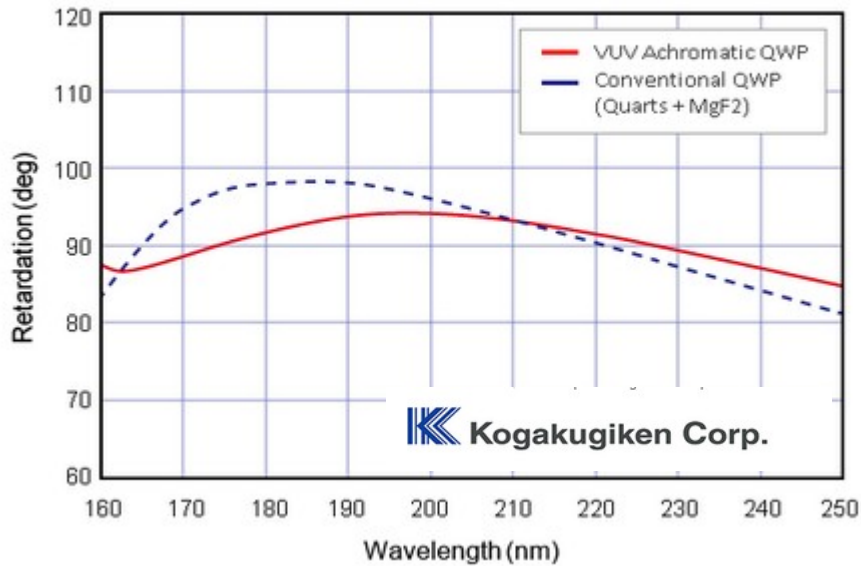
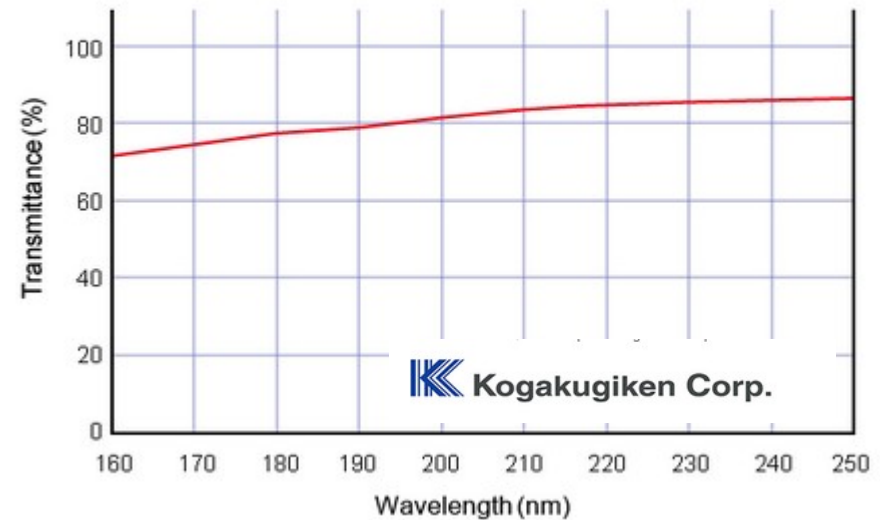


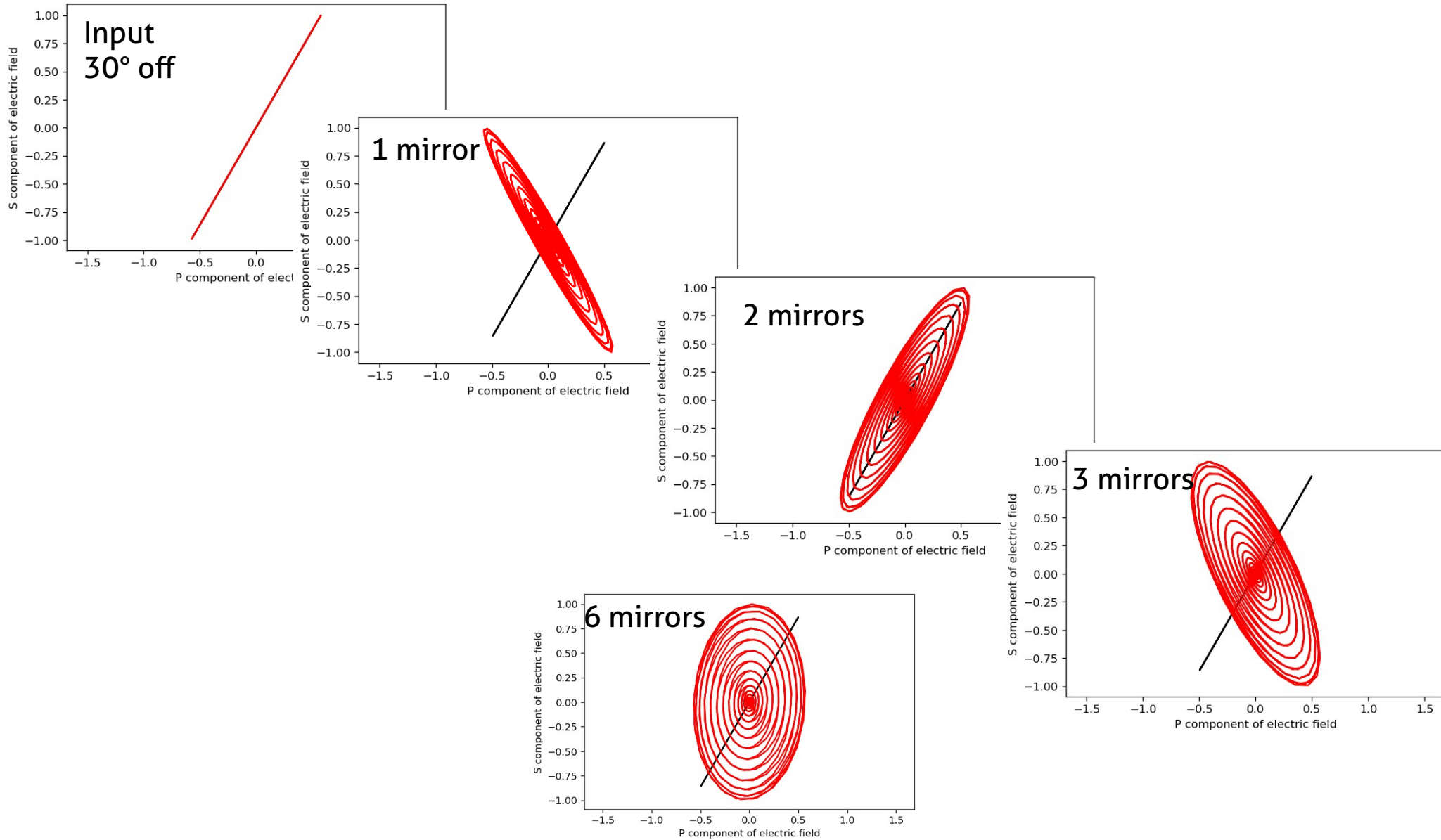
Fig.3 Transmittance Spectrum of VUV Achromatic QWP/HWP with optical contact Type (measured)



Dispersion is not provided...

Phase-shifts introduced by metallic reflections can be an alternative solution

Polarization by reflections



Calculation: reflection of a 5fs 400 nm pulse on Al mirrors: in the practical

Polarization by reflections

SU5: a calibrated variable-polarization synchrotron radiation beam line in the vacuum-ultraviolet range

Laurent Nahon and Christian Alcaraz

1024 APPLIED OPTICS / Vol. 43, No. 5 / 10 February 2004

Used as analysis QWP for synchrotron radiation

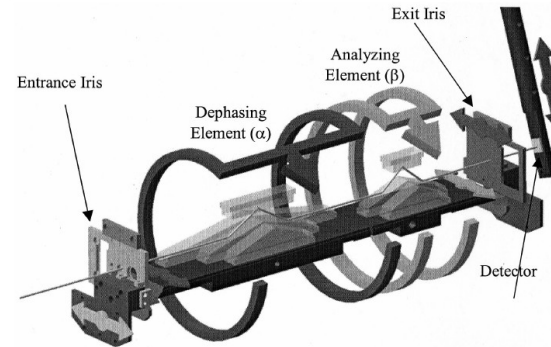


Fig. 3. Schematic of the SU5 (3 + 3)-reflection polarimeter, showing the dephasing and analyzing elements to be rotated by respective angles α and β , which involve, respectively, three (140°, 150°, and 160°) and two (130° and 140°) prisms. One can also see the two irises and the movable UV-XUV detector. The prisms can be moved out of the way of the photon beam to allow the beam to move toward the sample.

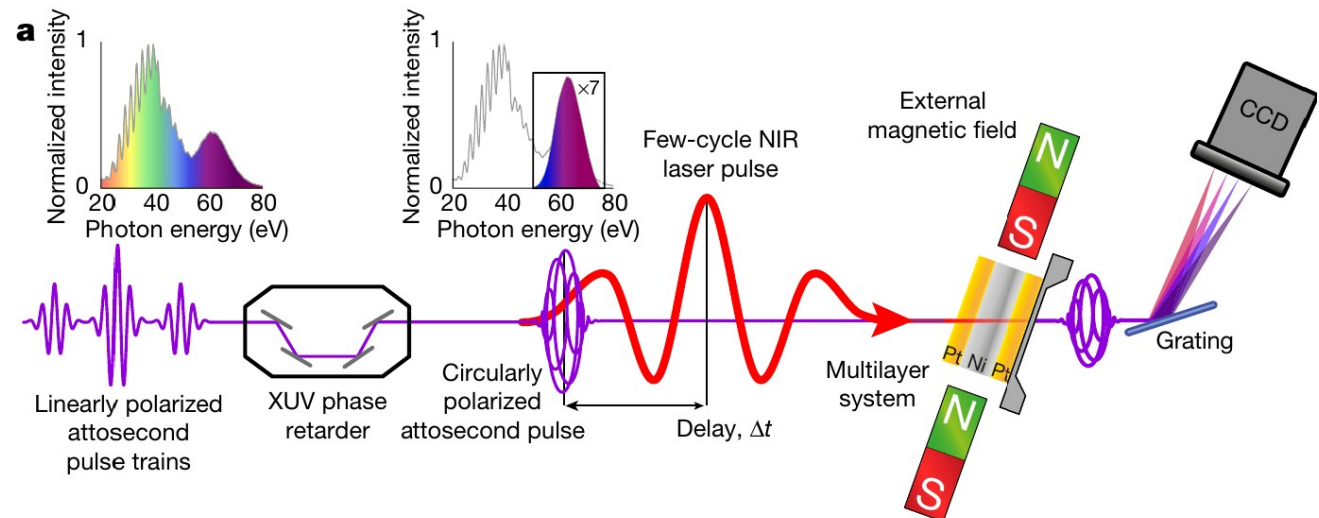
LETTER

<https://doi.org/10.1038/s41586-019-1333-x>

Light-wave dynamic control of magnetism

Florian Siegrist^{1,2}, Julia A. Gessner^{1,2}, Marcus Ossiander¹, Christian Denker³, Yi-Ping Chang¹, Malte C. Schröder¹, Alexander Guggenmos^{1,2}, Yang Cui², Jakob Walowski³, Ulrike Martens³, J. K. Dewhurst⁴, Ulf Kleineberg^{1,2}, Markus Münzenberg³, Sangeeta Sharma³ & Martin Schultze^{1,6*}

Used to convert linear atto pulses to circular



Introduction: time-frequency travel

Keeping ultrashort pulses ultrashort

Self-phase modulation – the enemy within

Mirror mirror

Producing circularly polarized pulses – a perfect circle

Focus

Most straightforward tool: lenses

But:

Glass introduces GDD and SPM

The refractive index depends on wavelength → The focal length depends on wavelength
chromatic aberration

+ spherical aberrations...

Focusing femtosecond pulses

Directly measuring the spatio-temporal electric field of focusing ultrashort pulses

Pamela Bowlan, Pablo Gabolde, and Rick Trebino

Georgia Institute of Technology, School of Physics
837 State St NW, Atlanta, GA 30332 USA



30 nm bandwidth pulse
Focused by $f=50\text{mm}$
Aspheric lens

While chromatic aberration plays only a small role in the pulse temporal phase, it does become evident, however, in the pulse's temporal intensity and its distortions. For a lens free of aberrations, the pulse fronts are curved and perfectly symmetrical about the focus, and flat at the focus. Chromatic aberration shifts the position of the flat pulse front to a value of z after the focus, resulting in pulse fronts that are not symmetric about the focus [3]. In Fig. 2, it is clear that the pulse fronts are, in fact, not symmetric about the focus, and the pulse front is flat at $z = 1.5\text{ mm}$ in both the simulation and experimental data.

Chromatic aberration and GDD,
GDD dominates

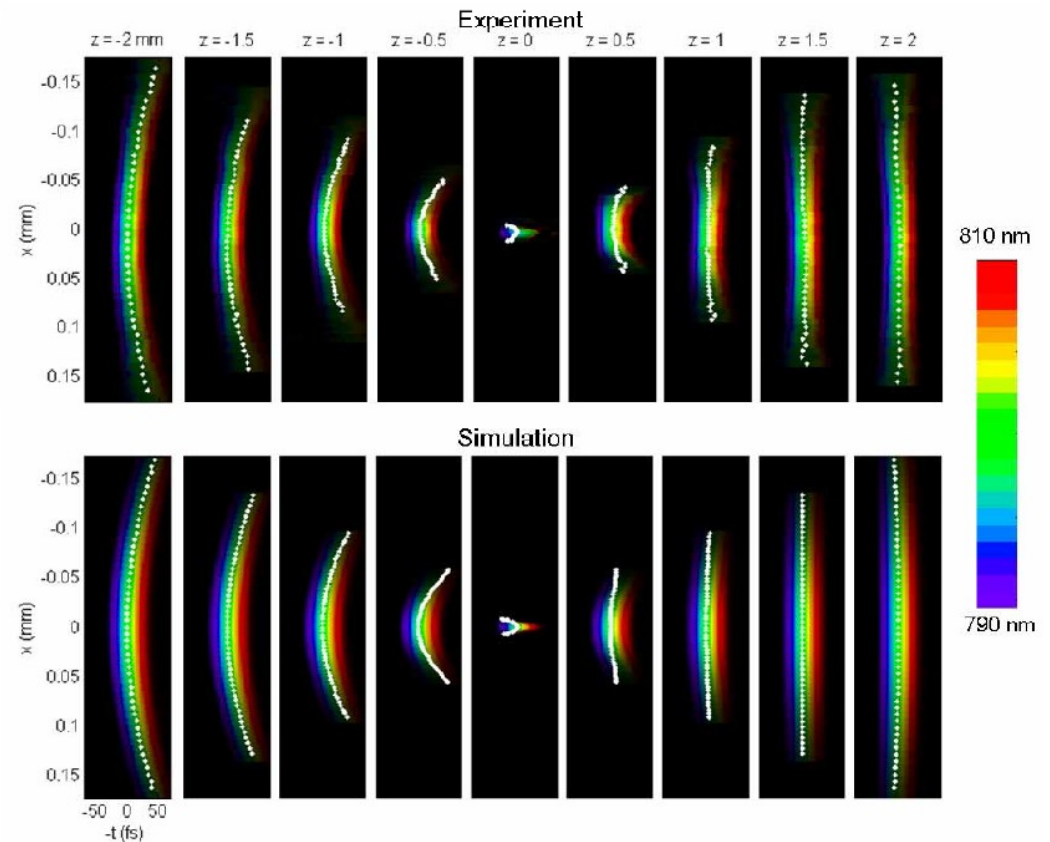


Fig. 2. $E(x,z,t)$ in the focal region of an aspheric lens. The experimental results are displayed in the top plots, and the simulations are in the bottom plots. Each box displays the amplitude of the electric field versus x and t at a distance z from the geometric focus. The color represents the instantaneous wavelength as designated by the color bar on the right. Each set of plots displays the amplitude of the electric field versus $-t$ (so that the leading edge of the pulse appears on the right) and x at a particular longitudinal distance away from the focus. The white dots display the pulse front (defined as the maximum temporal intensity at each x). The same conventions are used for the next several plots as well. In this case, as expected, chromatic aberration causes a flat pulse front to occur after the focus, at about $z = 1.5\text{ mm}$.

Focusing femtosecond pulses

Directly measuring the spatio-temporal electric field of focusing ultrashort pulses

Pamela Bowlan, Pablo Gabolde, and Rick Trebino

Georgia Institute of Technology, School of Physics
837 State St NW, Atlanta, GA 30332 USA



30 nm bandwidth pulse
Focused by $f=50\text{mm}$
Achromatic Doublet lens

In Fig. 3, most of the color variation is again due to the GDD of the lens. Because the doublet is very thick (9.8 mm) and, made of very dispersive glass, it introduces significant GDD, and this lengthens the pulse by about three times more than the aspheric lens does (using rms temporal width of the pulse averaged over x). Also, the pulse fronts are not symmetric about the focus, revealing the presence of chromatic aberration.

No chromatic aberration
GDD dominates

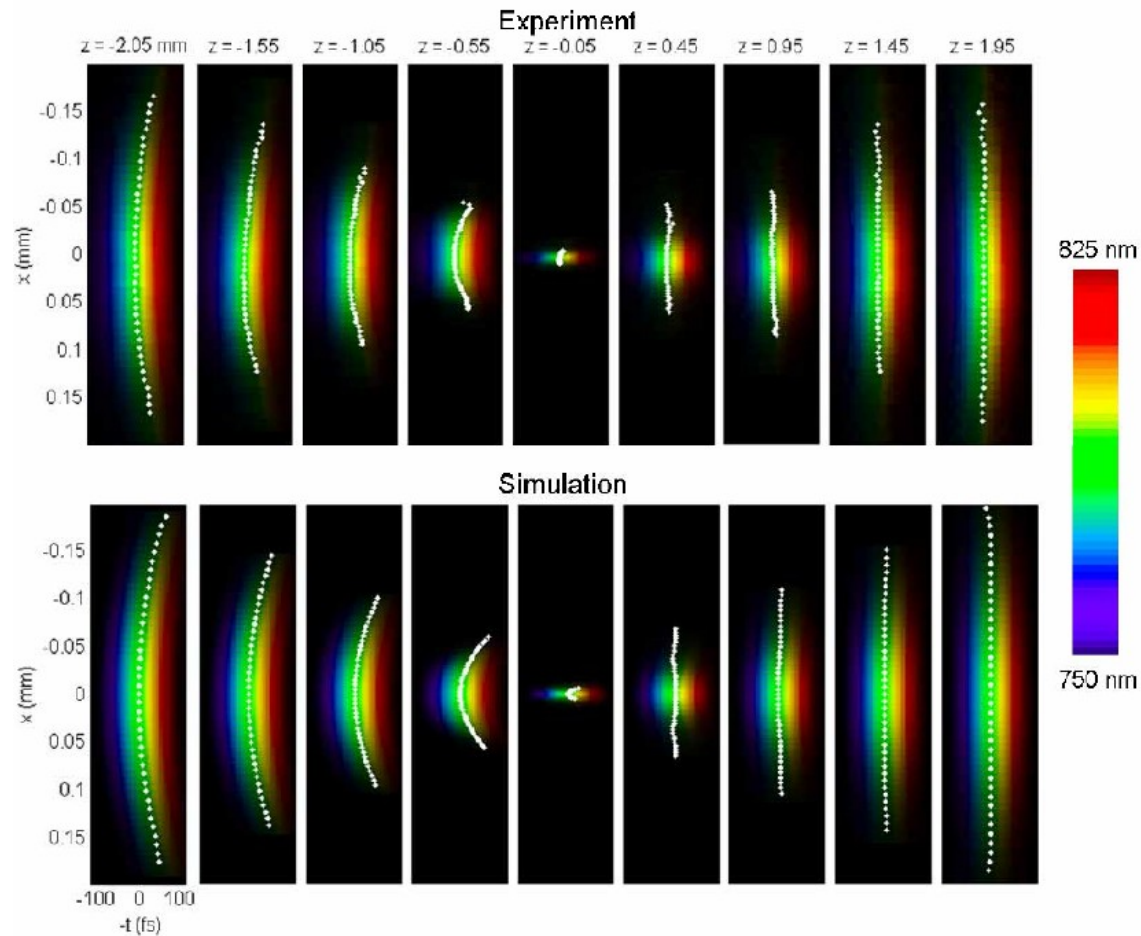


Fig. 3. $E(x,z,t)$ in the focal region of an achromatic doublet designed for visible light. Significant GDD is apparent due to the thickness of the lens. Because this lens was designed for the visible, and not 800 nm, the pulse fronts are not symmetric about the focus, revealing that some chromatic aberration is also present.

Focusing femtosecond pulses

Directly measuring the spatio-temporal electric field of focusing ultrashort pulses

Pamela Bowlan, Pablo Gabolde, and Rick Trebino

Georgia Institute of Technology, School of Physics
837 State St NW, Atlanta, GA 30332 USA



30 nm bandwidth pulse
Focused by $f=50\text{mm}$
Plano-convex lens

Spherical aberration and GDD dominates

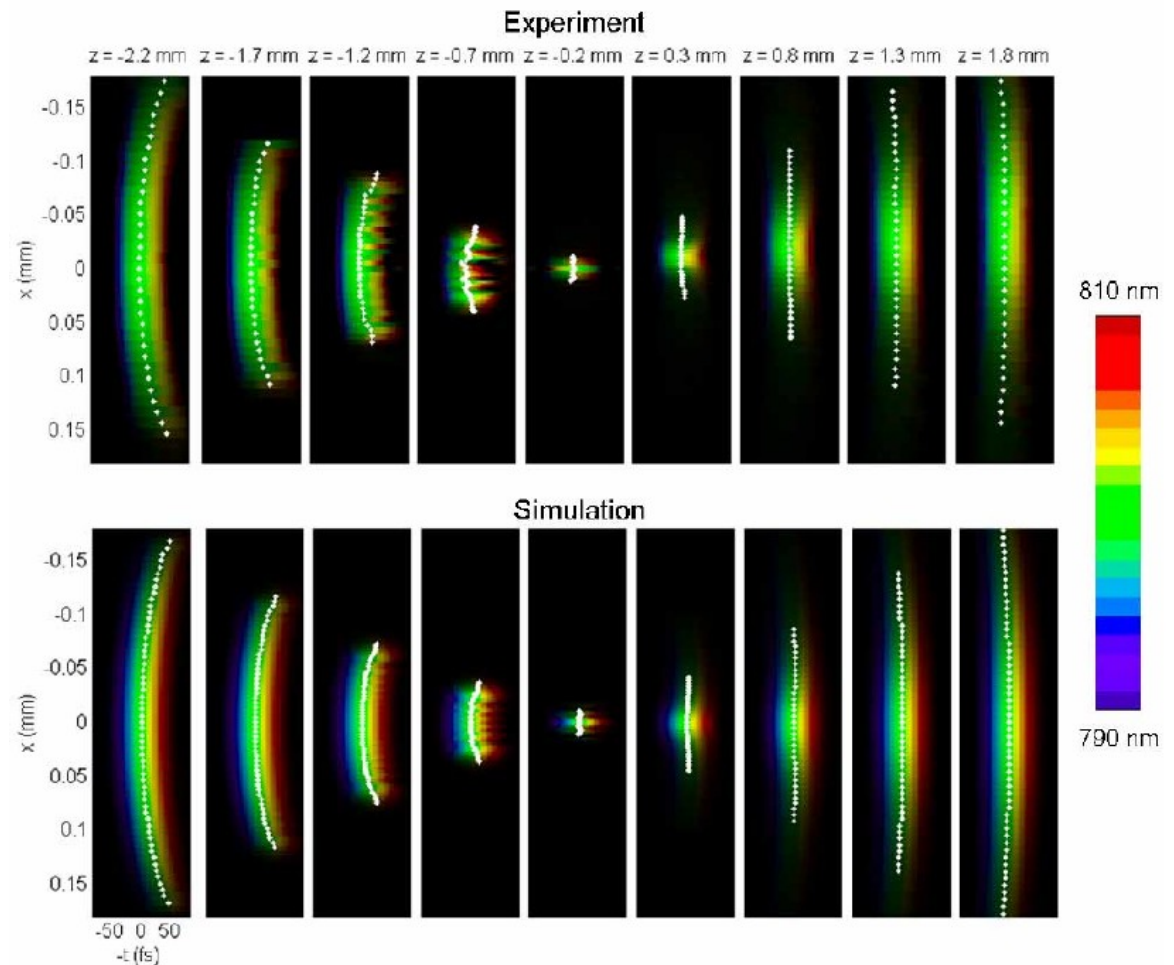


Fig. 4. $E(x,z,t)$ in the focal region of a plano-convex lens. The spherical aberrations introduced by this lens result in ripples in the spatial profile that are particularly visible at $z = -0.7\text{mm}$.

Focusing femtosecond pulses

Directly measuring the spatio-temporal electric field of focusing ultrashort pulses

Pamela Bowlan, Pablo Gabolde, and Rick Trebino

Georgia Institute of Technology, School of Physics
837 State St NW, Atlanta, GA 30332 USA



30 nm bandwidth pulse
Focused by $f=50\text{mm}$
Plano-convex lens
With chirp compensation

Pure effect of chromatic aberration
→ Pulse duration $\times 1.3$ w/r Fourier Limit

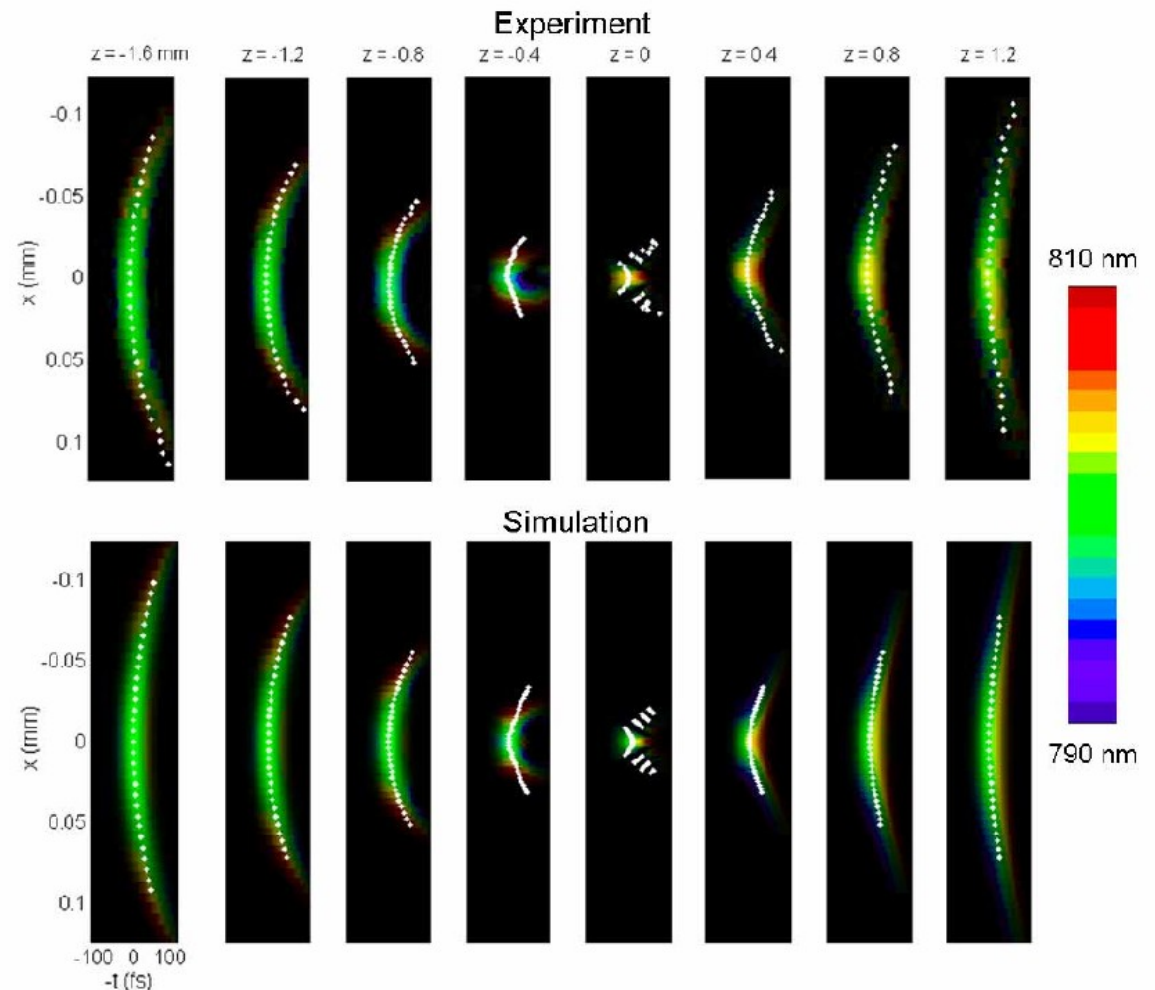


Fig. 5. $E(x,z,t)$ in the focal region of a ZnSe lens with chirp compensation. In these plots, all of the color variation is due to chromatic aberration.

Focusing femtosecond pulses

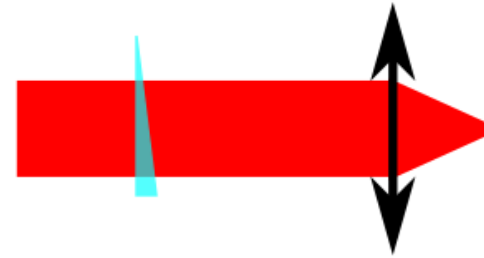
Bowlan *et al.* Vol. 25, No. 6/June 2008/J. Opt. Soc. Am. B

Measuring the spatiotemporal electric field of ultrashort pulses with high spatial and spectral resolution

Pamela Bowlan,^{1,*} Pablo Gabolde,¹ Matthew A. Coughlan,² Rick Trebino,¹ and Robert J. Levis²

¹School of Physics, Georgia Institute of Technology, 837 State Street NW, Atlanta, Georgia 30332, USA

²Department of Chemistry, Center for Advanced Photonics Research, Temple University, Philadelphia, Pennsylvania 19122, USA

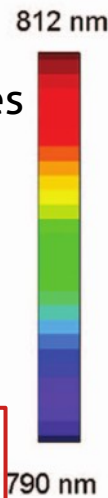


30 nm bandwidth pulse with angular dispersion
Focused by $f=25\text{mm}$ lens

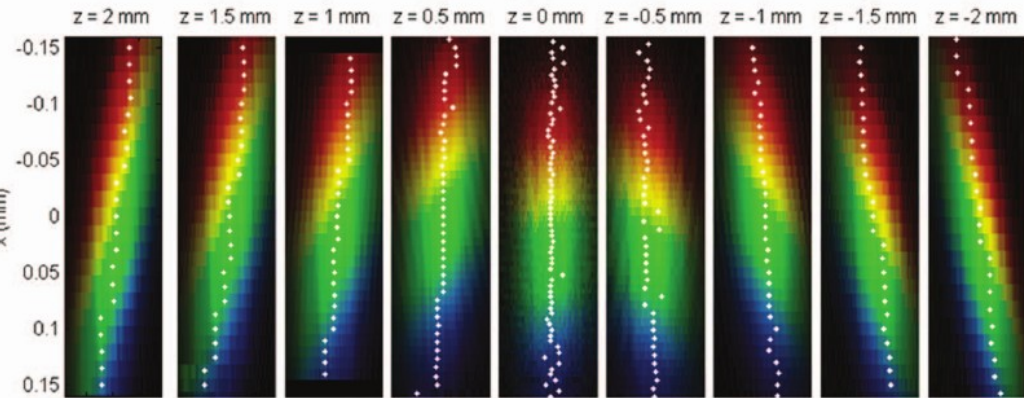
Different colors sent to different angles
→ Spatial chirp at focus

30 nm bandwidth pulse with angular dispersion
Focused by $f=25\text{mm}$ lens

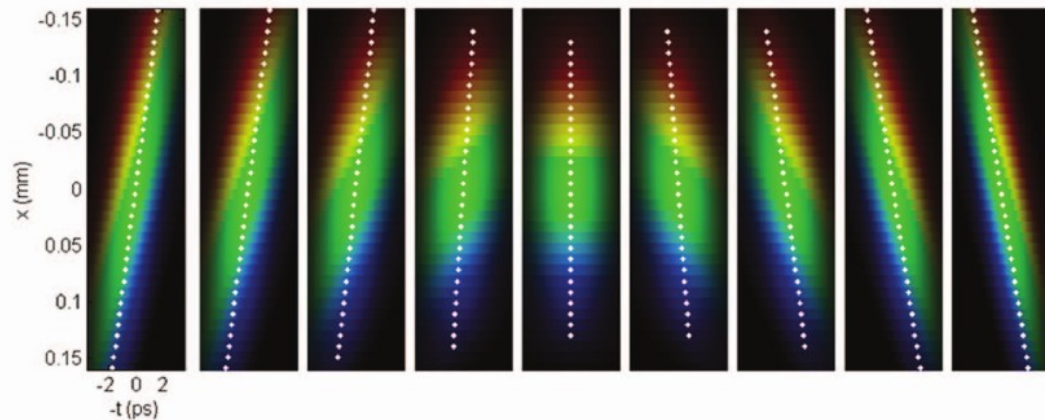
Different colors sent to different angles
→ Spatial chirp at focus



Experiment



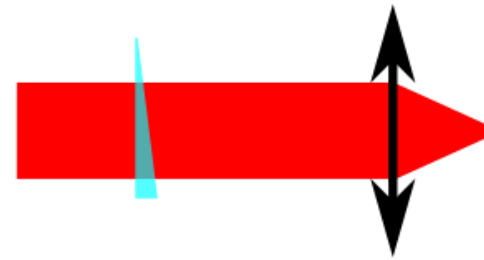
Simulation



Angular dispersion can be caused by misaligned compressor or wedged components

Fig. 5. $E(x,z,t)$ in the focal region of the beam that had angular dispersion. The data is displayed in the same way as in Fig. 4. The angular dispersion becomes purely spatial chirp at the focus because a lens is a Fourier transformer.

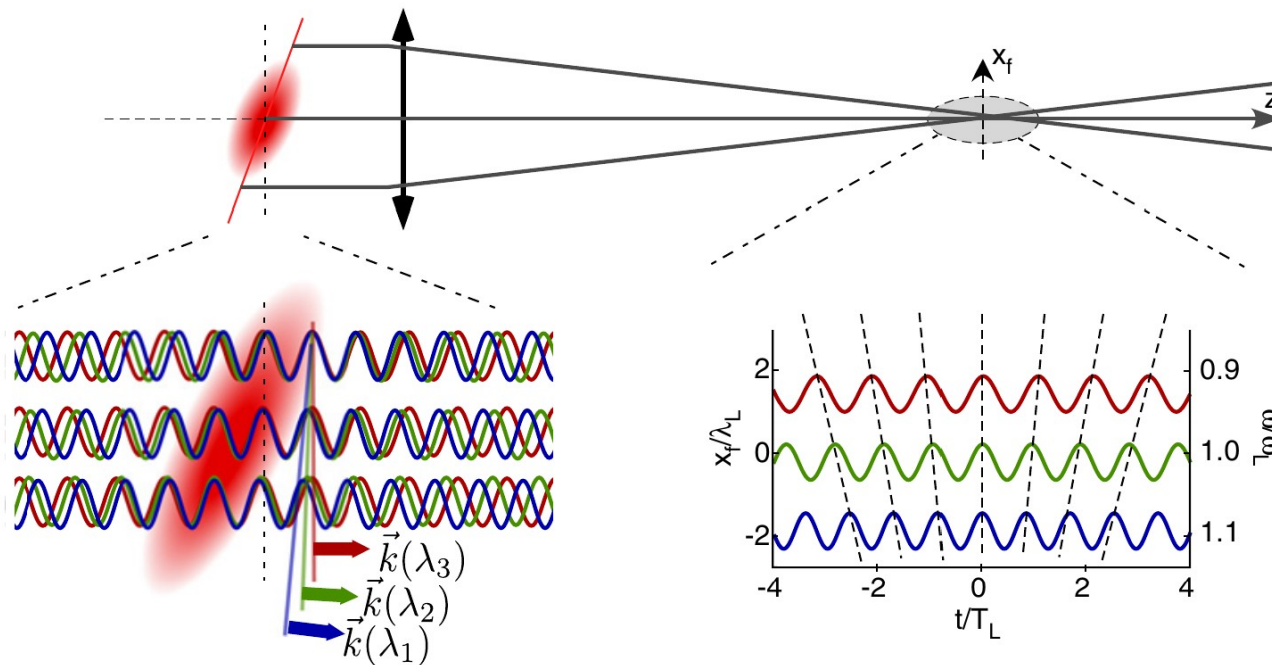
Focusing femtosecond pulses



30 nm bandwidth pulse
with angular dispersion
Focused by $f=25\text{mm}$ lens

Different colors sent to
different angles
→ Spatial chirp at focus

Angular dispersion causes pulse front tilt: the femtosecond pulse arrival time depends on space



Generally detrimental, but can be useful – the attosecond lighthouse

The attosecond lighthouse

Review Article

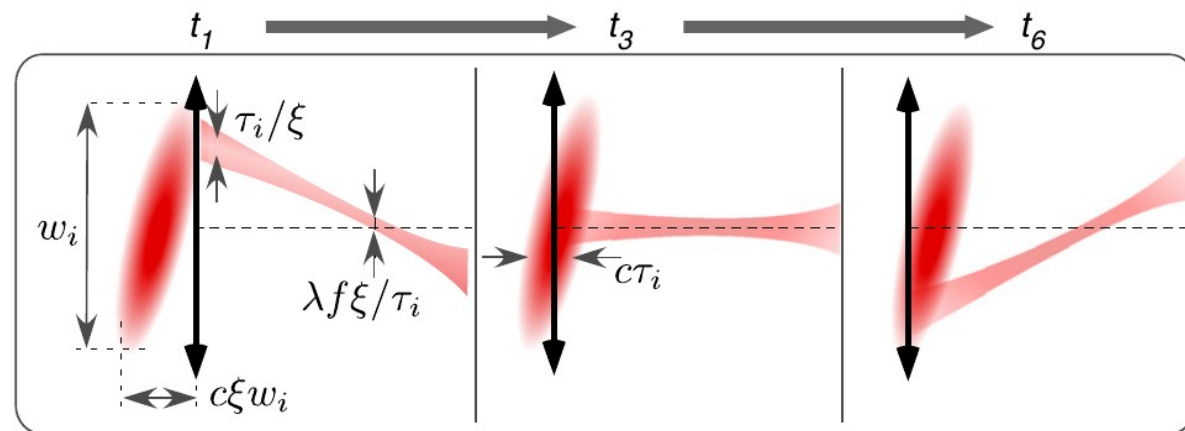
Applications of ultrafast wavefront rotation in highly nonlinear optics

F Quéré¹, H Vincenti^{1,2}, A Borot², S Monchocé¹, T J Hammond³,
 Kyung Taec Kim³, J A Wheeler¹, Chunmei Zhang³, T Ruchon¹,
 T Auguste¹, J F Hergott¹, D M Villeneuve³, P B Corkum³
 and R Lopez-Martens²

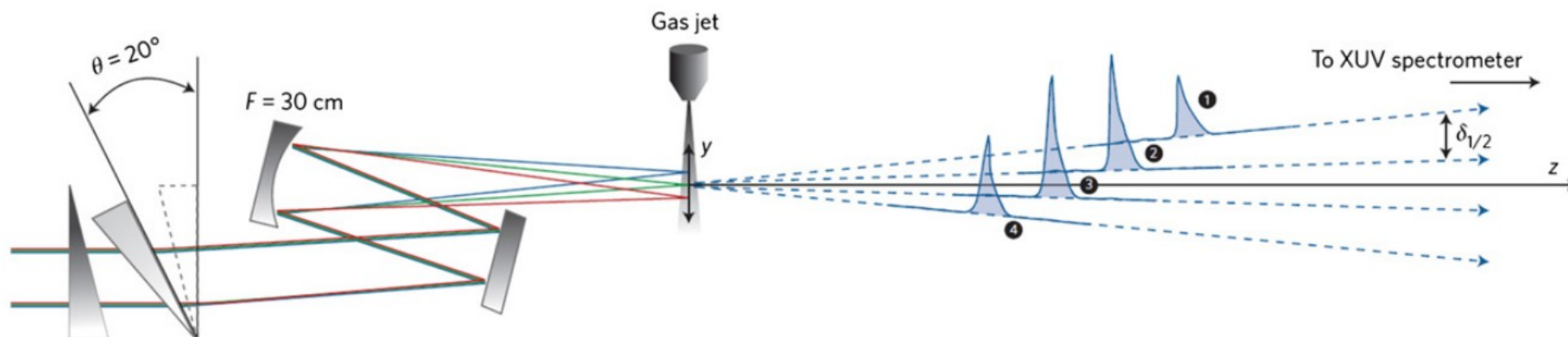
¹ Commissariat à l'Energie Atomique, Lasers, Interactions and Dynamics Laboratory (LIDyL),
 DSM/IRAMIS, CEN Saclay, F-91191 Gif sur Yvette, France

² Laboratoire d'Optique Appliquée, ENSTA-Paristech, Ecole Polytechnique, CNRS, F-91761 Palaiseau,
 France

³ Joint Attosecond Science Laboratory, National Research Council and University of Ottawa, 100 Sussex
 Drive, Ottawa ON, K1A 0R6, Canada



Attosecond lighthouse: ultrafast wavefront rotation, sending consecutive attosecond bursts to different directions



Focusing femtosecond pulses

Most straightforward tool: lenses

But:

Glass introduces GVD and SPM

The refractive index depends on wavelength → The focal length depends on wavelength
chromatic aberration

Spherical mirrors are broadly used

But:

Astigmatism is an issue when the incidence angle is too large

Off-axis parabola solve this issue

But:

They are more difficult to align

(large incidence angles also destroy circular polarization...)



Introduction: time-frequency travel

Keeping ultrashort pulses ultrashort

Self-phase modulation – the enemy within

Mirror mirror

Producing circularly polarized pulses – a perfect circle

Focus

Many effects can degrade the pulse quality in an experiment

The most obvious issue is the increase of pulse duration

We'll see how to characterize this next course

Polarization issues and spatial inhomogeneities / space-time couplings can be tricky

In general one tries to avoid measuring stuff as long as things work

This can be risky and lead you to investigate artifacts believing they are interesting physics